Design, Synthesis and Characterization of Coenzyme-substrate Inhibitors Targeting Intracellular Pyridoxal 5'-phosphate - dependent Enzymes

Dissertation

zur

Erlangung der naturwissenschaftlichen Doktorwürde

(Dr. sc. nat.)

vorgelegt der

Mathematisch- naturwissenschaftlichen Fakultät

der

Universität Zürich

von

Wu Fang

aus China

Promotionskomitee

Prof. Dr. Peter Sonderegger (Vorsitz)

Prof. Dr. Heinz Gehring (Leitung der Dissertation)

Zürich, 2007

Dedicated to my family

The results of this work have been or will be published elsewhere:

Wu F, Grossenbacher D, Gehring H. New transition state based-inhibitor of human ornithine decarboxylase inhibiting growth of tumor cells
Mol. Cancer Ther. 2007 Jun;6(6):1831-9.

Wu F, Yu J, Gehring H. Inhibitory and structural studies of novel coenzyme-substrate analogs of human histidine decarboxylase
FASEB J. 2007, *In press*

Wu F, Lo P, Gehring H. Structural requirements for novel coenzyme-substrate derivatives to inhibit intracellular ornithine decarboxylase and cell proliferation
(in preparation)

Additional publication, not part of this dissertation

Zakaryan R.P., Wu F, Pahlich S, Grossenbacher D, Sedda MJ, Gehring H.
Tyrosine phosphorylation in the C-terminal nuclear localization and retention signal (C-NLS) of the EWS protein (in preparation)

Presentations:

Gehring H., Wu F. Working Group 2 meeting of European Concerted Research COST922 "Health Implications of Dietary Amines. Lodz, Poland, *Nov. 2004.* Design and synthesis of a new cellular ODC inhibitor.

Wu F., Gehring H. Targeting the Kinome. Basel, *Dez*.2006. New transition state based-inhibitor of human ornithine decarboxylase inhibits growth of tumor cells.

Ingrid B. Müller, Fang Wu, Bärbel Bergmann, Marie-Luise Eschbach, Julia Knöckel, Heinz Gehring, Rolf D. Walter, Carsten Wrenger. European Concerted Research COSTB22. Dundee, UK, 2007, *Jun.* Poisoning pyridoxal 5’ phosphate (PLP)-dependent enzymes as a new strategy to target *P. falciparum*

Table of contents

ABBREVIATIONS

APAO	Acetyl polyamine oxidase
AZ	Antizyme
BOC	Tert-butoxycarbonyl
BOL	BOC-protected lysine methyl ester
BOM	BOC-protected ornithine methyl ester
DDC	Dopa decarboxylase
DENspm	*N*1, *N*11- di(ethyl)- norspermine
DFMO	α-DL-difluoromethylornithine
ERE	Estrogen response elements
GBM	Glioblastoma multiforme
HAT	Histone acetyltransferases
HDAC	Histone deacetylases
HDC	Histidine decarboxylase
HMC	Human mast cell
HME	Histidine methyl ester
LCMB	Lung cancer metastasizing cells in brain
NO	Nitric oxide
NOS	Nitric oxide synthase
ODC	Ornithine decarboxylase
PAO	Polyamine oxidase
PHME	Pyridoxyl-histidine methyl ester
PLP	Pyridoxal 5'-phosphate
POB	*N*-(4'-pyridoxyl)-ornithine-BOC

PT	Polyamine transporter
PUT	Putrescine
SMO	Spermine oxidase
SPD	Spermidine
SPM	Spermine
SSAT	Spermine/spermidine *N*1- acetyltransferase
TPA	12-*O*-Tetradecanoylphorbol-13-acetate

Zusammenfassung

Pyridoxal 5'-phosphat (PLP)-abhängige Enzyme katalysieren vielfältige Umwandlungen von Aminosäuren, wie Transaminierung, α-Decarboxylierung und Razemisierung sowie β/γ-Eliminierungs- und Substitutionsreaktionen. Vitamin B_6-abhängige Enzyme spielen eine zentrale Rolle im Aminosäure- und Aminmetabolismus und sind interessante Zielobjekte für Medikamente, um auf spezifische, zu pathologischen Zuständen führende Prozesse einzuwirken. Hemmstoffe, welche der Struktur des Übergangszustands entsprechen, binden mit hoher Affinität an ihre Zielenzyme. Unter Anwendung dieses Prinzips wurde in dieser Doktorarbeit eine Strategie erarbeitet, um spezifische, intrazellulär wirkende Inhibitoren für bestimmte PLP-abhängige Enzyme zu entwickeln.

Die PLP-abhängige Ornithindecarboxylase (ODC) ist ein Schlüssenenzym der Polyaminsynthese und wurde als erstes Zielobjekt ausgewählt. ODC ist in vielen Tumorzellen überexprimiert und deren Hemmung ist daher von grossem therapeutischem Interesse. Im ersten Teil der Doktorarbeit werden Design und Synthese eines solchen ODC-Inhibitors vorgestellt. Eine genaue Analyse der 3-D-Struktur von hODC offenbarte eine zusätzliche hydrophobe Tasche, welche die ε-Aminogruppe des Substrats Ornithins umhüllt. Molekülmodellierung mit einem BOC-geschützten Pyridoxyl-Ornithin-Konjugat (POB) in der aktiven Stelle der hODC deuteten auf eine starke Wechselwirkung des Enzyms mit der BOC-Gruppe hin. Das synthetisierte und gereinigte POB hemmte die Aktivität neu induzierter ODC in verschiedenen Tumorzellen. Das Ausmass der Hemmung der ODC-Aktivität korrelierte mit der zeitabhängigen Hemmung des Zellwachstums. Menschliche nicht-cancerogene glatte Muskelzellen der Aorta wurden nicht gehemmt. Die Proliferationshemmung von Tumorzellen durch POB war beträchtlich wirksamer als die von α-DL-Difluoromethylornithine (DFMO), des medizinisch am häufigsten verwendeten irreversiblen ODC-Inhibitors.

Um die hemmende Wirkung dieser Art von intrazellulärem ODC-Inhibitoren zu verbessern, wurden im zweiten Teil der Doktorarbeit die strukturellen Anforderungen für das Binden und Hemmen von hODC und für die Zellproliferation genauer untersucht. Strukturell unterschiedliche Enzym-Substrat-Analoge wurden entwickelt, synthetisiert und auf Hemmwirkung getestet. Von 23 untersuchten Konjugaten zeigten zwei, nämlich Phosphorpyridoxyl- und Pyridoxyl-Tryptophanmethylester (pPTME, PTME), eine signifikant grössere Zellproliferationshemmung als POB und insbesondere eine viel grössere als DFMO. Alle aktiven Verbindungen besitzen ein hydrophobes Seitenkettenfragment und ein

polyaminähnliches Motiv. Wie sich aus Untersuchungen mittels molekularem Modellieren vermuten liess, haben pPTME und PTME eine grössere Bindungsaffinität zu ODC als POB und hemmen die intrazelluläre ODC-Aktivität auch stärker. Zusätzlich induzieren diese drei Verbindungen, wie bereits von Polyaminanalogen bekannt, die Aktivitäten der Polyaminoxidase und der Spermin/Spermidin-*N*1-Acetyltransferase bis zu 250 % bzw. 780 %. Beide Enzyme sind im katabolen Polyaminstoffwechsel wirksam. Die duale Wirkung dieser Verbindungen, d.h. die Hemmung der ODC und die Induktion der katabolischen Enzyme, beeinflusst die intrazellulären Polyaminpools und könnte der Grund sein für den im Vergleich zu DFMO viel besseren Hemmeffekt auf die Zellproliferation.

Histamin, ein biogenes Amin mit wichtigen biologischen Funktionen, wird durch die Decarboxylierung von Histidin mittels Histidin-Decarboxylase (HDC), einem PLP-abhängigen Enzym, gebildet. HDC ist demzufolge ein wichtiges Zielenzym für Hemmstoffe, um die Histaminproduktion in bestimmten pathologischen Zuständen zu verringern. Die Entwicklung neuer Inhibitoren der hHDC und die Aufklärung von deren strukturellen Voraussetzungen ist eine grosse Herausforderung, da die 3D-Struktur der HDC von Säugetieren noch immer unbekannt ist. Im letzten Teil der Dissertation wurden potentiell membrandurchlässige Pyridoxylsubstratkonjugate entwickelt, synthetisiert und als Inhibitoren der hHDC getestet. Ferner wurde ein Modell der aktiven Stelle der hHDC entworfen, das mit den experimentellen Daten kompatibel ist. Von den 9 mit menschlichen Mastzellen getesteten strukturellen Varianten hemmte das Pyridoxyl-Histidin-Methylesterkonjugat (PHME) die HDC am stärksten, was darauf schliessen lässt, dass die Bindungsstelle von hHDC keine andere Gruppe als die Imidazol-Seitenkette von Histidin akzeptiert. PHME vermochte vor allem die induzierte neu synthetisierte HDC zu hemmen und zeigte auch Hemmwirkung in Zellextrakten. Das vorgeschlagene Modell des aktiven Zentrums der hHDC, welches Phosphopyridoxyl-Histidin enthält, erklärte die Bindungsspezifizität von HDC für ihr Substrat und erhellt die Struktur-Aktivitätsbeziehung der entwickelten und untersuchten Verbindungen.

Zusammenfassend zeigen die Ergebnisse, dass die Anwendung strukturell verschiedener Verbindungen zur Abklärung der Bindungsanforderungen der Zielproteine ein effizienter Weg zur Entwicklung neuer Inhibitoren von PLP-abhängiger Enzyme ist. ODC-Inhibitoren, wie sie hier vorgestellt wurden, können von Zellen aufgenommen werden und das Zellwachstum klinisch wichtiger bösartiger Tumorzelllinien, wie Gliomazellen, effizient hemmen.

SUMMARY

Pyridoxal 5'-phosphate (PLP)-dependent enzymes catalyze manifold transformations of amino acids such as transamination, α-decarboxylation, and racemization, as well as β- or γ-elimination and replacement reactions. Vitamin B_6-dependent enzymes play a central role in amine and amino acid metabolism and are interesting targets for drugs to intervene in specific processes that lead to pathological states. As transition-state-based inhibitors bind with high affinity to their target enzymes, a strategy was explored to develop inhibitors on the basis of mimics of a transition-state intermediate of PLP-dependent enzymic reactions.

The PLP-dependent ornithine decarboxylase (ODC) is the key enzyme in polyamine synthesis and was chosen as the first target. ODC is overexpressed in many tumor cells and thus a potential drug target. The thesis reports the design and synthesis of an analog of covalent coenzyme-substrate adducts as a novel precursor inhibitor of ODC. Structural analysis of the crystal structure of hODC disclosed a hydrophobic pocket adjacent to the ε-amino group of its substrate ornithine. Molecular modeling showed favorable interactions of a BOC-protected pyridoxyl-ornithine conjugate, termed POB, in the active site of hODC. The synthesized and purified POB at the concentration of 100 μM completely inhibited the activity of newly induced ODC in glioma LN229 and COS7 cells. In correlation with the inhibition of intracellular ODC activity, a time-dependent inhibition of cell growth was also observed in various tumor cell lines, but not in non-tumorigenic human aortic smooth muscle cells. POB was much more efficient in inhibiting proliferation of several types of tumor cells than α-DL-difluoromethylornithine (DFMO), the most widely used irreversible inhibitor of ODC.

In the second part of the thesis, the structural requirements for binding to and inhibiting hODC and for inhibition of cell proliferation were elucidated in more detail to improve the inhibitory effect of this kind of inhibitors of intracellular hODC. Structurally diverse enzyme-substrate mimics were designed, synthesized and tested for their inhibitory potential. Out of 23 conjugates, phosphopyridoxyl- and pyridoxyl-tryptophan methyl ester (pPTME, PTME) showed a significantly more potent cell proliferation inhibition of glioma cells than POB and particularly more than DFMO. All the active compounds possess a hydrophobic side chain and polyamine motif (-NH-$(CH_X)_4$-NH-). As predicted from the molecular modeling results, pPTME and PTME have an improved binding affinity for ODC in comparison to POB and strongly inhibited the intracellular ODC activity of glioma cells. Additionally, these three compounds induce, as polyamine analogs do, the activity of the enzymes of polyamine

catabolism, polyamine oxidase and spermine/spermidine *N*1-acetyltransferase, up to 250% and 780%, respectively. The dual mode of these compounds in cells, i.e. inhibition of ODC and induction of polyamine catabolic enzymes, influences the intracellular polyamine pools and might be the cause for their inhibitory effect on cell proliferation that compares favorably with that of DFMO.

Histamine, a biogenic amine with important biological functions, for example in gastric acid secretion and allergic reactions, is produced from histidine by histidine decarboxylase (HDC), a PLP-dependent enzyme. HDC is thus a potential target to attenuate histamine production in certain pathological states. Targeting mammalian HDC with novel inhibitors and elucidating the structural basis of their specificity for HDC are particularly challenging tasks, because the 3D structure of mammalian HDC is still unknown. In the last part of my dissertation, potentially membrane-permeable pyridoxyl-substrate conjugates were designed, synthesized and tested as inhibitors for human HDC and an active site of hHDC was modeled that is compatible with the experimental data. The most potent inhibitory compound among 9 tested structural variants was the pyridoxyl-histidine methyl ester conjugate (PHME), indicating that the binding site of hHDC does not tolerate other groups than the imidazole side chain of histidine. PHME inhibited induced HDC in human HMC-1 cells and proved also inhibitory in cell extracts. The proposed model of hHDC, containing phosphopyridoxyl-histidine in the active site, explains the binding specificity of HDC towards its substrate and the structure-activity relationship of the investigated compounds.

In conclusion, analogs of covalent coenzyme-substrate adducts and their structural variations provide promising lead compounds for the development of inhibitors for PLP-dependent enzymes such as ODC and HDC. ODC inhibitors of the kind presented in this thesis seem to be efficient agents for preventing proliferation of clinically interesting malignant tumor cell lines, such as gliomas.

1. General introduction

1.1 Pyridoxal 5'-phosphate dependent enzymes as therapeutic targets

Pyridoxal 5'-phosphate (PLP)-dependent enzymes widely exist in both prokaryotes (1.5% of all genes) and eukaryotes, and have important biological functions (Amadasi *et al*, 2007). PLP-dependent enzymes are involved in many cellular processes, including the biosynthesis of amino acids, amino acid-derived metabolites and amino sugars (Eliot & Kirsch, 2004). They catalyze various types of reactions, featured by the heterolytic cleavage of sigma bonds at the substrate Cα atom (Fig. 1). These enzymes can be classified according to the reactions proceeding through: i) α -decarboxylation (Fig. 1, (b)); ii) proton elimination, e.g. racemization and transamination (Fig. 1(a)); and iii) elimination of the side chain of amino acids, e.g. aldolic cleavage (Fig. 1(c)) as well as ß, γ elimination and substitution. The external aldimine (Fig. 1), a Schiff base of PLP with the α-amino group of the amino acid substrate, is the common intermediate in all transformation of amino acid catalyzed by PLP-dependent enzymes (Christen & Mehta, 2001). All PLP-dependent enzymes have a Lys residue in the active site which forms the internal Schiff base with the cofactor PLP, and specific protein motifs to tightly bind the cofactor.

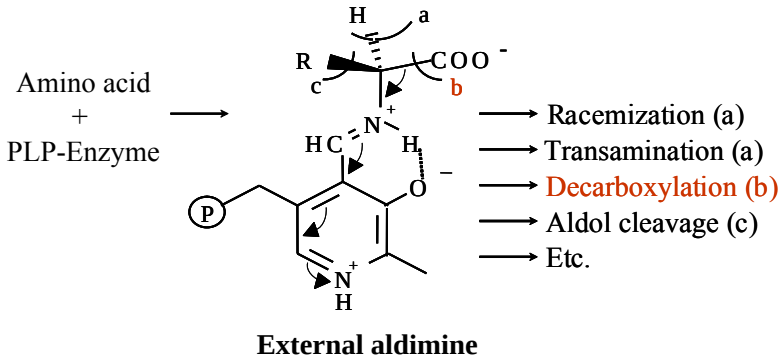

Fig. 1 Reactions catalyzed by PLP-dependent enzymes.

The common mechanistic features of PLP-dependent enzymes are not historical traits passed on from a common ancestor enzyme but rather reflect evolutionary or chemical necessities (Mehta & Christen, 2000). According to the amino acid sequences, supported by comparisons of the available three-dimensional crystal structures, vitamin B6-dependent enzymes can be classified into four independent evolutionary lineages of homologous proteins, i.e. the α family with aspartate aminotransferase as the prototype enzyme, the ß family with tryptophan synthase b as the prototype enzyme, the D-alanine aminotransferase family and the alanine racemase family (Mehta & Christen, 2000).

PLP-dependent enzymes are key enzymes in many metabolic pathways, such as ornithine decarboxylase in polyamine metabolism; glutamate decarboxylase, aromatic amino acid or dopa decarboxylase and histidine decarboxylase in the biosynthesis of neurotransmitters and biogenic amines such as dopamine, serotonin and histamine; GABA transaminase in the degradation of γ-aminobutyric acid (http://www.biocarta.com and (Duffy et al, 2004)); and serine palmitoyltransferase in sphingolipid metabolism (Hanada, 2003). These enzymes are targets for treatment of diseases, such as sleeping sickness, cancer, epilepsy and Parkinson's disease (Duffy *et al*, 2004; Rabasseda, 1999). Several inhibitors, that target these enzymes are already on the market as clinical drugs. Gamma-Vinyl-GABA (Vigabatrin) an inhibitor of GABA aminotransferase is used as epileptic drug; carbidopa, an inhibitor of dopa decarboxylase in Parkinson's disease; α-DL-difluoromethylornitine (DFMO), an irreversible inhibitor of ornithine decarboxylase (ODC) against sleeping sickness, and D-cycloserine, an inhibitor of alanine racemase to treat tuberculosis (Casero & Marton, 2007)). All of them are substrate analogs (Fig. 2).

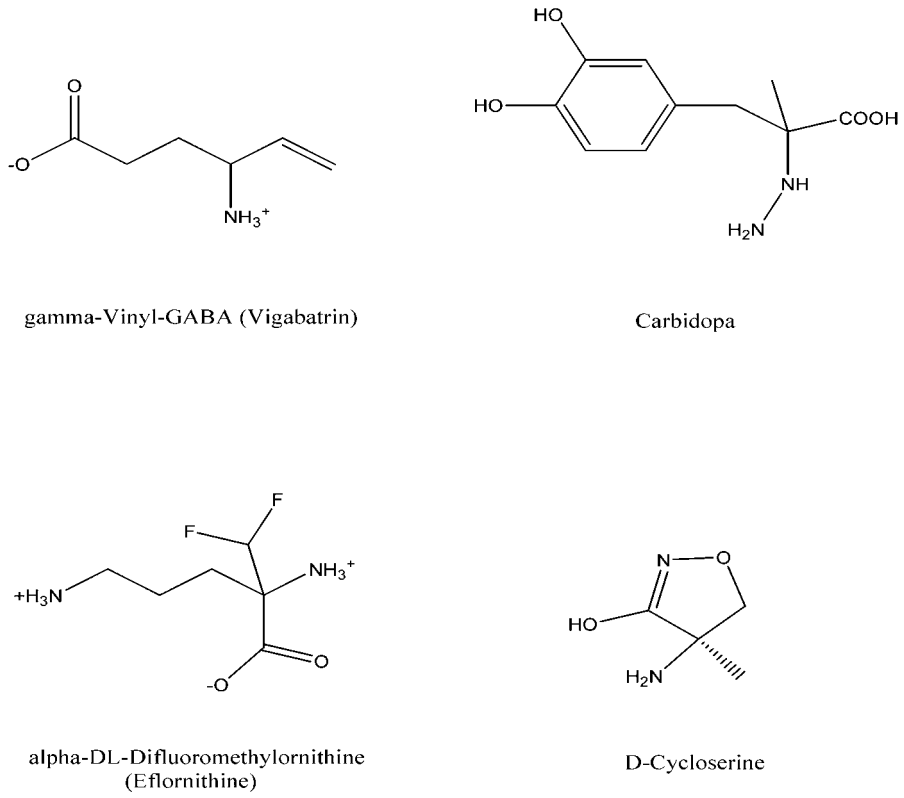

Fig. 2 Chemical structures of commercial drugs targeting PLP-dependent enzymes.

1.2 Polyamine pathway

1.2.1 Polyamines

Polyamines, namely spermine (SPM), spermidine (SPD) and putrescine (PUT), are multi-charged biogenic amines. They are essential for eukaryotic and in most cases also for prokaryotic cell growth and differentiation (Casero & Marton, 2007). Polyamines were originally thought to be DNA-binding agents, allowing DNA condensation and controlling DNA conformations (Childs et al, 2003; Seiler, 2003).

Polyamines are required for the proliferation of both normal and neoplastic cell (Li *et al*, 2007). The metabolism of polyamines (Fig. 3) comprises polyamine biosynthesis catalyzed by ornithine decarboxylase and spermine/spermidine synthase, polyamine

catabolism catalyzed by spermine/spermidine N^1-acetyltransferase (SSAT) and polyamine oxidase (PAO) as well as polyamine uptake and secretion by a polyamine transport system (PT) (Casero & Marton, 2007). All these enzymes and PT (red, Fig3.) are regarded as potential anti-cancer targets.

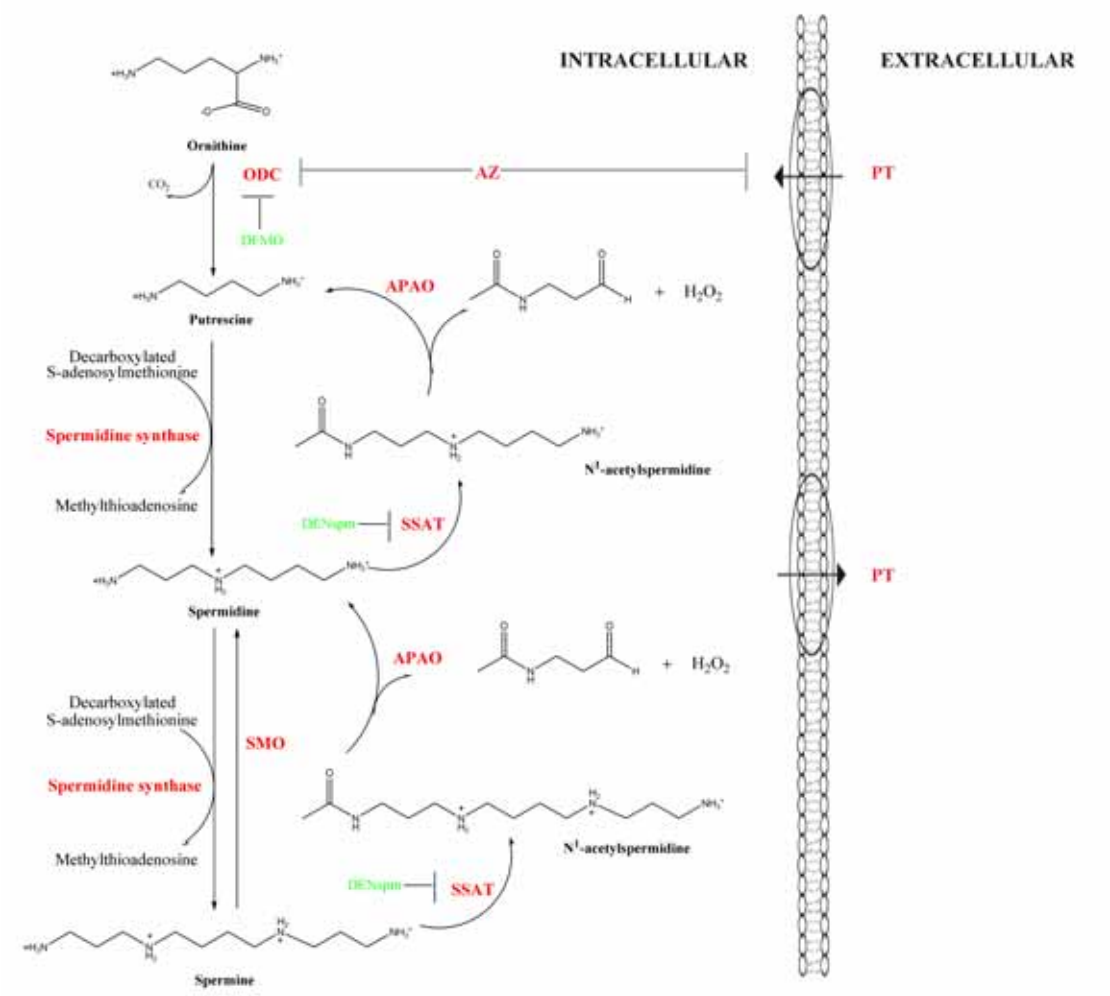

Fig. 3 The metabolic pathway of polyamines in cells. Red, enzymes; Green, inhibitors.

1.2.2 Human ornithine decarboxylase

Human ornithine decarboxylase (ODC), a PLP-dependent enzyme, catalyzes the first and rate–limiting step in polyamine biosynthesis by converting ornithine to putrescine (Fig. 3). ODC is a highly inducible and short-lived enzyme with a half life of 20 ~ 60 min (Seiler, 2003). Transcription, translation and degradation of ODC are highly

regulated by different mechanisms in cells (Origanti & Shantz, 2007; Pegg, 2006). *Odc* is the first target of the oncogene c-*myc* and the increased activity of the Myc/Max transcription complex increases the expression of ODC mRNA (Wagner *et al*, 1993). Many other regulatory factors have also been shown to stimulate the synthesis of ODC mRNA due to a promoter region in the *Odc* gene that contains multiple sequences such as a cAMP response element, CAAT and LSF motifs, AP-1 and AP-2 sites, GC-rich Sp1 binding sites and a TATA box, allowing responses to hormones, growth factors, and tumor promoters (Bercovich & Kahana, 2004; Zhao & Butler, 2001). Numerous studies have indicated that translation of ODC mRNA is reduced by excessive polyamines (Pegg, 2006). However, the mechanism underlying this effect is not clear. Antizyme, a protein inhibitor of mammalian ODC, is a negative regulator of intracellular polyamine levels. The expression of antizyme can be induced by polyamines through a ribosomes shift (+1) mechanism (Childs *et al*, 2003). The antizyme guides ODC into 26S proteasomes for degradation without the involvement of ubiquitin (Murakami *et al*, 1992).

ODC is considered as a potential anti-cancer target (Casero *et al*, 2005; Seiler, 2003). ODC is frequently upregulated in proliferating cells and has been implicated as an oncogene in multiple types of tumors. The amount of ODC is closely related to tumor promotion, and inhibition of ODC is associated with suppression of tumor development in animals (Lan *et al*, 2000; Love *et al*, 1993). Overexpression of ODC can also induce transformation of cells (Kubota *et al*, 1997) and ODC-overexpressing cells are tumorigenic in mice (Peralta Soler *et al*, 1998). Even moderate reductions of intracellular ODC activity can lead to a resistance in tumor development (Pegg, 2006). Overexpression of ODC in hair follicle cells of mice can also lead to hair loss (Soler *et al*, 1996; Wheeler *et al*, 2003). The effect seems to be attributable to an interference of putrescine with hair development (Pietila *et al*, 1997).

Several crystal structures of eukaryotic ODC were reported that include ODC from human and *Trypanosoma brucei* and showed that the active site is composed by both subunits of the homodimeric ODC (Almrud *et al*, 2000; Dufe *et al*, 2007; Grishin *et al*, 1999; Jackson *et al*, 2004; Jackson *et al*, 2000; Jackson *et al*, 2003). Mutations of

residues of the dimer interface of ODC significantly decrease the catalytic efficiency of ODC (Myers *et al*, 2001). These ODCs (~ 53 kD) belongs to the alanine racemase family (Mehta & Christen, 2000). The crystal structure of human ODC (PDB code: 1D7K, (Almrud *et al*, 2000)) has been determined to 2.1 Å resolution with PLP in the active site, however it contains no ligands (Fig. 4). The 3D structures of *Trypanosoma brucei* ODC have been solved together with the product putrescine or DFMO (an irreversible inhibitor of ODC). In these structures, the ε-amino group of putrescine or DFMO is bound between two aspartic acid residues (Asp332 and Asp361) and in comparison to the unliganded enzyme the catalytic residue Cys360 is also rotated towards the active site (Grishin *et al*, 1999). The aldehyde group of PLP forms an internal Schiff base with Lys69 in hODC or tODC. The pyridine ring of the PLP interacts with the side chain of His197 and the *N*1 of PLP forms a hydrogen bond with the side chain oxygens of Glu274. The phosphate group binds into the pocket formed by Ala67, Pro275, Gly276, Arg277 and Tyr389 (Red circle, Fig. 4).

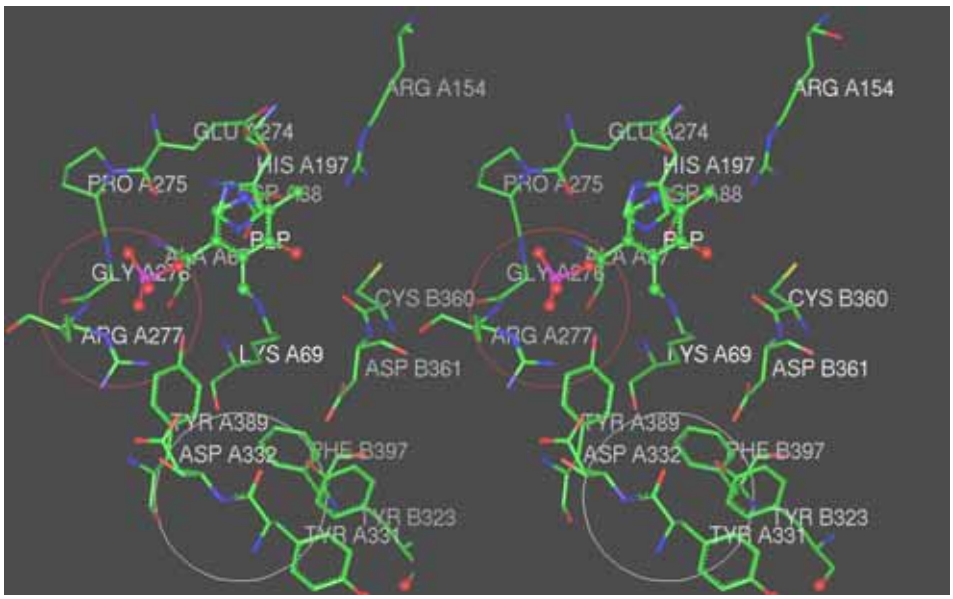

Fig. 4 The crystal structure of the active site of human ornithine decarboxylase (PDB code: 1D7K; (Almrud et al, 2000)). PLP is displayed in ball-stick mode and residues in stick mode. Red circle, the phosphate binding region; White circle, the putative binding region of the ε-amino group of ornithine.

1.2.3 Spermine/spermidine N^1-acetyltransferase and acetyl polyamine oxidase

Spermine/spermidine N^1-acetyltransferase (SSAT) and acetyl polyamine oxidase (APAO) are highly inducible enzymes in polyamine catabolic pathway and are in charge of the conversion of the more charged SPM or SPD into the less charged SPD or PUT, respectively (Fig. 3, (Casero & Pegg, 1993; Pavlov *et al*, 2002; Vujcic *et al*, 2003)). SSAT catalyzes the formation of N^1-acetylspermine or N^1-acetylspermidine by transfering an acetyl group from acetyl-coenzyme A to the N^1 position of either SPM or SPD (Casero & Marton, 2007). APAO oxidizes N^1-acetylated polyamines and produces H_2O_2, 3-acetoamidopropanal, and either spermidine or putrescine, depending on the starting substrate in the presence of molecular oxygen (Fig. 3, (Wang & Casero, 2006)). Recently, Vujcic *et al* discovered a novel oxidase, spermine oxidase (SMO), which directly oxidizes SPM to SPD, 3-aminopropanl and H_2O_2, independent of SSAT (Vujcic *et al*, 2003).

The 3D structure of SSAT (~ 20 kD), the potential drug target, is already known together with its inhibitor N^1, N^{11}- di(ethyl)- norspermine (DENspm, Fig. 3; (Bewley *et al*, 2006)) or with N^1-spermine-acetyl-coenzyme A, the bisubstrate analog (Hegde *et al*, 2007). The SSAT-catalyzed reaction was confirmed to be the rate-limiting step in the two-step catabolic conversion from spermine to spermidine and from spermidine to putrescine (Wang & Casero, 2006). The SSAT with a half life of 15 min is normally present in very small amounts in the cell and is induced by a number of factors including various toxic agents, hormones as well as growth factors, the polyamines themselves and polyamine analogs (Casero & Pegg, 1993). Induction of SSAT decreases cell growth and increased apoptosis (Babbar *et al*, 2006). In animal studies, this response to polyamine analogs has been demonstrated to be a tumor cell–specific response (Gabrielson *et al*, 2004). Oxidases, APAO and SMO, are regarded to be responsible for producing reactive oxygen species that contribute to the bioactivity of these polyamine analogs (Casero & Marton, 2007). The H_2O_2 generated in these processes is considered as the main cause for cell death. SMO, like SSAT, is significantly induced by polyamine analogs in a dose- and time-dependant manner (Devereux *et al*, 2003). APAO is a generally constitutively expressed, FAD-dependent

oxidase. Although APAO activity was not altered significantly under pathophysiological conditions, it is also induced by polyamines or polyamine analogs in a manner that parallels the induction of SSAT and SMO (Casero & Pegg, 1993; Pavlov *et al*, 2002; Vujcic *et al*, 2003). This suggests the existence of a common regulatory mechanism for all three genes (SSAT, APAO and SMO) (Vujcic *et al*, 2003).

1.2.4 Antizyme

The protein antizyme (AZ) is known to be a regulator of polyamine metabolism that inhibits the activity of ODC and polyamine transport, thus restricting cellular polyamine levels (Fig. 3, (Coffino, 2001; Pegg, 2006)). The inhibition of ODC by AZ functions via the formation of a tight heterodimic complex between AZ and the ODC monomer, which prevents enzymic activity and leads to the ubiquitine-independent degradation of ODC (Murakami *et al*, 1992). The half-life of the ODC-AZ complex is less than 5 min (Ivanov *et al*, 2000). The AZ-mediated degradation of ODC has been found to be conserved from yeast to human (Palanimurugan et al, 2004). Multiple forms of antizyme are expressed in many eukaryotes. AZ-1 (~ 25 kD) and AZ-2 (~ 21 kD) exist ubiquitously in cells, and AZ-3 (~ 21 kD) only in germ cells of testis (Ivanov *et al*, 2000). The NMR structure of a fragment of the AZ protein (residues 87–227) has been determined and shows a fold similar to some acetyltransferases including SSAT (Hoffman et al, 2005), another regulatory protein of the polyamine metabolism. The sequence of AZ-1 contains a group of conserved acidic amino acids (Glu161, Glu164, and Glu165) on an external face that may interact with the binding element in ODC, which includes an electropositive surface formed by the residues 117–140 (Coffino, 2001). The production of AZ depends on the polyamine levels through an unusual regulatory mechanism, namely a +1 frameshifting, which is obligatory for functional AZ production in mammalians (Coffino, 2001). AZ was also found to interact with both cyclin D1 and cyclin D1-associated cyclin-dependent kinase cdk4. Cyclin D1, like ODC, is degraded by proteasomes in an ubiquitin-independent manner (Coffino, 2001; Matsufuji *et al*, 1995). Overexpression

of AZ can also induce apoptosis of cells triggered by mitochondrial membrane depolarization and caspases (Liu et al, 2006).

1.2.5 Polyamine transporter

Besides biosynthesis and catabolism, cells are also able to take up polyamines from the extracellular environment by an efficient and ATP-dependent polyamine transporting system, which is still not well-characterized (Fig. 3, (Igarashi & Kashiwagi, 1999; Seiler, 2003)). Moreover, PT can efficiently transport SPD and SPM conjugates into cells. Recently, the intracellular concentration of an iron chelator conjugate was strongly increased in cells with a factor of 1900 by conjugating with spermine. The bioactivity of the conjugate was improved more than 230-fold in comparison to the iron chelator alone (Bergeron et al, 2005; Bergeron *et al*, 2003).

1.2.6 Other functions of polyamines

Recently, polyamines were found to interfere also with different processes or molecules in cells, such as inflammation, acetylation and membrane receptors. Spermine was identified to have anti-inflammatory properties, and depletion of polyamines by DFMO could abolish neurodegeneration and increase the survival rate of mice, which were exposed to severe innate immune reactions in the CNS (Soulet & Rivest, 2003; Zhang et al, 2000). Endogenous polyamines can regulate the expression of nitric oxide synthase (Baydoun & Morgan, 1998) which is an inducible enzyme involved in the early phase response to inflammatory insults and produces high-output of NO (Satriano, 2004).

Intracellular polyamines can also alter the expression and activity of both histone acetyltransferases (HAT) and histone deacetylases (HDAC). These two enzymes determine steady-state levels of histone acetylation (Hobbs & Gilmour, 2000) in proliferating cells (Wei *et al*, 2007). HDAC is an emerging anti-cancer target and the inhibition of HDAC can lead to a cell-cycle arrest, apoptosis and, in some cases,

differentiation (Carey & La Thangue, 2006; McLaughlin & La Thangue, 2004). Many pharmaceutical companies are developing HDAC inhibitors and several have passed the earlier clinical trials and exhibited generally a favourable toxicity profile (Carey & La Thangue, 2006; Inche & La Thangue, 2006). The intracellular ODC activity was also reported to closely correlate with the sensitivity of cells to HDAC inhibitor–induced apoptosis (Saunders & Verdin, 2006). Polyamines are also known to bind membrane or intracellular receptors. Polyamines have been suggested to interact with several ion channels and receptors involved in the regulation of calcium, sodium, and potassium homeostasis (Li *et al*, 2007). Spermine was also found to facilitate binding of the estrogen-ER_α complex to estrogen-responsive elements (ERE) (Thomas *et al*, 1999) and polyamine analogs were also reported to down-regulate ER_α expression in human breast cancer cells (Huang *et al*, 2006).

1.3 Inhibitors of polyamine metabolism

1.3.1 DFMO, an irreversible inhibitor of ODC

Numerous inhibitors of hODC are known and some of them are in clinical studies as anti-cancer agents. The best-known is DFMO, an irreversible inhibitor of hODC. DFMO (Fig. 2) is a suicide inhibitor of ODC and binds irreversibly to Cys360 of the holo enzyme after being activated by ODC. It was initially developed as an anti-cancer agent in the eighties with the aim of targeting human ODC. Later on, it turned out to be a potent therapeutic agent against sleeping sickness as it targets ODC of *Trypanosoma brucei* even better. Nowadays, DFMO is still used as a first-line drug to cure sleeping sickness (Heby *et al*, 2007) and as a remedy against facial hair growth in women (Shapiro & Lui, 2005).

Clinical studies proved that DFMO is a well-tolerated agent but not as efficient, as initially thought, to treat cancers. This seems to be due to its low affinity (Ki ~ 40

μM), fast clearance, inefficient uptake into cells, and development of cell resistance that is due to up-regulation of ODC expression and polyamine transport (Casero *et al*, 2005; Marton & Pegg, 1995; Seiler, 2003). Never the less, some positive results with DFMO have been achieved in the treatment of recurrent anaplastic gliomas (Wallace & Fraser, 2004). Clinical phase II and III studies of DFMO as an anti-cancer or chemopreventive agent are still on going be it as a single agent or in combination with other drugs (Messing *et al*, 2006; Raul *et al*, 2007; Vlastos *et al*, 2005).

A lot of attempts have been made to modify the ornithine skeleton of DFMO to improve the efficiency of DFMO (Seiler, 2003). Although the modified compounds had improved binding affinity for ODC *in vitro*, they were not more effective inhibiting cell proliferation *in vitro* and *in vivo* (Seiler, 2003). Thus, inhibitors of hODC with better efficiency in suppressing the proliferation of tumor cells are in high demand.

1.3.2 Polyamine analogs or mimics

Polyamine analogs are derivatives of natural polyamines and sufficiently similar in structure to the parent compound to allow their recognition and subsequent uptake by the polyamine transporter. However, they cannot be converted further in cells by polyamine catabolic enzymes due to missing free amino groups (Wallace *et al*, 2003). These analogs cause a multi-target inhibitory effect. They not only compete with the natural polyamines for uptake by the polyamine transporter but also induce the activities of AZ, SSAT and PAO and decrease ODC activity. The development of polyamine analogs or mimics has been started more than 20 years ago (Seiler, 2005). The original idea was to develop mimics of natural polyamines to modulate directly polyamines biosynthesis (Berger & Porter, 1986). Further studies revealed that one class, the bis(ethyl)polyamine analogs, drastically induce the SSAT activity more than 1700-fold (Casero *et al*, 1989), and inhibit cell proliferation significantly. This finding prompted the cloning of SSAT (Casero & Marton, 2007). DENspm is one of the most effective inducers (Fig. 5) and also known as BENspm or BE333. Now, it is in clinical

studies, but showed some unacceptable toxicity similar to that of the polyamine SPM in the high-dose range (Casero & Marton, 2007; Seiler, 2003).

Fig. 5 The chemical structure of DENspm.

1.4 Human histidine decarboxylase

L-Histidine decarboxylase (HDC), a dimeric PLP-dependent enzyme, is the rate-limiting enzyme for histamine synthesis in mammals (Medina *et al*, 2003). The biogenic amine histamine plays physiologically and pathologically important roles in inflammation, gastric acid secretion, neurotransmission, and immune modulation, particularly in allergic reactions by acting on its specific membrane receptors, H_1, H_2, H_3, and H_4 (Furuta *et al*, 2007). The formation and release of histamine have been implicated in gastric mucosal damage caused by drugs like aspirin (Parmar *et al*, 1984). Therefore, HDC can be regarded as a potential target to attenuate histamine production in certain pathological states (Medina *et al*, 2003; Moya-Garcia *et al*, 2005).

A 3D model has been constructed using the crystal structure of pig dopa decarboxylase as the template (Fig. 6A), as described in more details in **4.2**. Different types of inhibitors of histidine decarboxylase have been discovered already 20 years ago, i.e. histidine methyl ester, α-fluoromethylhistidine and His-Phe or more recently, i.e. epigallocatechin gallate (EGCG) (Fig. 6B).

A

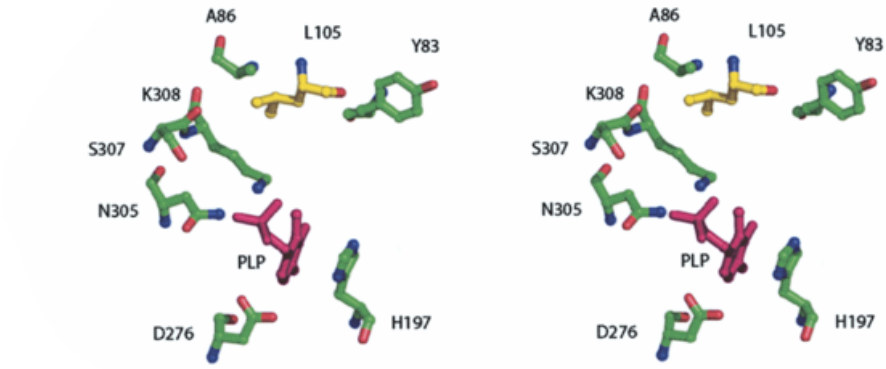

B

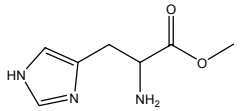

Histidine methyl ester

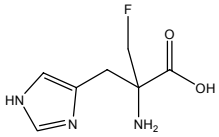

a-Fluoromethylhistidine

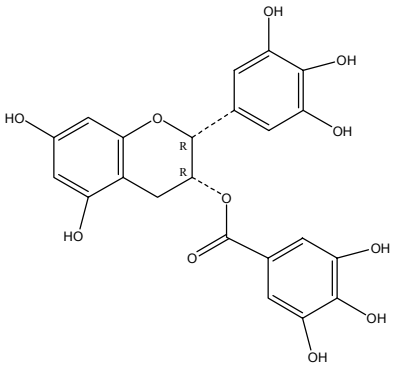

Epigallocatechin-3-gallate (EGCG)

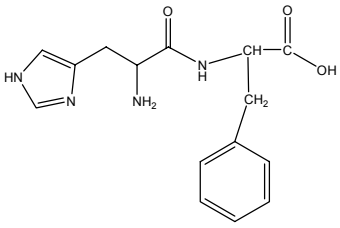

His-Phe

Fig. 6 Structures of rat histidine decarboxylase and inhibitors. A) Stereo view of the predicted active site of rat HDC with the cofactor PLP (pink) (Fleming *et al*, 2004). B) Known inhibitors of mammalian HDC.

1.5 Inhibitor design

1.5.1 Transition state-based ligand design

Transition-state-based inhibitors bind with high affinity to their target enzyme. Designing of transition-state inhibitors is used frequently in drug discovery (Robertson, 2005). Recently, a class of transition state-based inhibitor (intermediate mimics) of purine nucleoside phosphorylase showed excellent binding affinity (Taylor Ringia & Schramm, 2005). The designed immucillinH, an inhibitor of human purine nucleoside phosphorylase, with a K_d of 56 pM, is in clinical phase IIa to treat T cell leukemia (www.biocryst.com) (Basu *et al*, 2007; Singh *et al*, 2005).

Designing inhibitors by mimicking well-defined reaction intermediates is a powerful strategy in developing potent and specific inhibitors for PLP-dependent enzymes. In all PLP-dependent enzymes, the external aldimine, a Schiff base of PLP with the α-amino group of the amino acid substrate, is a common intermediate. Reduction of the Schiff base produces phosphopyridoxyl-amino acid conjugates, analogs of the covalent intermediates (Fig. 1 and 7). These compounds are a kind of transition state analogs that bind to the apoprotein with high affinity (Heller JS, 1975; Khomutov *et al*, 1971; Raso & Stollar, 1975). They cannot be transformed by the enzymes and thus inhibit them very potently. A future advantage of these analogs is that they bind with high specificity to the respective apoenzymes. Binding studies with phosphopyridoxyl-amino acids showed that phosphopyridoxyl-L-aspartate and phosphopyridoxyl-L-glutamate, in contrast to phosphopyridoxyl-L-tyrosine and phosphopyridoxyl-L-alanine, bind so tightly to aspartate aminotransferase that they could not be competed away by PLP, which has a high affinity for this enzyme. Phosphopyridoxyl-ornithine was found to be an inhibitor of ornithine decarboxylase (ODC) but did not affect S-adenosylmethionine decarboxylase (Heller JS, 1975). The drawback of these compounds in their *in vivo* application is the impermeability to the cell membranes for these substances due to their negative charges. On incubation of fibroblasts with phosphopyridoxyl-L-aspartate or L-glutamate, neither uptake nor any

effect on the cells could be demonstrated (H. Gehring personal communication) which is in agreement with results reported for phosphopyridoxyl-L-ornithine (Coward & Pegg, 1987). Thus, if one succeeds to expose newly synthesized cellular ODC to phosphopyridoxyl-ornithine, ODC activity can be expected to be completely and specifically inhibited (no mammalian α-transaminase for ornithine is known) and consequently stop the cell proliferation. Human ODC, the potential anti-cancer target, decarboxylates the substrate through a well defined process (Jackson *et al*, 2000). CO_2 release, accompanied by formation of the quinonoid intermediate, is an irreversible step and has been identified as the likely rate-determining step in the enzymic reaction (Fig. 7). Therefore, designing cell-permeable analogs that mimicking the external aldimine intermediate could be a strategy to develop novel inhibitors for hODC.

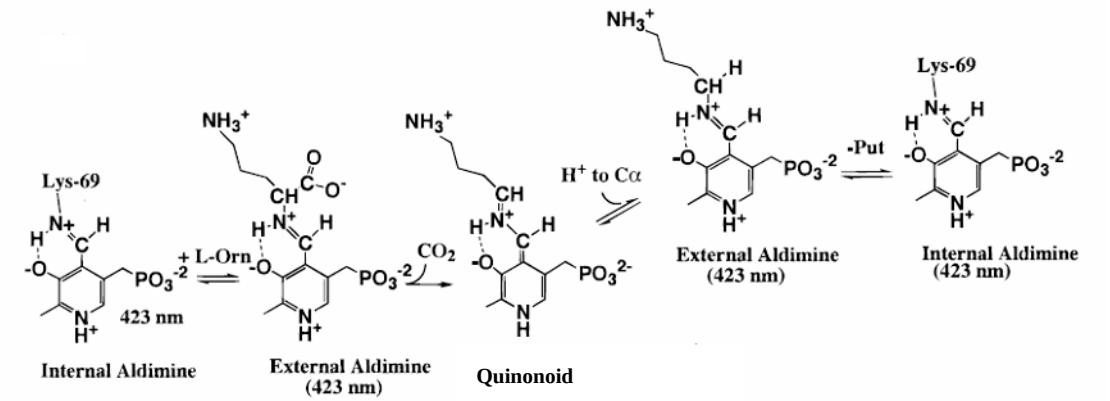

Fig. 7 Reaction mechanism for ODC. Obtained from K. Laurie (Jackson *et al*, 2000).

1.5.2 Structure-based ligand design

Structure-based drug design becomes more and more important in developing inhibitors due to the increased numbers of 3D structures of proteins, the high computational efficiency in molecular modeling and calculation and the accessibility of user-friendly software. Up to now, there are several drugs on the market that originated from structure-based approaches (Singh *et al*, 2006). Agenerase and Viracept, e.g., were developed using the crystal structure of HIV protease (Lapatto *et*

al, 1989) and the flu drug Relenza was also designed based on the crystal structure of neuraminidase (Wade, 1997). Dozens of compounds (>40) have been discovered with the aid of structure-guided methods and have entered clinical trials. Identifying novel hydrophobic sites in the active site of enzymes and designing additional molecular fragments that will occupy them can improve the binding affinity and is a common strategy to develop improved inhibitors based on the structure of known inhibitors (Knight *et al*, 2006; Singh *et al*, 2005). PIK-294, a newly reported inhibitor of phosphoinositide 3-kinases (PIK3), which has an additional m-phenol group compared to the parent compound PIK-293 projects into a deeper binding pocket that is not accessed by the co-substrate ATP and by PIK-293. It potency was increased 10-60 folds towards the different isoforms of phosphoinositide 3-kinases (Knight *et al*, 2006).

Structure-based drug design can be classified into two applicable strategies, namely high-throughput database screening and fragment-based ligand *de novo* design. High-throughput database screening requires high computational efficiency, as usually a known chemical database containing hundreds of thousands of compounds have to be screened against the whole binding site of targeted proteins. Fragment-based *de novo* drug design usually identifies fragments of a few atoms to fit in specific pockets of the binding site. Fragment-based *de novo* drug design can also generate new chemical entities with desired properties in a cost- and time-efficient manner (Singh *et al*, 2006). LUDI, a structure-based *de novo* drug design software, was developed in the early nineties, based on an empirical scoring function (Bohm, 1994). It can efficiently identify small molecular fragments (5-30 atoms) from a fragment library (~1000) to fit into the binding pocket of proteins *de novo* and/or append new substitutions to an already existing anchor ligands under consideration of steric constraints (Bohm, 1992). Successful applications of LUDI have been reported in many cases, such as the design of improved inhibitors for HIV protease and dihydrofolate reductase. Using LUDI to place fragments in the binding pocket also helps mapping binding constraints in the binding sites (Singh *et al*, 2006).

1.5.3 Design of improved and cell-permeable ligands for hODC and hHDC

Studying the interaction between analogs of reaction intermediates as discussed above and the active site of enzymes and exploring the 3D geometry of the binding site by using structurally diverse mimics is a reasonable strategy for discovering improved inhibitors.

To find more potent cell-permeable inhibitors for intracellular hODC or hHDC, different molecular mimics of reaction intermediates were designed and synthesized by conjugating pyridoxal or pyridoxal 5'-phosphate with substrate derivatives. These conjugates with a methyl ester-protected carboxylate group may be expected to be cell-permeable precursors of potentially intracellular active inhibitors because they have no negative net charge and very likely cross the cell membrane as it was reported for several pyridoxyl-amines (Zhang & McCormick, 1992; Zhang & McCormick, 1991) and a pyridoxyl-methionine analog (Ogier *et al*, 1993). Intracellular pyridoxal kinase, an enzyme that seems to tolerate considerable variation in C4' position of the pyridoxyl moiety (Tang *et al*, 2005; Zhang & McCormick, 1991), is expected to phosphorylate these compounds (Zhang *et al*, 1993) after they have been taken up by the cells; whereas the carboxymethyl ester will be hydrolyzed intracellularly (Kelley *et al*, 1977). The active form of the conjugates formed in the cells will bind with very high affinity to the newly synthesized apoenzymes, thus affecting only proliferating cells, in which hODC or hHDC is obligatorily induced.

1.6 Aims of the thesis

PLP-dependent enzymes catalyze manifold transformations of amino acids such as transamination, α-decarboxylation, and racemization, as well as β- or γ-elimination and replacement reactions. As vitamin B_6-dependent enzymes play a central role in amine and amino acid metabolism, they are interesting targets for drugs to intervene in specific processes that lead to pathological states. Human ornithine decarboxylase (ODC) and histidine decarboxylase (HDC) are pyridoxal 5'-phosphate (PLP)-dependent enzymes. They are responsible for synthesis of biogenic polyamine or histamine in cells and regarded as anti-cancer or anti-histamine targets, respectively. Cell-permeable inhibitors of these enzymes are in demand as (see **1.3.1** and **1.5.1**) to antagonize the production of polyamines and histamines in certain pathologic conditions. Phosphopyridoxyl-amino acid adducts, a kind of transition state analogs of vitamin B_6-dependent enzymes, bind with very high affinity and specificity to their respective enzymes. The drawback of these compounds in their *in vivo* application is, however, the impermeability of the cell membranes due to their negative charges. Thus, derivatives of phosphopyridoxyl-amino acid adducts that are expected to be taken up by cells should be developed and tested for their inhibitory capability for a particularly intracellular vitamin B_6-dependent enzyme and/or for cell proliferation in the case of ODC. From this investigations, information on the structural features of covalent pyridoxyl-amino acid derivates that facilitate their uptake by cells were expected as well as whether such compounds could be potentially useful anti-neoplastic drugs.

1.8 References

Almrud JJ, Oliveira MA, Kern AD, Grishin NV, Phillips MA, Hackert ML (2000) Crystal structure of human ornithine decarboxylase at 2.1 A resolution: structural insights to antizyme binding. J Mol Biol 295: 7-16

Amadasi A, Bertoldi M, Contestabile R, Bettati S, Cellini B, di Salvo ML, Borri-Voltattorni C, Bossa F, Mozzarelli A (2007) Pyridoxal 5'-phosphate enzymes as targets for therapeutic agents. Current medicinal chemistry 14: 1291-1324

Babbar N, Hacker A, Huang Y, Casero RA, Jr. (2006) Tumor necrosis factor alpha induces spermidine/spermine N1-acetyltransferase through nuclear factor kappaB in non-small cell lung cancer cells. J Biol Chem 281: 24182-24192

Basu I, Cordovano G, Das I, Belbin TJ, Guha C, Schramm VL (2007) A transition state analog of 5'-methylthioadenosine phosphorylase induces apoptosis in head and neck cancers. J Biol Chem 282: 21477-21486

Baydoun AR, Morgan DM (1998) Inhibition of ornithine decarboxylase potentiates nitric oxide production in LPS-activated J774 cells. British journal of pharmacology 125: 1511-1516

Bercovich Z, Kahana C (2004) Degradation of antizyme inhibitor, an ornithine decarboxylase homologous protein, is ubiquitin-dependent and is inhibited by antizyme. J Biol Chem 279: 54097-54102

Berger FG, Porter CW (1986) Putrescine does not mediate the androgen-response in mouse kidney. Biochem Biophys Res Commun 138: 771-777

Bergeron RJ, Bharti N, Wiegand J, McManis JS, Yao H, Prokai L (2005) Polyamine-vectored iron chelators: the role of charge. J Med Chem 48: 4120-4137

Bergeron RJ, McManis JS, Franklin AM, Yao H, Weimar WR (2003) Polyamine-iron chelator conjugate. J Med Chem 46: 5478-5483

Bewley MC, Graziano V, Jiang J, Matz E, Studier FW, Pegg AE, Coleman CS, Flanagan JM (2006) Structures of wild-type and mutant human spermidine/spermine N1-acetyltransferase, a potential therapeutic drug target. Proc Natl Acad Sci U S A 103: 2063-2068

Bohm HJ (1992) LUDI: rule-based automatic design of new substituents for enzyme inhibitor leads. Journal of computer-aided molecular design 6: 593-606

Bohm HJ (1994) The development of a simple empirical scoring function to estimate the binding

constant for a protein-ligand complex of known three-dimensional structure. Journal of computer-aided molecular design 8: 243-256

Carey N, La Thangue NB (2006) Histone deacetylase inhibitors: gathering pace. Current opinion in pharmacology 6: 369-375

Casero RA, Jr., Celano P, Ervin SJ, Porter CW, Bergeron RJ, Libby PR (1989) Differential induction of spermidine/spermine N1-acetyltransferase in human lung cancer cells by the bis(ethyl)polyamine analogs. Cancer Res 49: 3829-3833

Casero RA, Jr., Frydman B, Stewart TM, Woster PM (2005) Significance of targeting polyamine metabolism as an antineoplastic strategy: unique targets for polyamine analogs. Proceedings of the Western Pharmacology Society 48: 24-30

Casero RA, Jr., Marton LJ (2007) Targeting polyamine metabolism and function in cancer and other hyperproliferative diseases. Nature reviews 6: 373-390

Casero RA, Jr., Pegg AE (1993) Spermidine/spermine N1-acetyltransferase--the turning point in polyamine metabolism. Faseb J 7: 653-661

Childs AC, Mehta DJ, Gerner EW (2003) Polyamine-dependent gene expression. Cell Mol Life Sci 60: 1394-1406

Christen P, Mehta PK (2001) From cofactor to enzymes. The molecular evolution of pyridoxal-5'-phosphate-dependent enzymes. Chem Rec 1: 436-447

Coffino P (2001) Regulation of cellular polyamines by antizyme. Nat Rev Mol Cell Biol 2: 188-194

Coward JK, Pegg AE (1987) Specific multisubstrate adduct inhibitors of aminopropyltransferases and their effect on polyamine biosynthesis in cultured cells. Advances in enzyme regulation 26: 107-113

Devereux W, Wang Y, Stewart TM, Hacker A, Smith R, Frydman B, Valasinas AL, Reddy VK, Marton LJ, Ward TD, Woster PM, Casero RA (2003) Induction of the PAOh1/SMO polyamine oxidase by polyamine analogs in human lung carcinoma cells. Cancer chemotherapy and pharmacology 52: 383-390

Dufe VT, Ingner D, Heby O, Khomutov AR, Persson L, Al-Karadaghi S (2007) A structural insight into the inhibition of human and Leishmania donovani ornithine decarboxylases by 1-amino-oxy-3-aminopropane. Biochem J 405: 261-268

Duffy S, Nguyen PV, Baker GB (2004) Phenylethylidenehydrazine, a novel GABA-transaminase inhibitor, reduces epileptiform activity in rat hippocampal slices. Neuroscience 126: 423-432

Eliot AC, Kirsch JF (2004) Pyridoxal phosphate enzymes: mechanistic, structural, and evolutionary considerations. Annu Rev Biochem 73: 383-415

Fleming JV, Sanchez-Jimenez F, Moya-Garcia AA, Langlois MR, Wang TC (2004) Mapping of catalytically important residues in the rat L-histidine decarboxylase enzyme using bioinformatic and site-directed mutagenesis approaches. Biochem J 379: 253-261

Furuta K, Nakayama K, Sugimoto Y, Ichikawa A, Tanaka S (2007) Activation of histidine decarboxylase through post-translational cleavage by caspase-9 in a mouse mastocytoma P-815. J Biol Chem 282: 13438-13446

Gabrielson E, Tully E, Hacker A, Pegg AE, Davidson NE, Casero RA, Jr. (2004) Induction of spermidine/spermine N1-acetyltransferase in breast cancer tissues treated with the polyamine analog N1, N11-diethylnorspermine. Cancer chemotherapy and pharmacology 54: 122-126

Grishin NV, Osterman AL, Brooks HB, Phillips MA, Goldsmith EJ (1999) X-ray structure of ornithine decarboxylase from Trypanosoma brucei: the native structure and the structure in complex with alpha-difluoromethylornithine. Biochemistry 38: 15174-15184

Hanada K (2003) Serine palmitoyltransferase, a key enzyme of sphingolipid metabolism. Biochim Biophys Acta 1632: 16-30

Heby O, Persson L, Rentala M (2007) Targeting the polyamine biosynthetic enzymes: a promising approach to therapy of African sleeping sickness, Chagas' disease, and leishmaniasis. Amino Acids

Hegde SS, Chandler J, Vetting MW, Yu M, Blanchard JS (2007) Mechanistic and structural analysis of human spermidine/spermine N1-acetyltransferase. Biochemistry 46: 7187-7195

Heller JS CE, Bussolotti DL, Coward JK (1975) Potent inhibition of ornithine decarboxylase by N-(5'-phosphopyridoxyl)-ornithine. Biochim Biophys Acta 403: 197-207

Hobbs CA, Gilmour SK (2000) High levels of intracellular polyamines promote histone acetyltransferase activity resulting in chromatin hyperacetylation. Journal of cellular biochemistry 77: 345-360

Hoffman DW, Carroll D, Martinez N, Hackert ML (2005) Solution structure of a conserved domain of antizyme: a protein regulator of polyamines. Biochemistry 44: 11777-11785

Huang Y, Keen JC, Pledgie A, Marton LJ, Zhu T, Sukumar S, Park BH, Blair B, Brenner K, Casero RA, Jr., Davidson NE (2006) Polyamine analogs down-regulate estrogen receptor alpha expression in human breast cancer cells. J Biol Chem 281: 19055-19063

Igarashi K, Kashiwagi K (1999) Polyamine transport in bacteria and yeast. Biochem J 344 Pt 3:

633-642

Inche AG, La Thangue NB (2006) Chromatin control and cancer-drug discovery: realizing the promise. Drug discovery today 11: 97-109

Ivanov IP, Rohrwasser A, Terreros DA, Gesteland RF, Atkins JF (2000) Discovery of a spermatogenesis stage-specific ornithine decarboxylase antizyme: antizyme 3. Proc Natl Acad Sci U S A 97: 4808-4813

Jackson LK, Baldwin J, Akella R, Goldsmith EJ, Phillips MA (2004) Multiple active site conformations revealed by distant site mutation in ornithine decarboxylase. Biochemistry 43: 12990-12999

Jackson LK, Brooks HB, Osterman AL, Goldsmith EJ, Phillips MA (2000) Altering the reaction specificity of eukaryotic ornithine decarboxylase. Biochemistry 39: 11247-11257

Jackson LK, Goldsmith EJ, Phillips MA (2003) X-ray structure determination of Trypanosoma brucei ornithine decarboxylase bound to D-ornithine and to G418: insights into substrate binding and ODC conformational flexibility. J Biol Chem 278: 22037-22043

Kelley JL, Miller CA, White HL (1977) Inhibition of histidine decarboxylase. Derivatives of histidine. J Med Chem 20: 506-509

Khomutov RM, Dixon HB, Vdovina LV, Kirpichnikov MP, Morozov YV, Severin ES, Khurs EN (1971) N-(5'-phosphopyridoxyl)glutamic acid and N-(5'-phosphopyridoxyl)-2-oxopyrrolidine -5-carboxylic acid and their action on the apoenzyme of aspartate aminotransferase. Biochem J 124: 99-106

Knight ZA, Gonzalez B, Feldman ME, Zunder ER, Goldenberg DD, Williams O, Loewith R, Stokoe D, Balla A, Toth B, Balla T, Weiss WA, Williams RL, Shokat KM (2006) A pharmacological map of the PI3-K family defines a role for p110alpha in insulin signaling. Cell 125: 733-747

Kubota S, Kiyosawa H, Nomura Y, Yamada T, Seyama Y (1997) Ornithine decarboxylase overexpression in mouse 10T1/2 fibroblasts: cellular transformation and invasion. Journal of the National Cancer Institute 89: 567-571

Lan L, Trempus C, Gilmour SK (2000) Inhibition of ornithine decarboxylase (ODC) decreases tumor vascularization and reverses spontaneous tumors in ODC/Ras transgenic mice. Cancer Res 60: 5696-5703

Lapatto R, Blundell T, Hemmings A, Overington J, Wilderspin A, Wood S, Merson JR, Whittle PJ, Danley DE, Geoghegan KF, et al. (1989) X-ray analysis of HIV-1 proteinase at 2.7 A resolution confirms structural homology among retroviral enzymes. Nature 342: 299-302

Li J, Doyle KM, Tatlisumak T (2007) Polyamines in the Brain: Distribution, Biological Interactions, and their Potential Therapeutic Role in Brain Ischaemia. Current medicinal chemistry 14: 1807-1813

Liu GY, Liao YF, Hsu PC, Chang WH, Hsieh MC, Lin CY, Hour TC, Kao MC, Tsay GJ, Hung HC (2006) Antizyme, a natural ornithine decarboxylase inhibitor, induces apoptosis of haematopoietic cells through mitochondrial membrane depolarization and caspases' cascade. Apoptosis 11: 1773-1788

Love RR, Carbone PP, Verma AK, Gilmore D, Carey P, Tutsch KD, Pomplun M, Wilding G (1993) Randomized phase I chemoprevention dose-seeking study of alpha-difluoromethylornithine. Journal of the National Cancer Institute 85: 732-737

Marton LJ, Pegg AE (1995) Polyamines as targets for therapeutic intervention. Annu Rev Pharmacol Toxicol 35: 55-91

Matsufuji S, Matsufuji T, Miyazaki Y, Murakami Y, Atkins JF, Gesteland RF, Hayashi S (1995) Autoregulatory frameshifting in decoding mammalian ornithine decarboxylase antizyme. Cell 80: 51-60

McLaughlin F, La Thangue NB (2004) Histone deacetylase inhibitors open new doors in cancer therapy. Biochem Pharmacol 68: 1139-1144

Medina MA, Urdiales JL, Rodriguez-Caso C, Ramirez FJ, Sanchez-Jimenez F (2003) Biogenic amines and polyamines: similar biochemistry for different physiological missions and biomedical applications. Critical reviews in biochemistry and molecular biology 38: 23-59

Mehta PK, Christen P (2000) The molecular evolution of pyridoxal-5'-phosphate-dependent enzymes. Advances in enzymology and related areas of molecular biology 74: 129-184

Messing E, Kim KM, Sharkey F, Schultz M, Parnes H, Kim D, Saltzstein D, Wilding G (2006) Randomized prospective phase III trial of difluoromethylornithine vs placebo in preventing recurrence of completely resected low risk superficial bladder cancer. The Journal of urology 176: 500-504

Moya-Garcia AA, Medina MA, Sanchez-Jimenez F (2005) Mammalian histidine decarboxylase: from structure to function. Bioessays 27: 57-63

Murakami Y, Matsufuji S, Kameji T, Hayashi S, Igarashi K, Tamura T, Tanaka K, Ichihara A (1992) Ornithine decarboxylase is degraded by the 26S proteasome without ubiquitination. Nature 360: 597-599

Myers DP, Jackson LK, Ipe VG, Murphy GE, Phillips MA (2001) Long-range interactions in the

dimer interface of ornithine decarboxylase are important for enzyme function. Biochemistry 40: 13230-13236

Ogier G, Chantepie J, Deshayes C, Chantegrel B, Charlot C, Doutheau A, Quash G (1993) Contribution of 4-methylthio-2-oxobutanoate and its transaminase to the growth of methionine-dependent cells in culture. Effect of transaminase inhibitors. Biochem Pharmacol 45: 1631-1644

Origanti S, Shantz LM (2007) Ras transformation of RIE-1 cells activates cap-independent translation of ornithine decarboxylase: regulation by the Raf/MEK/ERK and phosphatidylinositol 3-kinase pathways. Cancer Res 67: 4834-4842

Palanimurugan R, Scheel H, Hofmann K, Dohmen RJ (2004) Polyamines regulate their synthesis by inducing expression and blocking degradation of ODC antizyme. Embo J 23: 4857-4867

Parmar NS, Hennings G, Gulati OP (1984) Histidine decarboxylase inhibition: a novel approach towards the development of an effective and safe gastric anti-ulcer drug. Agents and actions 15: 494-499

Pavlov V, Lin PK, Rodilla V (2002) Biochemical effects and growth inhibition in MCF-7 cells caused by novel sulphonamido oxa-polyamine derivatives. Cell Mol Life Sci 59: 715-723

Pegg AE (2006) Regulation of ornithine decarboxylase. J Biol Chem 281: 14529-14532

Peralta Soler A, Gilliard G, Megosh L, George K, O'Brien TG (1998) Polyamines regulate expression of the neoplastic phenotype in mouse skin. Cancer Res 58: 1654-1659

Pietila M, Alhonen L, Halmekyto M, Kanter P, Janne J, Porter CW (1997) Activation of polyamine catabolism profoundly alters tissue polyamine pools and affects hair growth and female fertility in transgenic mice overexpressing spermidine/spermine N1-acetyltransferase. J Biol Chem 272: 18746-18751

Rabasseda X (1999) Perspectives in the treatment of Parkinson's disease: COMT inhibitors open up new treatment strategies. Drugs Today (Barc) 35: 701-717

Raso V, Stollar BD (1975) The antibody-enzyme analogy. Characterization of antibodies to phosphopyridoxyltyrosine derivatives. Biochemistry 14: 584-591

Raul F, Gosse F, Osswald AB, Bouhadjar M, Foltzer-Jourdainne C, Marescaux J, Soler L (2007) Follow-up of tumor development in the colons of living rats and implications for chemoprevention trials: assessment of aspirin-difluoromethylornithine combination. International journal of oncology 31: 89-95

Robertson JG (2005) Mechanistic basis of enzyme-targeted drugs. Biochemistry 44: 5561-5571

Satriano J (2004) Arginine pathways and the inflammatory response: interregulation of nitric oxide and polyamines: review article. Amino Acids 26: 321-329

Saunders LR, Verdin E (2006) Ornithine decarboxylase activity in tumor cell lines correlates with sensitivity to cell death induced by histone deacetylase inhibitors. Mol Cancer Ther 5: 2777-2785

Seiler N (2003) Thirty years of polyamine-related approaches to cancer therapy. Retrospect and prospect. Part 1. Selective enzyme inhibitors. Curr Drug Targets 4: 537-564

Seiler N (2005) Pharmacological aspects of cytotoxic polyamine analogs and derivatives for cancer therapy. Pharmacology & therapeutics 107: 99-119

Shapiro J, Lui H (2005) Treatments for unwanted facial hair. Skin therapy letter 10: 1-4

Singh S, Malik BK, Sharma DK (2006) Molecular drug targets and structure based drug design: A holistic approach. Bioinformation 1: 314-320

Singh V, Evans GB, Lenz DH, Mason JM, Clinch K, Mee S, Painter GF, Tyler PC, Furneaux RH, Lee JE, Howell PL, Schramm VL (2005) Femtomolar transition state analog inhibitors of 5'-methylthioadenosine/S-adenosylhomocysteine nucleosidase from Escherichia coli. J Biol Chem 280: 18265-18273

Soler AP, Gilliard G, Megosh LC, O'Brien TG (1996) Modulation of murine hair follicle function by alterations in ornithine decarboxylase activity. The Journal of investigative dermatology 106: 1108-1113

Soulet D, Rivest S (2003) Polyamines play a critical role in the control of the innate immune response in the mouse central nervous system. The Journal of cell biology 162: 257-268

Tang L, Li MH, Cao P, Wang F, Chang WR, Bach S, Reinhardt J, Ferandin Y, Galons H, Wan Y, Gray N, Meijer L, Jiang T, Liang DC (2005) Crystal structure of pyridoxal kinase in complex with roscovitine and derivatives. J Biol Chem 280: 31220-31229

Taylor Ringia EA, Schramm VL (2005) Transition states and inhibitors of the purine nucleoside phosphorylase family. Current topics in medicinal chemistry 5: 1237-1258

Thomas T, Shah N, Klinge CM, Faaland CA, Adihkarakunnathu S, Gallo MA, Thomas TJ (1999) Polyamine biosynthesis inhibitors alter protein-protein interactions involving estrogen receptor in MCF-7 breast cancer cells. Journal of molecular endocrinology 22: 131-139

Vlastos AT, West LA, Atkinson EN, Boiko I, Malpica A, Hong WK, Follen M (2005) Results of a phase II double-blinded randomized clinical trial of difluoromethylornithine for cervical intraepithelial neoplasia grades 2 to 3. Clin Cancer Res 11: 390-396

Vujcic S, Liang P, Diegelman P, Kramer DL, Porter CW (2003) Genomic identification and biochemical characterization of the mammalian polyamine oxidase involved in polyamine back-conversion. Biochem J 370: 19-28

Wade RC (1997) 'Flu' and structure-based drug design. Structure 5: 1139-1145

Wagner AJ, Meyers C, Laimins LA, Hay N (1993) c-Myc induces the expression and activity of ornithine decarboxylase. Cell Growth Differ 4: 879-883

Wallace HM, Fraser AV (2004) Inhibitors of polyamine metabolism: review article. Amino Acids 26: 353-365

Wallace HM, Fraser AV, Hughes A (2003) A perspective of polyamine metabolism. Biochem J 376: 1-14

Wang Y, Casero RA, Jr. (2006) Mammalian polyamine catabolism: a therapeutic target, a pathological problem, or both? Journal of biochemistry 139: 17-25

Wei G, Hobbs CA, Defeo K, Hayes CS, Gilmour SK (2007) Polyamine-mediated regulation of protein acetylation in murine skin and tumors. Mol Carcinog 46: 611-617

Wheeler DL, Ness KJ, Oberley TD, Verma AK (2003) Inhibition of the development of metastatic squamous cell carcinoma in protein kinase C epsilon transgenic mice by alpha-difluoromethylornithine accompanied by marked hair follicle degeneration and hair loss. Cancer Res 63: 3037-3042

Zhang M, Wang H, Tracey KJ (2000) Regulation of macrophage activation and inflammation by spermine: a new chapter in an old story. Critical care medicine 28: N60-66

Zhang Z, McCormick DB (1992) Uptake and metabolism of N-(4'-pyridoxyl)amines by isolated rat liver cells. Arch Biochem Biophys 294: 394-397

Zhang Z, Smith E, Surowiec SM, Merrill AH, Jr., McCormick DB (1993) Synthesis of N-(4'-pyridoxyl)sphingosine and its uptake and metabolism by isolated cells. Membrane biochemistry 10: 53-59

Zhang ZM, McCormick DB (1991) Uptake of N-(4'-pyridoxyl)amines and release of amines by renal cells: a model for transporter-enhanced delivery of bioactive compounds. Proc Natl Acad Sci U S A 88: 10407-10410

Zhao B, Butler AP (2001) Core promoter involvement in the induction of rat ornithine decarboxylase by phorbol esters. Mol Carcinog 32: 92-99

2. New transition state-based inhibitor for human ornithine decarboxylase inhibits growth of tumor cells

Fang Wu, Doris Grossenbacher, Heinz Gehring

2.1 Abstract

Pyridoxal 5'-phosphate (PLP)-dependent ornithine decarboxylase (ODC) is the key enzyme in polyamine synthesis. ODC is overexpressed in many tumor cells and thus a potential drug target. Here we show the design and synthesis of a coenzyme-substrate analog as a novel precursor inhibitor of ODC. Structural analysis of the crystal structure of hODC disclosed an additional hydrophobic pocket surrounding the ε-amino group of its substrate ornithine. Molecular modeling methods showed favorable interactions of the BOC-protected pyridoxyl-ornithine conjugate, termed POB, in the active site of hODC. The synthesized and purified POB completely inhibited the activity of newly induced ODC activity at 100 μM in glioma LN229 and COS7 cells. In correlation with the inhibition of ODC activity, a time dependent inhibition of cell growth was observed in myeloma, glioma LN18 and LN229, Jurkat, COS7 and SW2 small-cell lung cancer cells if DNA synthesis and cell number were measured, but not in the non-tumorigenic human aortic smooth muscle cells. POB not only strongly inhibited cell proliferation of low grade glioma LN229 cells in a dose dependent manner (IC_{50} ~ 50 μM) but also high grade glioblastoma multiforme cells. POB is much more efficient in inhibiting proliferation of several types of tumor cells than α-DL-difluoromethylornithine (DFMO), the best known irreversible inhibitor of ODC.

2.2 Introduction

Polyamines, such as putrescine (PUT), spermidine (SPD) and spermine (SPM) are multi-charged aliphatic cations and exist in all organisms (1). Ornithine decarboxylase (ODC), a pyridoxal 5'-phosphate-dependent enzyme, catalyzes the conversion of ornithine to putrescine, the first and rate–limiting step in polyamine synthesis (Fig. 1A) (2). ODC expression is rapidly induced after exposing cells with cell proliferation-stimulating agents (2-4). High levels of ODC observed in cancer cells are closely related to tumor promotion (1, 5). Overexpression of ODC induces transformation of cells (6) and inhibition of ODC abolishes transformation and is associated with tumor suppression (2, 7). Even modest reductions in ODC activity can lead to a marked resistance in tumor development (2, 7). ODC-overexpressing cells are tumorigenic and expression of ODC in hair follicle cells is linked to growth and maintenance of hair follicles (8). Thus, ODC is an interesting target for anti-cancer or chemopreventive drugs (2, 5).

Several inhibitors of ODC are known and the most widely used compound is α-DL-difluoromethylornithine (DFMO), an enzyme-activated irreversible inhibitor, which was introduced more than 20 years ago. DFMO irreversibly binds into the active site of ODC by covalently attaching to Cys360 after it is activated by ODC itself (5). Although DFMO has been shown to be effective in some experimental models and therapeutical approaches, it seems not to be as effective in vivo against tumor cells (9). One explanation of why DFMO is not sufficiently blocking ODC activity in vivo might be that DFMO is displaced, due to its relatively low affinity (Ki ~ 40 μM), by endogenous ornithine (Km ~ 90 μM), the substrate of ODC (5). The concentration of ornithine in human plasma seems to be in the range of this Km value. Fast clearance, inefficient uptake into cells and development of resistance, such as up-regulation of ODC expression and polyamine transporter, are further drawbacks of DFMO (5, 10, 11). Thus, other ODC inhibitors which have higher potency, better pharmacokinetics and the ability to overcome the cell resistance are demanded (5, 10).

A lot of attempts have been made by modifying the ornithine skeleton structure of DFMO to improve the efficiency (5). Although the modified compounds got improved binding affinity for ODC in vitro, they had no favorable effect in inhibiting cell proliferation in vitro and in vivo (5).

Pyridoxal 5'-phosphate (PLP) is the functional cofactor of PLP-dependent enzymes which catalyze a wide variety of amino acid transformations (12, 13). An obligatory step in all these reactions is the intermediary formation of an aldimine, i.e. a Schiff base of PLP with the amino group of the amino acid substrate (Fig. 1A) (12, 13). Reduction of the Schiff base produces phosphopyridoxyl-amino acids, which are analogs of the covalent coenzyme-substrate adducts. These compounds are a kind of transition state analogs that bind to the apoprotein with high affinity (14-16). They cannot be transformed by the enzymes and thus inhibit them very potently. A further advantage of these analogs of coenzyme-substrate adducts is the high degree of specificity. Phosphopyridoxyl-ornithine was found to be a very potent inhibitor of ornithine decarboxylase without affecting S-adenosylemethionine decarboxylase (15).

Successful exposure of newly synthesized cellular ODC to phosphopyridoxyl-ornithine would inhibit ODC activity completely and specifically (no mammalian α-transaminase for ornithine is known), and thus induce the inhibition of cell proliferation. However, the drawback of these compounds in their in vivo application is the impermeability of the cell membrane for these substances due to their negative charges.

Here we report the design and synthesis of a phosphopyridoxyl-ornithine based precursor inhibitor for human ornithine decarboxylase which can be taken up by cells. POB (Fig 1B) inhibited ODC activity in cells and inhibited proliferation of many types of tumor or transformed cells much more effectively than DFMO.

2.3 Materials and Methods

Chemicals and Cell lines

Pyridoxal•HCl was purchased from Merck. H-Orn(BOC)-OMe•HCl and DFMO were from Bachem. L-[1-^{14}C]ornithine and [^{3}H]thymidine were from American Radiolabeled Chemicals Inc.

NIH3T3 cells were purchased from American Type Culture Collection. Glioma cell line LN18, LN229 (both from brain), primary tumor cells from lung cancer metastasis in brain (LCMB) and from glioblastoma multiforme (GBM) were generous gifts from Dr. K. Frei (Department of Neurosurgery, University Hospital Zurich). COS7 cells (monkey kidney, SV40 T antigen transformed) and a murine myeloma cell line were generous gifts from Prof. P. Sonderegger (Department of Biochemistry, University Zürich). Jurkat cells (a tumor T lymphoma cell line) and a human small-cell lung cancer cell line (SW2) were kindly provided by Dr. J. Kemler-Carraneo (Abteilung Klinische Immunologie, University Hospital Zurich). Human aortic smooth muscle cells were gifts from Dr. C. Dumrese (Anatomische Institut, Universität Zürich)**.**

Synthesis of POB

N-(4'-pyridoxyl)- ornithine(BOC)-OMe•HCl (POB, Fig. 1B) was synthesized as described for the synthesis of phosphopyridoxyl-ornithine or pyridoxyl-ornithine (15). Briefly, pyridoxal (1mmol) and KOH (2 mmol) were dissolved in 5 ml methanol as was H-Orn(BOC)-OMe•HCl (1 mmol) and KOH (1 mmol) in 8 ml MeOH. Both solutions were mixed at 0 ºC and stirred at room-temperature for 20 min. Then, 125 mg of $NaBH_4$ was added in small portions and the solution was put on ice for further 30 min. Acetic acid (100%) was added until pH 5 was reached to stop the reaction. The solvents were removed with a vacuum dryer and the residue was dissolved in water and subjected to HPLC for purification and analysis.

HPLC analysis and purification of POB

The compound was analyzed and purified with a Jasco HPLC equipped with a Nova Pack C_{18} column (3.9×150 mm, 5 μm from Millipore) and a multiwavelengh detector. The sample was loaded and separated with a flow rate of 0.5 ml/min using the following gradient: 0-12 min, 100% solvent A (3% ACN/0.1% TFA) and 0% solvent B (80% ACN/0.1% TFA); 12-22 min, 0-80% B; 22-92 min, 80-100% B, followed by 100% B. The detection was carried out at 290 and 215 nm. Under these conditions the synthetic compounds eluted at the retention time of 21.4 min and the MS peak of this purified compound is 398.22 Dalton (purity >95%, Supplementary Fig. S1).

The extinction coefficient used for this compound was 8400 $M^{-1}cm^{-1}$ at 296 nm under acidic conditions (17). A semi-prep column (aquapore octyl, 10×250 mm, 20 μm) was used under similar conditions to prepare larger amounts of POB. The purified POB was vacuum-dried several times after adding water and stored at a concentration of about 10 mM (water stock solution) in –20 °C.

Cell culture

LN18, LN229, LCMB and GBM were maintained in DMEM supplemented with 1 g/L glucose, 10% FBS (Life Technologies), 20 μg/ml gentamycine (Fluka) in a humidified 5% CO_2 atmosphere at 37 °C. Jurkat cells were grown in RPMI 1640 medium (Sigma) supplemented with 10% NBCS (Life Technologies), 15 mM Hepes (Life Technologies), 2 mM L-glutamine, 50 μM β-mercaptoethanol, and 1% (w/v) penicillin and streptomycin (Life Technologies) in a humidified 5% CO_2 atmosphere at 37 °C. SW2 cells were grown in RPMI 1640 supplemented with 10% FBS. NIH3T3 and myeloma cells were maintained in DMEM medium with 10% NBCS or FBS. The human aortic smooth muscle cells were cultured in DMEM containing 10% FBS, 20 mM HEPES buffer solution in a humidified atmosphere (5% CO_2).

For measuring cell growth, cells (2.5 - 5 x 10^4 cells per well) were seeded and incubated in 0.5 ml medium containing 5% FBS or NBCS and 1%

penicillin/streptomycin in 24-well plate. After one day, cells were incubated in the absence or presence of the indicated concentrations of POB or DFMO for the indicated times. Cells were counted with a Coulter counter (ZM Coulter Electronics) as described (18). Data in the figures represent a typical experiment out of at least two independent experiments.

[^{3}H]thymidine incorporation

Cells were seeded and pretreated as described above. Then, [^{3}H]thymidine (0.25 μCi) was added into each well and incubated together with cells for the indicated times. Radioactivity of incorporated [^{3}H]thymidine was measured in a Wallac 1450 MicroBeta liquid scintillation counter according to the procedure described by Koga et al. (19). The numbers in the figures are the mean of at least three wells.

ODC activity

ODC activity was measured by the released $^{14}CO_2$ from labeled ornithine as described (20). For measuring the serum-induced ornithine decarboxylase activity, cells were cultured in 6-well plate at a density of ~1.6 x 10^5 per well with 5% FBS or NBCS for one day and then treated in the absence or in the presence of POB for the indicated times. The cells were then induced by fresh medium containing 10% FBS for 6 h, collected after trypsine/EDTA treatment and washed twice with ice-cold phosphate-buffered saline, pH 7.4 (PBS). The collected cells were lysed two times by freezing (liquid nitrogen) and thawing (37 °C, 2 min) in 320 μL lysis buffer (1 mM EDTA, 100 μM pyridoxal phosphate, 2.5 mM DTT and protease inhibitor cocktail (Roche) in 50 mM PBS, pH 7.4). The reaction was started by adding 30 μl L-[1-^{14}C] ornithine (100 μM, 0.09 μCi) to 270 μl supernatant of lysed cells. After 75 min incubation, the reaction was stopped by injecting 200 μL 4 N H_2SO_4 and kept for one hour at room temperature in order to ensure complete absorption of released CO_2 in the capture reagent (tissue solubilizer NCSII, Amersham). The captured $^{14}CO_2$ was measured by scintillation counting using a Wallac 1450 MicroBeta liquid scintillation counter. The protein concentration in the lysed supernatant was determined by the

BioRad protein assay kit. The numbers in the figures are the mean of at least two wells.

Western blotting

LN229 Cells were seeded in 25-cm^2 flasks (~4 x 10^5 cells) and treated in the absence or presence of POB for three days and lysed as described above. Cell lysates were fractionated on 10% SDS-PAGE and subjected to immunoblotting analysis as described (21).

Polyamine analysis

LN229 cells were seeded in 6-well plate at a density of ~1.6 x 10^5 per well with 5% FBS for one day and then treated in the absence or presence of POB (100 μM) for the indicated times. Cells were collected, counted and lysed. Polyamines were extracted with 0.2 M perchloric acid and measured by Dr. L. Persson and coworkers (Department of Experimental Medical Research, Lund University) as described (22). The numbers in the figures are the mean of triplicates.

Polyamine oxidase

Polyamine oxidase activity was determined as described (23). LN229 cells were seeded in 6-well plate at a density of ~1.6 x 10^5 per well with 5% FBS for one day and treated in the absence or presence of POB (200 μM) or DFMO (500 μM) for the 2 days. Then, cells were lysed and polyamine oxidase activities measured. The numbers in the figures are the mean of triplicates.

Molecular modeling

The model containing human ODC, PLP and putrescine was generated by superposition of the crystal structure of the human ODC (PDB code: 1D7K, Fig 2A (24)) with the crystal structure of Trypanosoma Brucei ODC (PDB code: 1F3T, (25)) containing PLP and putrescine as ligands. In order to optimize the structure of the

complex formed with PLP, putrescine and human ODC protein, energy minimization was performed by using InsightII software (version 2000, Accelrys Corporate) under amber force field. The putative binding sites of hODC in this model were analyzed with InsightII binding site module and prepared for further docking analysis by using DOCK4 (USCF) without considering the solvent effect. DOCK4 was employed for predicting the geometry of the ligands bound to the protein (26). Electrostatic and van der Waals energies were evaluated on a grid with a 0.3 Å spacing in the region spanning all residues within 6 Å of phosphopyridoxyl-putrescine adduct (see Fig. 1A and 2B). The structures of phosphopyridoxyl-ornithine (Schiff base analog, Fig. 1) and the putative active form of POB (Fig. 2C) were drawn based on the known 3D coordinates of the phosphopyridoxyl-putrescine conjugate followed by energy minimization. The optimized structures were rigidly docked into the modeled active site of ODC using the program DOCK4 and the complexes of ODC and analogs were further optimized by energy minimization (InsightII) (Fig. 2C). The de novo design program LUDI (27) of InsightII was used to retrieve putative fragments which can fit into the binding pocket (Fig. 2B). The standard default parameter and a fragment library supplied with the program were used for the LUDI search.

2.4 Results

Design and modeling of an inhibitor for human ornithine decarboxylase

The phosphopyridoxyl-ornithine precursor which we designed, synthesized, purified (see Materials and Methods) and expected to be able to pass the cell membrane, is shown in Fig. 1B. In this pyridoxyl-ornithine derivative, the 5'-phosphate group is eliminated and the carboxyl group is esterified with methanol. The crystal structure of human ODC (PDB code: 1D7K) contains the cofactor pyridoxal 5'-phosphate (PLP) but no substrate or product (24). In order to study the potential interaction between inhibitors and hODC, we built a model composed of the reaction intermediate phosphopyridoxyl-putrescine adduct and the active site of hODC (Fig. 1A and 2B) (see Materials and Methods). Based on this model and by using the binding site analysis module of InsightII, we found a hydrophobic pocket, where the ε-amino group of ornithine was situated, that is formed by the aromatic residues TyrA389, TyrA331, PheB397 and TyrB323 between the two ODC subunits (Fig. 2B and 2C). Only the dimer of ODC is catalytically active, as the active sites are constructed of residues from subunit A and B. Applying the structure-based drug design software LUDI (InsightII) indicated that fragments such as 1-methylaminoethanol, 2-aminopyrrole, triethylamine and trimethylamine would fit into this additional pocket. Indeed, when the hydrophobic BOC group was added to the ε-amino group of ornithine (Fig. 1B), the interaction was more favorable if analyzed by the software DOCK or InsightII.

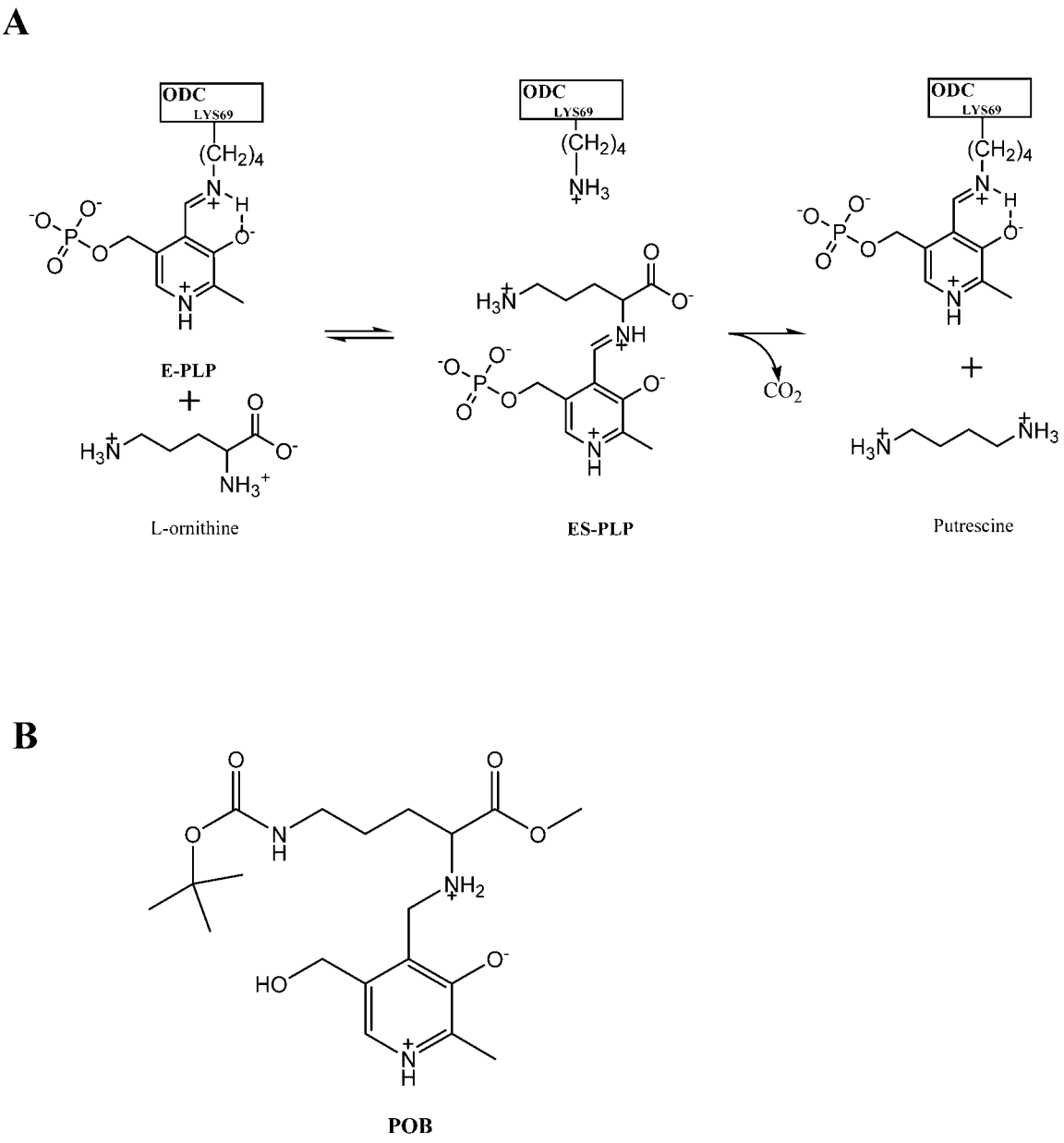

Figure 1. A, Reaction mechanism of ODC with L-ornithine. E-PLP, ODC-pyridoxal 5'-phosphate (internal aldimine); ES-PLP, enzyme-coenzyme-substrate intermediate (external aldimine) B, POB, the precursor analogue of phosphopyridoxyl-ornithine (see ES-PLP).

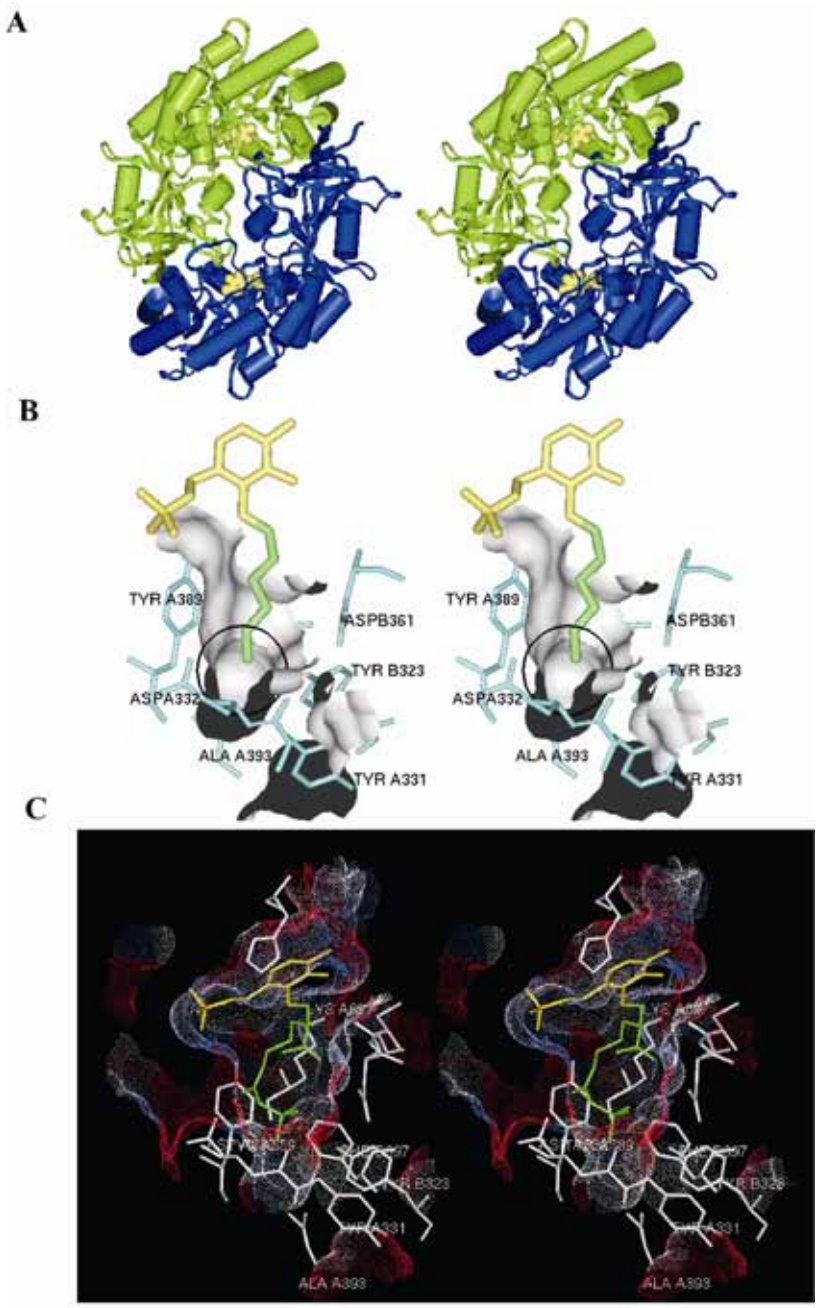

Figure 2. **Modeling the phosphopyridoxyl-ornithine analogs in the active site of human ODC**. A, Stereo view of the dimeric human ODC. The two subunits are colored in green (subunit A) and blue (subunit B) and the cofactor PLP in the active site of hODC is shown in CPK mode in yellow. B, The Connolly surface of part of the active site is displayed as grey solid surface (generated by residues TyrA331, TyrA389, AlaA393, TyrB323, and PheB397) together with the reaction intermediate phosphopyridoxyl-putrescine adduct (see Fig. 1A) in yellow (phosphopyridoxyl moiety) and green (putrescine moiety). The additional pocket is indicated by a black circle. C, Stereoview of the putative binding mode of the active form of POB in the active site of hODC. The Connolly surface of whole active site is displayed by dots. Blue, indicates positive charged surface; red, negative and white, neutral. The phosphopyridoxyl-ornithine-BOC conjugate is displayed in yellow (phosphopyridoxyl moiety) and green (ornithine-BOC moiety).

Inhibition of cellular ODC activity

To prove whether POB (synthesis and purification see Materials and Methods) could enter cells and is there converted to an active inhibitor of newly expressed ODC activity, COS7 and glioma LN229 cells were subjected to POB. In COS7 cells nearly complete inhibition of the activity of ODC was measured after two days of POB treatment at a concentration of 100 μM (Fig. 3A). A strong inhibition was also observed after 3 days of treatment of LN229 cells with POB at 100 μM, comparable with the inhibition of DFMO at a concentration of 500 μM (Fig. 3B). To demonstrate whether the diminished ODC activity was indeed due to the inhibition of enzymic activity and not to a decreased expression of ODC, Western blot was performed to estimate the amount of ODC in LN229 and COS7 cells after treating them with POB for 3 or 2 days, respectively (Fig. 3C, for COS7 see Supplementary Fig.S2). The result showed that the amount of ODC (53 KD) was similar in POB-treated and control cells. Although ODC activity was almost completely inhibited by POB, the amount of ODC seemed not to be affected by the inhibition. Thus, POB was taken up by cells and acted as proposed as an efficient inhibitor of ODC in cells.

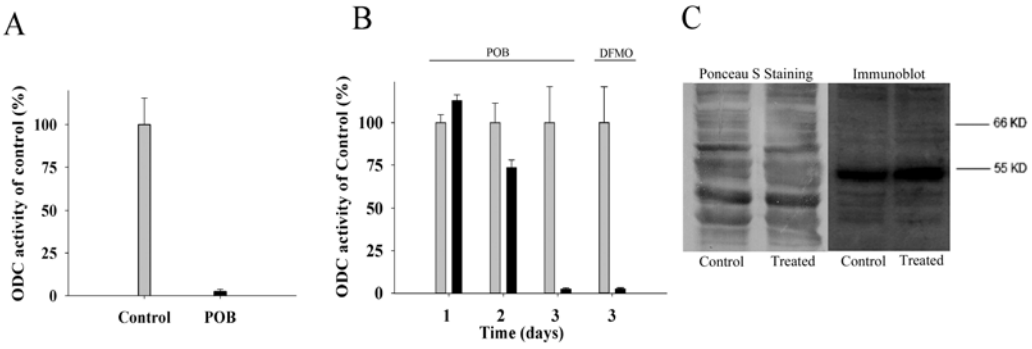

Figure 3. **Inhibition of ODC activity in cells by POB**. A, COS7 cells were treated with POB (100 μM) for 2 days. Cells were collected, lysed and ODC activity measured immediately by the release of labeled CO_2 from ornithine (see Materials and Methods). B, LN229 cells were treated with POB (100 μM) or with DFMO (500 μM) for the indicated times. Cells were collected, lysed and ODC activity of untreated cells (gray columns) or treated cells (black columns) was measured immediately. C, Western blot of ODC after treatment of LN229 cells with POB (100 μM) for 3 days. Cells were collected, lysed and twofold Laemmli buffer was added to aliquots of the supernatant. The same amount of total proteins (47μg) was subjected to SDS-PAGE followed by immunoblotting and Ponceau S staining (see Materials and Methods). The main band of 53 KD represents ODC (Control 100%, Treated 106%). Error bars represent the standard deviation.

Effect of POB on cellular DNA synthesis

As POB was found effective in inhibiting activity of ODC, and ODC is associated with cell proliferation and tumor growth (see Introduction), the effect of POB on cancer cell proliferation was investigated with cell lines such as myleoma, human small-cell lung cancer cells (SW2), glioma LN229 cells and recently isolated primary tumor cells derived from lung cancer metastasis in brain (LCMB) as well as glioblastoma multiforme primary tumor cells (GBM) (see Materials and Methods). The result showed that in these cells, the DNA synthesis was strongly inhibited upon POB treatment (Fig. 4). Myeloma cells were highly sensitive to POB (Fig. 4A). Even after adding 50 μM POB only for one day, DNA synthesis measured after a 13-h pulse with [^{3}H]dThd was less than 20% of untreated cells. In SW2 cells, the DNA synthesis of cells treated with 200 μM POB was reduced to about 15%, whereas the incubation with DFMO at the same concentration had no influence. DNA synthesis of LN229 was decreased to about 25% of the control when exposing them to 100 μM POB for one day (Fig. 4C), and that of LCMB and GBM cells to about 33% and 60% of the control, respectively after four days treatment (Fig. 4D).

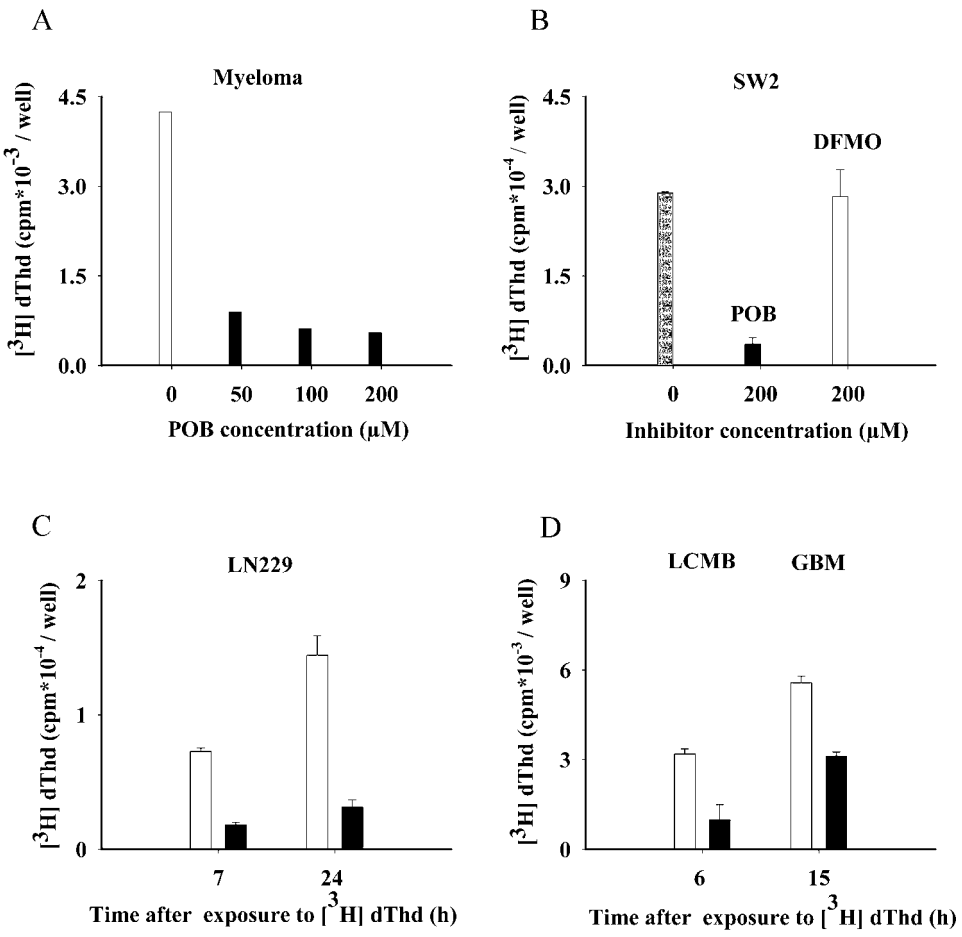

Figure 4. **Inhibition of cell DNA synthesis by POB**. A, Myeloma cells were pretreated with POB at the indicated concentrations for one day, then [^{3}H]dThd was added, incubated for 13 hours and the incorporated [^{3}H]dThd was measured (see Materials and Methods). B, SW2 cells were pretreated with POB or DFMO for half a day and then incubated with [^{3}H]dThd for 25 hours. C, LN229 cells were pretreated with 100 μM POB for one day, and [^{3}H]dThd was added and incubated for the indicated times. D, Lung cancer metastasizing cells in brain (LCMB) or glioblastoma multiforme cells (GBM) were pretreated with 100 μM POB for four days, and [^{3}H]dThd was added and incubated for the indicated times. Gray columns, without treatment; black columns, with POB treatment. Error bars represent the standard deviation.

Inhibiting tumor cell growth

Cell growth of several different types of cell lines in culture was investigated by counting the cell number. After treating them with POB or DFMO for the indicated time and concentration (Fig. 5A-C), POB at 100 μM was a stronger inhibitor of cell growth than DFMO even at 5 or 10-fold higher concentrations in LN229 and COS7 cells, respectively. Whereas in myeloma cells, POB acted at the indicated

concentration without a delay, in other cells, growth decreased drastically after a delay of one or two days. POB also inhibited other cells from different tissues, for instance, Jurkat (T cell line), LN18 (brain), and NIH3T3 (fibroblast) cells, whereas non-tumorigenic human aortic smooth muscle cells were resistance to inhibition with POB (Fig. 5D, the cell number of human aortic smooth muscle cells increased 2.5-fold during the indicated times). The dose and time dependence of inhibition of cell growth by POB varied and was dependent on the cells used and the treatment period. For LN229 cells, the IC_{50} value is around 50 μM when estimated by [^{3}H]dThd incorporation or by cell counting after 5 or 6 days of POB exposure (Fig. 6, data of 6 days treatment not shown). The cell inhibition with DFMO was less effective than that with POB at the indicated concentrations (Fig. 6).

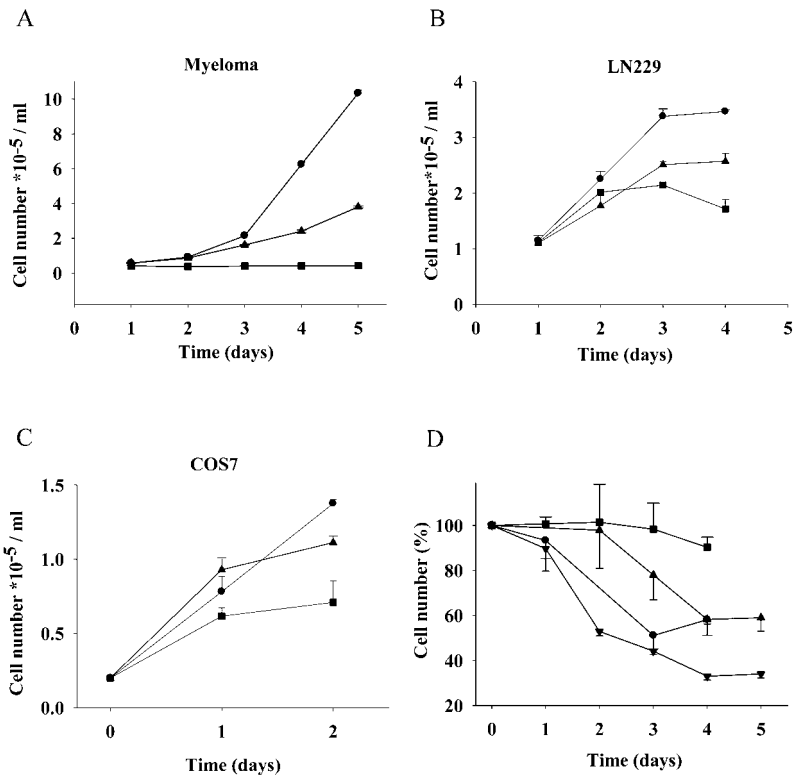

Figure 5. **Cell growth inhibition of POB and DFMO**. Myeloma cells A, Glioma LN229 cells (B) and COS7 cells (C) were treated without (●) or either with POB (■, 100 μM) or with DFMO (▲, 100 μM for myeloma cells, 500 μM for LN229 and 1 mM for COS7 cells) for the indicated times; D, Time-dependent inhibition of primary cultures of human aortic smooth muscle cells (■), of LN18 (▲), NIH3T3 (●) and Jurkat (▼) cells, subjected to 100 μM POB. Error bars represent the standard deviation.

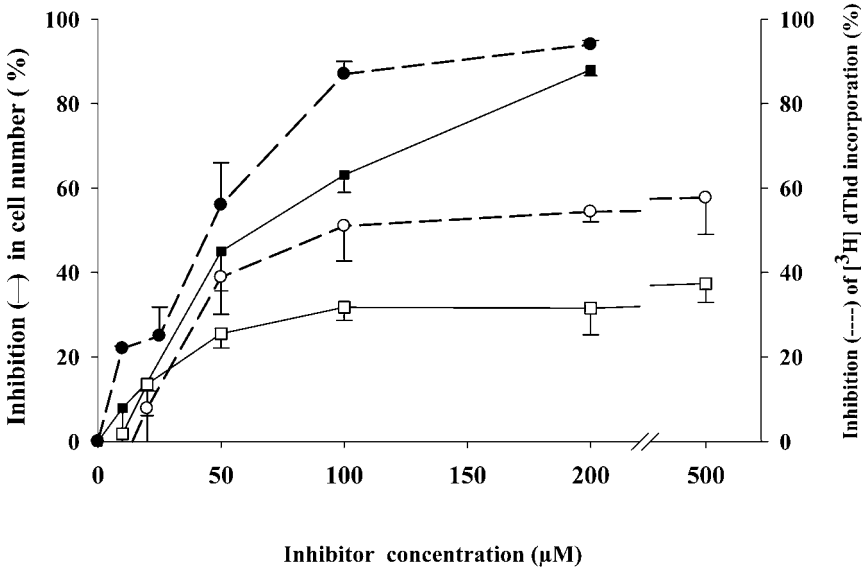

Figure 6. **Dose dependent cell growth inhibition by POB and DFMO**. Glioma LN229 cells were incubated with different concentrations of POB (■) or with DFMO (□) for 5 days, counted (——) and compared with the untreated controls. For measuring [^{3}H]dThd incorporation (- - -), LN229 cells were incubated with [^{3}H]dThd for 15 hours after 2 days pretreatment with POB (●) or DFMO (○). Error bars represent the standard deviation.

Treatment of cells with POB affects the morphology of cells in different ways. Only few dead cells were found in untreated LN229 cells but a high fraction of cells detached after treatment with POB (100 μM) for 3 days. DFMO-treated (500 μM) LN229 cells showed higher cell density with less detached cells (Supplementary Fig. S3A). The number of detached cells after POB treatment seemed to depend on the dose of POB. If COS7 cells were treated with POB, many cells died and detached (round floating cells) and a substantial percentage (~40%) of attached COS7 cells could be stained with trypan blue indicating dying cells (Supplementary Fig. S3B). Only few dead cells were found among untreated attached COS7 cells if stained with trypan blue (data not shown). SW2 cells tend to aggregate and form large clumps. As shown by the inhibition of DNA synthesis, treatment with POB inhibited cell proliferation of SW2 and substantially decreased the size and amount of cell aggregates (Supplementary Fig. S3C). The microscopic cell images indicate that inhibition of ODC arrested cell proliferation that is followed by cell death. The

change in morphology of cells might reflect the importance of ODC activity for maintaining the cell shape (28, 29).

2.5 Discussion

The present study describes the successful action of POB, a newly developed inhibitor of ODC, on various tumor cells. The development strategy bases on the external aldimine, an obligatory intermediate in the mechanism of action of ODC. In the pyridoxyl-ornithine derivative POB, the 5'-phosphate group is eliminated and the carboxyl group is esterified with methanol. The rationale behind the design was that this compound together with the additional hydrophobic BOC group of the ε-amino group of ornithine has no negative net charge and very likely crosses the cell membrane as it was reported for several pyridoxyl-amines (30, 31) and pyridoxyl-methionine analogs (32). Intracellular pyridoxal kinase, an enzyme that seems to tolerate considerable variation in C4' position of the pyridoxyl moiety (31, 33) is expected to phosphorylate this compound after it has been taken up by the cells whereas the carboxymethyl ester will be hydrolyzed intracellularly. The phosphopyridoxyl-ornithine analog formed in cells will bind with very high affinity to the newly synthesized apoornithine decarboxylase and affecting only proliferating cells in which ODC is obligatory induced.

POB, the synthesized precursor of a covalent coenzyme-substrate adduct of ODC is taken up by the cells. Intracellularly, the compound is transformed and binds as deduced and demonstrated by the inhibition of ODC activity to newly synthesized ODC. The response time of POB varied in different cell lines; with LN229 cells a lag of more than one day had been observed. The delayed inhibition might be due to the necessary transformation, i.e. ester hydrolysis and phosphorylation (as discussed above) of POB to an efficient ligand of ODC, processes that might well vary in different cells. Additionally, one has to consider that the active compound has to compete with intracellular pyridoxal phosphate (~ 20 to 50 μM (34)), a necessity for a cell to survive. Although the prominent ODC inhibitor DFMO acts directly with active ODC, less pronounced growth inhibition effects were observed even at higher concentrations of DFMO. The treatment of cells with POB does neither up-regulate

nor down-regulate significantly ODC expression whereas an up-regulation was reported with DFMO (5) and was also observed in our hand (Supplementary Fig. S2).

Consistent with the inhibition of ODC activity by POB is the inhibition of cell proliferation in the investigated tumor cells. Again, cells respond differently on dose and time of exposure to POB. The IC_{50} of POB is, under serum culture condition, in the μM-range (50 μM for LN229). Myeloma cells respond immediately, and COS7 or LN229 cells stopped cell proliferation after exposing them to POB for one to two days, whereas human aortic smooth muscle cells are not affected significantly by POB.

The proposed strategy suggests that the intracellularly transformed POB derivative binds most likely only to newly synthesized apo-ODC since competing bound PLP out of holo-ODC might be very unlikely to happen in the short life cycle of ODC due to the intrinsic high affinity of PLP. In addition to that, the transformed POB derivative seems to bind specifically ODC and does not inhibit human histidine decarboxylase another highly induced PLP dependent enzyme in cells (data not show).

DFMO, however, will interact only with active ODC. Adding POB or DFMO to cell extracts and measuring subsequently ODC activity showed indeed that DFMO (500 μM) inhibited ODC activity whereas POB (100 μM) had only a minor effect (data not shown). Although DFMO was able to suppress the activity of ODC in vitro and in cells, it was less efficient in preventing cancer cell proliferation. This indicates a different mechanism of action of these two inhibitors in inhibiting cell proliferation. This conclusion is further supported by the observation that cells supplied with excess of polyamines in culture medium responded differently if treated with POB or DFMO, respectively. The inhibition of DFMO-treated cells was reversed by addition of polyamines (Fig. S4), an already well-known effect (35, 36). Conversely, POB treated cells did not show much differences in the presence or absence of additional polyamines (Fig. S4).

This different behaviour could be explained by the observed intracellular polyamine pool. In POB treated cells putrescine declined at most after two days, when

the inhibition of ODC caused by POB became effective (Fig. S5 and 3B). However the polyamine level is not lower than that of the controls, whereas DFMO was reported to deplete the PUT, SPD, but not SPM pool already after a day (37) and was also observed in our hand with LN229 that were treated with 500 μM DFMO for two days (PUT: 0.09, SPD: 0.06, SPM: 2.5 nmol/10^6 cells). This clearly indicates that the inhibitory action caused by POB is different from that of DFMO, and is not simply caused by PUT and SPD depletion. Possible explanations could be that POB-derivatives might act as a kind of polyamine analogue and interfere with the polyamine conversion (as indicated by a two-fold increase of polyamine oxidase activity, see Fig. S6) and transport, a complex interplay whose regulation is not yet understood (23, 38, 39).

Modeling the inhibitor into the active site of hODC revealed a relatively large hydrophobic pocket formed by the two subunits of hODC at the position of the ε-amino group of ornithine suggesting to us not to remove the BOC-protecting group of POB (Fig. 1B). And indeed, the BOC group contributes substantially to the successful inhibitions as we could not find a comparable inhibition if it was removed. Besides the favourable binding suggested from the molecular modeling experiment, the improved bioavailability might also contribute to the efficiency of POB. The calculated logP (Log octanol/water partition coefficient, which is a theoretical tool for measuring the lipophilicity of a compound) of POB is 1.72 and without the BOC group -0.50 (calculated values were obtained from www.logp.com), which is a very strong indication that POB can more efficiently cross the cell membrane (40).

The attempt to develop a cell growth inhibitor by targeting ODC was successful and proved the proposed strategy. The newly designed and synthesized transition state-based analog (POB) was very effective in inhibiting newly induced cellular ODC activity and exceeded the potency of DFMO, the best and well characterized inhibitor of ODC so far, in inhibiting proliferation of many types of tumor cells. POB inhibits the proliferation of broad variety of tumor cell lines, such as myeloma, glioma LN18 and LN229, Jurkat, COS7 and SW2 cells, but not the non-tumorigenic human aortic smooth muscle cells. Glioblastoma multiforme (GBM) is the most aggressive

form of primary brain tumors known collectively as gliomas. Very few therapeutic options exist for the treatment of human glioblastoma (41). Here we report that POB can suppress the proliferation of low grade (IC_{50} ~50 μM) but also high grade glioblastoma cells (GBM). Future experiments will have to show whether the promising results with POB in culture studies can be confirmed in animal or even clinical studies. Structure modification of this inhibitor might improve its action and can be proposed and performed on the basis of the interaction model of POB with ODC.

In conclusion, the present study demonstrates that selected PLP-dependent enzymes in cells can be targeted with the proposed transition state-based inhibitors and the designed strategy might serve to develop inhibitors of this type for other PLP-dependent enzymes of pharmacological interest.

2.6 Acknowledgment

This work is supported by COST Switzerland, Action 922, grant number C02.0017. We would like to dedicate this paper to Livio Besio who did initial work but died in an accident. We thank Dr. S. Bienz (Institute of Organic Chemistry, University Zurich) for providing excellent chemistry equipments, Dr. L. Persson and co-workers for measuring the polyamines, Dr. K. Frei for kindly providing glioma cell lines, primary tumor cells from lung cancer metastasis in brain and from glioblastoma multiforme, Dr. C. Dumrese and coworkers for providing the experiments with human aortic smooth muscle cells and Dr. P. Christen (Department of Biochemistry, University Zurich) for his valuable advices and critical reading of the manuscript.

2.7 References

1. Gerner EW, Meyskens FL, Jr. Polyamines and cancer: old molecules, new understanding. Nat Rev Cancer 2004;4:781-92.
2. Pegg AE. Regulation of ornithine decarboxylase. J Biol Chem 2006;281:14529-32.
3. Nickel KP, Belury MA. Inositol hexaphosphate reduces 12-O-tetradecanoylphorbol-13-acetate-induced ornithine decarboxylase independent of protein kinase C isoform expression in keratinocytes. Cancer Lett 1999;140:105-11.
4. Glikman P, Manni A, Demers L, Bartholomew M. Polyamine involvement in the growth of hormone-responsive and -resistant human breast cancer cells in culture. Cancer Res 1989;49:1371-6.
5. Seiler N. Thirty years of polyamine-related approaches to cancer therapy. Retrospect and prospect. Part 1. Selective enzyme inhibitors. Curr Drug Targets 2003;4:537-64.
6. Auvinen M, Paasinen A, Andersson LC, Holtta E. Ornithine decarboxylase activity is critical for cell transformation. Nature 1992;360:355-8.
7. Nilsson JA, Keller UB, Baudino TA, et al. Targeting ornithine decarboxylase in Myc-induced lymphomagenesis prevents tumor formation. Cancer Cell 2005;7:433-44.
8. Wheeler DL, Ness KJ, Oberley TD, Verma AK. Inhibition of the development of metastatic squamous cell carcinoma in protein kinase C epsilon transgenic mice by alpha-difluoromethylornithine accompanied by marked hair follicle degeneration and hair loss. Cancer Res 2003;63:3037-42.
9. Vlastos AT, West LA, Atkinson EN, et al. Results of a phase II double-blinded randomized clinical trial of difluoromethylornithine for cervical intraepithelial neoplasia grades 2 to 3. Clin Cancer Res 2005;11:390-6.
10. Casero RA, Jr., Frydman B, Stewart TM, Woster PM. Significance of targeting

polyamine metabolism as an antineoplastic strategy: unique targets for polyamine analogues. Proc West Pharmacol Soc 2005;48:24-30.

11. Marton LJ, Pegg AE. Polyamines as targets for therapeutic intervention. Annu Rev Pharmacol Toxicol 1995;35:55-91.
12. Eliot AC, Kirsch JF. Pyridoxal phosphate enzymes: mechanistic, structural, and evolutionary considerations. Annu Rev Biochem 2004;73:383-415.
13. Christen P, Mehta PK. From cofactor to enzymes. The molecular evolution of pyridoxal-5'-phosphate-dependent enzymes. Chem Rec 2001;1:436-47.
14. Raso V, Stollar BD. The antibody-enzyme analogy. Characterization of antibodies to phosphopyridoxyltyrosine derivatives. Biochemistry 1975;14:584-91.
15. Heller JS CE, Bussolotti DL, Coward JK. Potent inhibition of ornithine decarboxylase by N-(5'-phosphopyridoxyl)-ornithine. Biochim Biophys Acta 1975;403:197-207.
16. Khomutov RM, Dixon HB, Vdovina LV, et al. N-(5'-phosphopyridoxyl)glutamic acid and N-(5'-phosphopyridoxyl)-2-oxopyrrolidine-5-carboxylic acid and their action on the apoenzyme of aspartate aminotransferase. Biochem J 1971;124:99-106.
17. Elbert A.Peterson HAS. Preparation of Crystalline Phosphorylated Derivatives of Vitamin B_6. J. Am. Chem. Soc. 1954;76:169-75.
18. Geistlich A, Gehring H. CDGF (chicken embryo fibroblast-derived growth factor) is mitogenically related to TGF-beta and modulates PDGF, bFGF, and IGF-I action on sparse NIH/3T3 cells. Exp Cell Res 1993;204:329-35.
19. Koga T, Nakano S, Nakayama M, et al. Identification and partial purification of a low-molecular-weight growth inhibitor formed by density-inhibited, tumorigenic V79 Chinese hamster cells. Cancer Res 1986;46:4431-7.
20. Gerhauser C, Mar W, Lee SK, et al. Rotenoids mediate potent cancer chemopreventive activity through transcriptional regulation of ornithine decarboxylase. Nat Med 1995;1:260-6.
21. Belyanskaya LL, Delattre O, Gehring H. Expression and subcellular

localization of Ewing sarcoma (EWS) protein is affected by the methylation process. Exp Cell Res 2003;288:374-81.

22. Nasizadeh S, Myhre L, Thiman L, et al. Importance of polyamines in cell cycle kinetics as studied in a transgenic system. Exp Cell Res 2005;308:254-64.
23. Dai H, Kramer DL, Yang C, et al. The polyamine oxidase inhibitor MDL-72,527 selectively induces apoptosis of transformed hematopoietic cells through lysosomotropic effects. Cancer Res 1999;59:4944-54.
24. Almrud JJ, Oliveira MA, Kern AD, et al. Crystal structure of human ornithine decarboxylase at 2.1 A resolution: structural insights to antizyme binding. J Mol Biol 2000;295:7-16.
25. Jackson LK, Brooks HB, Osterman AL, Goldsmith EJ, Phillips MA. Altering the reaction specificity of eukaryotic ornithine decarboxylase. Biochemistry 2000;39:11247-57.
26. Kuntz ID. Structure-based strategies for drug design and discovery. Science 1992;257:1078-82.
27. Bohm HJ. A novel computational tool for automated structure-based drug design. J Mol Recognit 1993;6:131-7.
28. Heiskala M, Zhang J, Hayashi S, Holtta E, Andersson LC. Translocation of ornithine decarboxylase to the surface membrane during cell activation and transformation. EMBO J 1999;18:1214-22.
29. Pomidor MM, Ruhl KK, Zheng P, et al. Relationship between ornithine decarboxylase and cytoskeletal organization in cultured human keratinocytes: cellular responses to phorbol esters, cytochalasins, and alpha-difluoromethylornithine. Exp Cell Res 1995;221:426-37.
30. Zhang Z, McCormick DB. Uptake and metabolism of N-(4'-pyridoxyl)amines by isolated rat liver cells. Arch Biochem Biophys 1992;294:394-7.
31. Zhang ZM, McCormick DB. Uptake of N-(4'-pyridoxyl)amines and release of amines by renal cells: a model for transporter-enhanced delivery of bioactive compounds. Proc Natl Acad Sci U S A 1991;88:10407-10.

32. Ogier G, Chantepie J, Deshayes C, et al. Contribution of 4-methylthio-2-oxobutanoate and its transaminase to the growth of methionine-dependent cells in culture. Effect of transaminase inhibitors. Biochem Pharmacol 1993;45:1631-44.

33. Tang L, Li MH, Cao P, et al. Crystal structure of pyridoxal kinase in complex with roscovitine and derivatives. J Biol Chem 2005;280:31220-9.

34. Robson LC, and Schwarz, MR. in Vitamin B6 Metabolism and Role in Growth. GP Tryfiates, editor. Westport Conn: Food and Nutrition Press; 1980. p.205.

35. Wallace HM, Fraser AV. Inhibitors of polyamine metabolism: review article. Amino Acids 2004;26:353-65.

36. Delcros JG, Tomasi S, Carrington S, et al. Effect of spermine conjugation on the cytotoxicity and cellular transport of acridine. J Med Chem 2002;45:5098-111.

37. Qu N, Ignatenko NA, Yamauchi P, et al. Inhibition of human ornithine decarboxylase activity by enantiomers of difluoromethylornithine. Biochem J 2003;375:465-70.

38. Vujcic S, Halmekyto M, Diegelman P, et al. Effects of conditional overexpression of spermidine/spermine N1-acetyltransferase on polyamine pool dynamics, cell growth, and sensitivity to polyamine analogs. J Biol Chem 2000;275:38319-28.

39. Duranton B, Holl V, Schneider Y, et al. Cytotoxic effects of the polyamine oxidase inactivator MDL 72527 to two human colon carcinoma cell lines SW480 and SW620. Cell Biol Toxicol 2002;18:381-96.

40. Eugene Kellogg G, Abraham DJ. Hydrophobicity: is LogP(o/w) more than the sum of its parts? Eur J Med Chem 2000;35:651-61.

41. Hui AM, Zhang W, Chen W, et al. Agents with selective estrogen receptor (ER) modulator activity induce apoptosis in vitro and in vivo in ER-negative glioma cells. Cancer Res 2004;64:9115-23.

2.8 Supplemental Data

Figure S1. Nanoelectrospray Mass Spectra of POB.

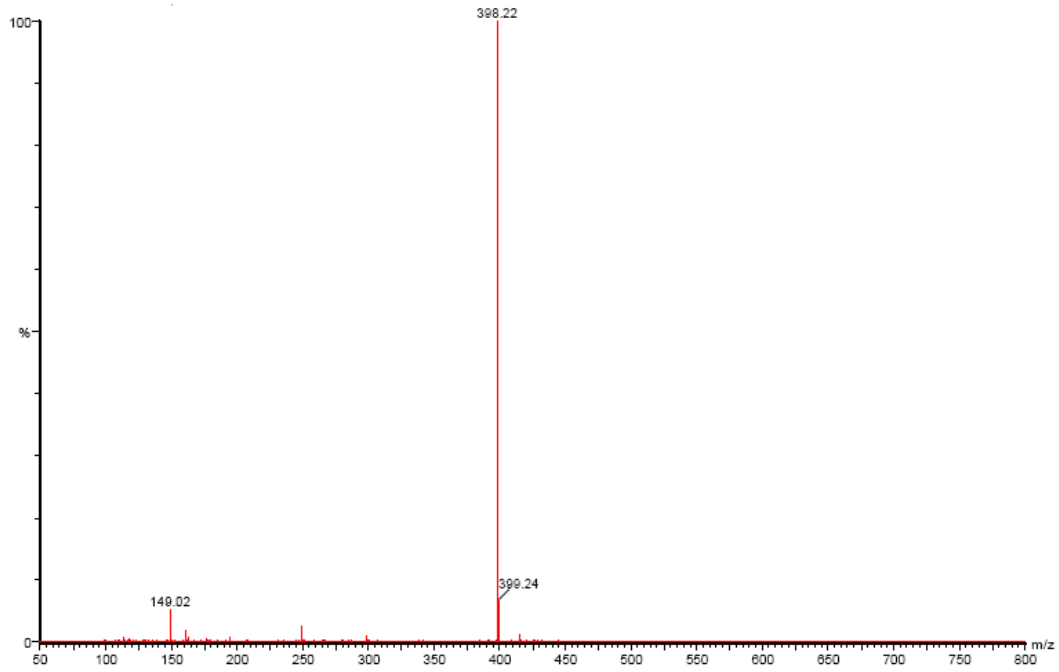

Figure S2. Western blot analysis of ODC after treatment of COS7 cells with POB (100 μM) and DFMO (500 μM) for 2 days. Cells were then collected and lysed. Two fold Laemmli buffer was added to aliquots of the supernatant. The same amount (20 μg) of total proteins was subjected to SDS-PAGE. The main band around 53 KD represents ODC.

Control	DFMO	POB
100%	160%	70%

Figure S3. Cell morphology and cell culture images. A, LN229 cells were treated with POB (100 μM) or DFMO (500 μM) for 3 days. B, COS7 cells were treated with POB (100 μM) for 2 days and stained with trypan blue. The black dots (right picture) indicated dead cells after trypan blue staining. Bar, 50 μm. C, SW2 cells were treated with POB (100 μM) for one day. Images from culture plates were made with an NIKON inverse light microscopy.

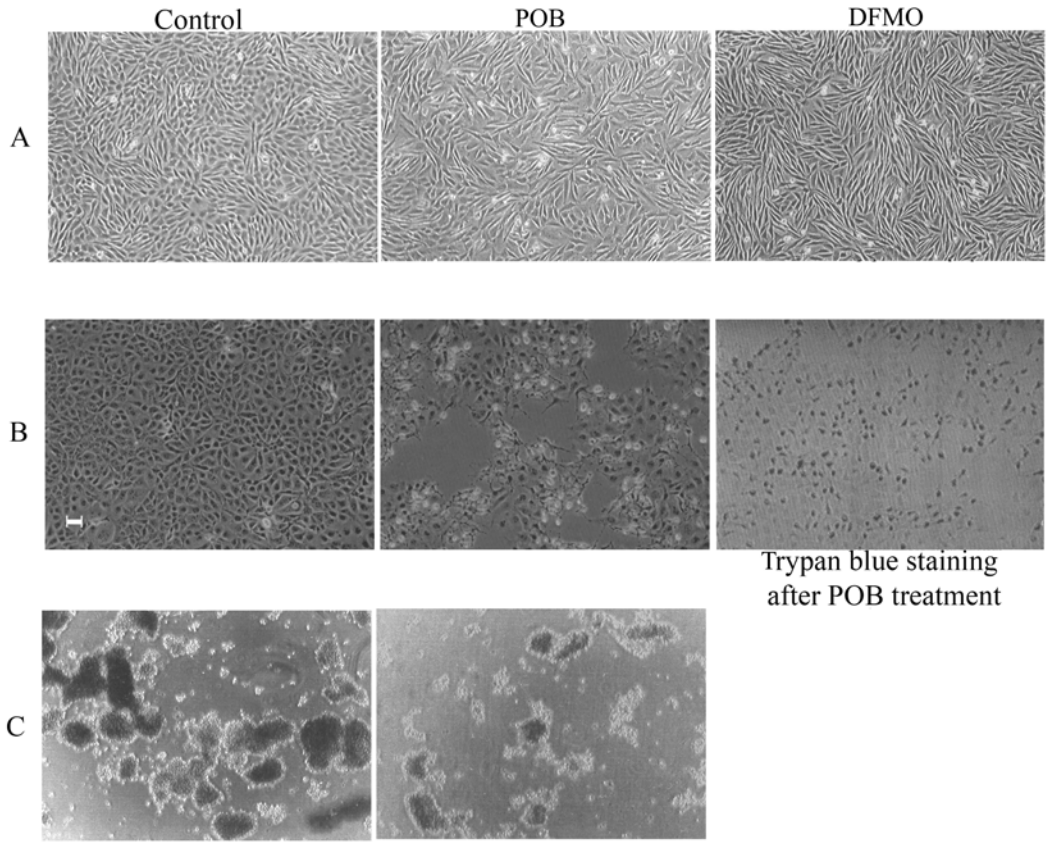

Figure S4. **Effect of added polyamines on cell growth inhibition caused by POB or DFMO**. LN229 cells were and treated as indicated in the figure for 4 days in the presence of 2 mM aminoguanidine (an inhibitor of serum oxidase). Error bars represent the standard deviation.

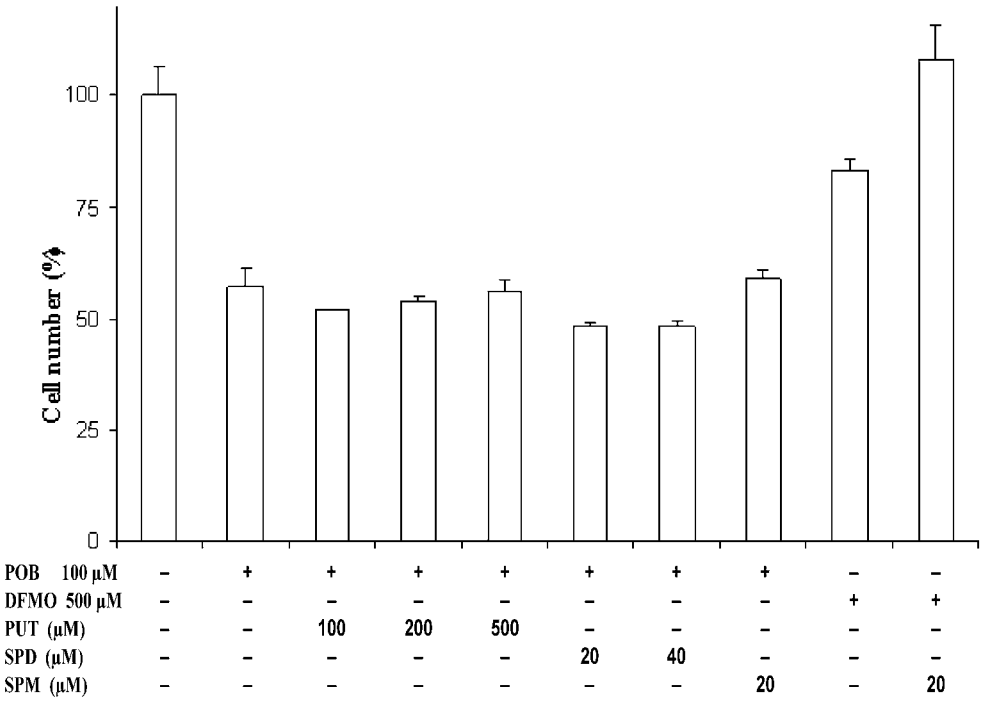

Figure S5. Polyamine contents in LN229 cells. LN229 cells were treated without (o) or with POB (■, 100 μM) for the indicated days. Cultures were then harvested and acid-soluble polyamine and cell number were determined as indicated in the Materials and Methods. Error bars represent the standard deviation.

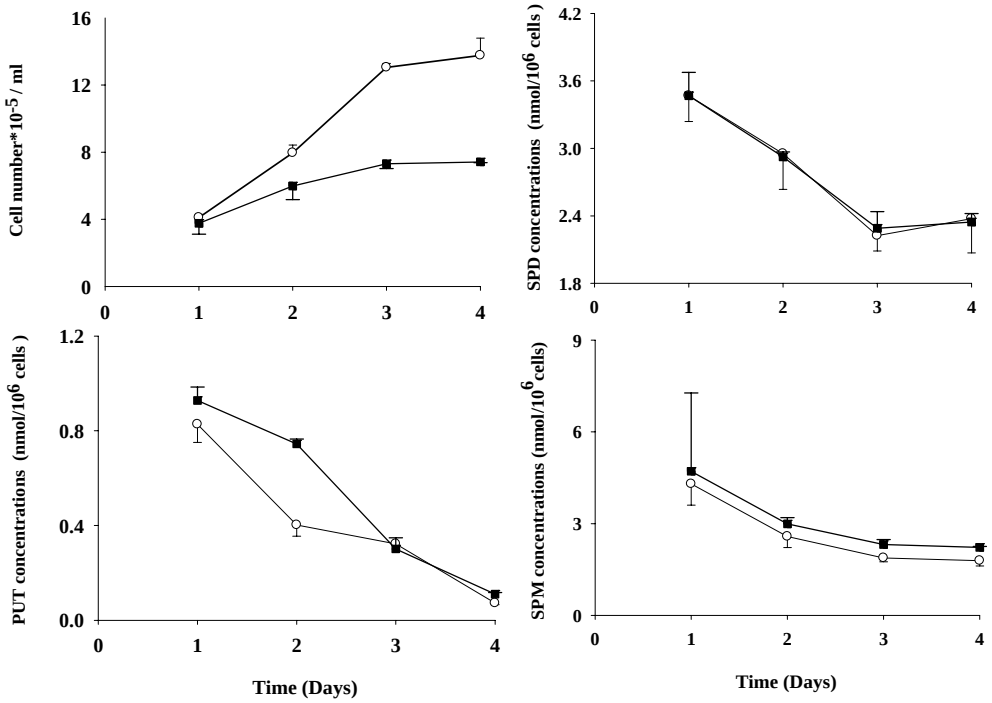

Figure S6. Induction of polyamine oxidase activity by POB. LN229 cells were treated with inhibitors (indicated in the figure) or without treatment (100%) for two days. Then cells were collected, lysed and polyamine oxidase acivity was measured as described in the Materials and Methods.

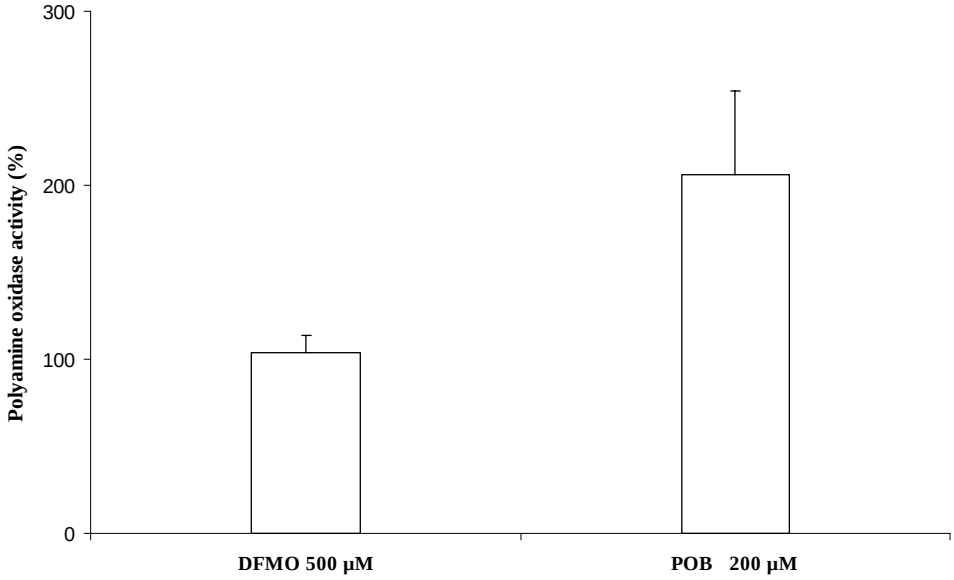

3. Structural requirements for novel coenzyme-substrate derivatives to inhibit intracellular ornithine decarboxylase and cell proliferation

Fang Wu, Lo Persson and Heinz Gehring

3.1 Abstract:

Transition-state-based inhibitors bind with high affinity to their target enzymes. Mimics of a transition-state intermediate of pyridoxal 5'-phosphate-dependent enzymic reactions were used to study the structural requirements for optimal inhibition of intracellular ornithine decarboxylase and proliferation of tumor cells. Previously, we had developed such a coenzyme-substrate analog (POB) as a new inhibitor of the short-lived inducible intracellular human ornithine decarboxylase (ODC). In the present study, structurally diverse enzyme-substrate mimics were designed, synthesized and tested for their inhibitory potential. Out of 23 conjugates, phosphopyridoxyl- and pyridoxyl-tryptophan methyl ester (pPTME, PTME) proved significantly more potent in proliferation inhibition of LN229 cells than POB, and particularly more than alpha-DL-difluoromethylornithine, a medically used irreversible inhibitor of ODC. All the active compounds have a hydrophobic side chain fragment and a kind of polyamine motif (-NH-$(CH_X)_4$-NH-). As predicted from the molecular modeling results, the binding affinity of pPTME and PTME was higher than that of POB. Phosphorylated pPTME and PTME strongly inhibited intracellular ODC activity of LN229 cells at a concentration of 50 μM and 100 μM, respectively. PTME, pPTME and POB induce, as polyamine analogs do, the activity of the enzymes of the polyamine catabolism, polyamine oxidase and spermine/spermidine *N*1-acetyltransferase, up to 250% and 780%, respectively. The dual mode of these compounds in LN229 cells, i.e. inhibition of ODC and induction of polyamine catabolic enzymes, influences the intracellular polyamine pools and might underlie their inhibitory effect on cell proliferation that compares favorably with that of difluoromethylornithine.

3.2 Introduction

Polyamine (PA) metabolism is closely linked to cancer and other hyperproliferative diseases and offers numerous potential targets for anti-cancer or chemopreventive agents (1). Biosynthesis, catabolism and transport of PAs interplay in a complex system still not fully understood (2). Ornithine decarboxylase (ODC), catalyzes the first and rate-limiting step in PA biosynthesis converting ornithine into putrescine (PUT) and is a highly inducible pyridoxal 5'-phosphate (PLP)-dependent enzyme with a half life of only 20 ~ 60 min (3). PUT is further transformed into spermidine (SPD) and SPD into spermine (SPM), the multi-charged PAs, by spermine/spermidine synthase, respectively (2, 4). Spermine/spermidine *N*1-acetyltransferase (SSAT) and polyamine oxidase (PAO) are inducible enzymes of the PA catabolism and produce PUT or SPD in a two-step process from SPD or SPM, respectively (1). Cells are also able to import and export PAs by an ATP-dependent and selective PA transporter, which is still not well characterized (3, 5).

ODC expression is rapidly induced after exposing cells with cell proliferation-stimulating agents (6-8). High levels of ODC observed in cancer cells are closely related to tumor promotion (3, 9). Overexpression of ODC induces transformation of cells (10) and inhibition of ODC abolishes transformation and is associated with tumor suppression (6, 11). Even modest reductions in ODC activity can lead to markedly reduced tumor development (6, 11). ODC-overexpressing cells are tumorigenic and expression of ODC in hair follicle cells is linked to growth and maintenance of hair follicles (12). Thus, ODC is a target in the development of anti-proliferative agents (3, 6). The most widely used inhibitor of ODC is α-DL-difluoromethylornithine (DFMO). This enzyme-activated irreversible inhibitor efficiently depletes intracellular PUT and SPD (13). DFMO shows a beneficial selectivity against tumor over normal cells by targeting the overexpressed ODC (1). Clinical studies proved that DFMO is a well-tolerated agent but not as efficient, as initially thought, to treat cancer (1, 14, 15). Never the less, some positive results have

been achieved in recurrent anaplastic gliomas (16, 17). Synthetic PA mimics or analogs, as well as natural PA derivatives, also decrease tumor cell growth rapidly together with or without depletion of intracellular PA pools (2, 18). In contrast to DFMO, these agents strongly induce the activity of SSAT and PAO, the polyamine catabolic enzymes, and downregulate ODC by a cellular feedback mechanism without directly inhibiting ODC activity (1). Different derivatives of SPD and SPM are currently in pre-clinical or clinical studies be it as a single agent or in combination with other drugs (3). However, they seem to exert, like SPM, unacceptable toxicities (1, 3). Therefore, novel types of inhibitors acting in the PA metabolism, which overcome or diminish these problems are in high demand.

Creating mimics of transition-state intermediates of enzymic reactions is a powerful strategy in developing potent and specific inhibitors for enzymes (19, 20). PLP is the cofactor of vitamin B_6-dependent enzymes, which catalyze a wide variety of amino acid transformations (21, 22). PLP binds with high affinity ($K_m \sim 90$ nM) to rat ODC (23). An obligatory step in all these reactions is the intermediary formation of an aldimine, i.e., a Schiff base of PLP with the α-amino group of the amino acid substrate. Reduction of the aldimine double bond produces phosphopyridoxyl-amino acids, which are analogs of the covalent coenzyme-substrate adducts. These compounds are a kind of transition-state analogs that bind to the apoprotein with high affinity (24-26). They cannot be transformed by the enzymes and thus inhibit them very potently. A further advantage of these analogs of coenzyme-substrate adducts is the high degree of specificity for the corresponding apoenzyme (25, 27, 28).

Based on this knowledge, we recently developed a strategy to deliver such a Schiff base analog as bioavailable prodrug for intracellular ODC (27). The precursor inhibitor POB, a pyridoxyl-ornithine methyl ester conjugate, which was taken up by cells and assumed to be phosphorylated by intracellular pyridoxal kinase (29, 30), efficiently suppressed ornithine decarboxylase activity in cells and the proliferation of many types of tumor cell lines with a better efficiency than DFMO, the most widely used inhibitor of ODC, and without affecting the proliferation of human non-tumorigenic smooth muscle cells (27). The inhibitory action caused by POB

(pyridoxyl-ornithine(BOC)-OMe, compound **14** in Figure 1) is different from that of DFMO, and it seems that POB-derivatives might act as a kind of PA analog and interfere with the PA conversion and transport, a complex interplay, whose regulation is not yet understood (31-33).

To improve the inhibitory effect of this kind of inhibitors of intracellular hODC, the structural requirements for binding to and inhibiting hODC and for inhibiting cell proliferation were investigated. Based on the structural model described previously (27), various structurally diverse conjugates of pyridoxal (PL) or PLP and substrate or PA analogs were synthesized and tested as potentially improved inhibitors and/or as inactive analogs to explore the mode of action of these compounds. Only compounds that have a hydrophobic side chain and a motif of PA inhibited the activity of intracellular ODC, induced the SSAT and PAO activity, the intracellular PA catabolic enzymes, and suppressed the proliferation of LN229 cells.

3.3 Materials and Methods

Materials

Compounds **1** to **3** (tyrosine, alanine and lysine analogs) were kind gifts from Dr. P. Christen (Department of Biochemistry, University Zurich) (34, 35). The starting materials for synthesis of other compounds (Figure 1), were bought from commercial sources: His-OMe·2HCl from Bachem (Bubendorf, Switzerland) for compounds **4** and **9**; His·HCl (Sigma, Missouri, USA), **5**; His(1-Me)-OMe His·HCl (Bachem), **6**; histamine·2HCl (Sigma), **7** and **8**; Trp-OMe·HCl (Bachem), **10** to **13**; Orn(BOC)-OMe·HCl (BOM, Bachem), **14** and **15**; Phe-OMe·HCl (Bachem), **16**; ß-(3-pyridyl)-D-Ala-OMe·2 HCl (Bachem), **17**; α,γ-diaminobutyric acid(Boc)-OMe·HCl (Bachem), **18** and **19**; putrescine·2HCl (Fluka, Buchs, Switzerland) for **20**, spermidine·3HCl (Fluka) for **21** and **23**, and spermine·4HCl

(Fluka) for **22**. Compounds **11**, **13**, **15** and **19** were hydrolyzed by-products generated during synthesis. Protease inhibitors were obtained from Roche (Basel, Switzerland). L-[1-^{14}C]Acetyl CoA (55 mCi/mmol) and L-[1-^{14}C]ornithine (55 mCi/mmol) were from American Radiolabeled Chemicals Inc (Missouri, USA). Pyridoxal·HCl and pyridoxal 5'-phosphate were purchased from Fluka, pyridoxamine 5'-phosphate and aminoguanidine dicarbonate from Sigma, and BOC-protected lysine methyl ester (BOL; from Bachem).

Procedure for synthesis

Compounds **4** to **7**, **9** to **13** and **20** to **23** (Figure 1) were synthesized as described (36). Briefly, PL or PLP (1 mmol) and $NaHCO_3$ (2 mmol) were dissolved in 5 ml ethanol and the substrate analogs (1.05 mmol) together with $NaHCO_3$ (3 mmol) in 10 ml ethanol. Both solutions were mixed at 0 ºC and stirred at room temperature for 2 h. $NaBH_4$ (125 mg) was then added in small portions to the solution on ice. After 30 min acetic acid (100%) was added to pH 5 to stop the reaction. The solvents were removed with a vacuum dryer; the residue was dissolved in water and subjected to FPLC or HPLC for analysis and purification. Compounds **15** to **19** were synthesized as described for POB (compound **14,** see ref. 27). Compound **8** was obtained according to procedures described (37). Briefly, histamine (1.02 mmol) and KOH (4.2 mmol) was dissolved in 2.5 mL water and stirred at 0 °C for 10 min. Solid PL (1 mmol) was then added followed by ethanol (20 ml). The reaction mixture was stirred at 30 °C for 7 h and the solvent evaporated, yielding a white powder.

Compound **4** to **9** and **20** to **23** were analyzed and purified with FPLC equipped with a mono S HR5/5 column (Amersham pharmacia biotech, Sweden) and a multiwavelengh detector. The samples were loaded and separated with a flow rate of 0.5 ml/min using the following elution steps: 0-5 min, 100% solvent A (50 mM acetic acid pH 4.6) and 0% solvent B (50 mM acetic acid, pH 4.6, 1 M NaCl); 5-30 min, 0-100% B; 30-40 min, 100% B. Detection was at 290 nm. Compounds **10** to **19** were analyzed and purified with a Kromasil C_{18} column (4.6 × 250 mm; Akzo Nobel,

Sweden). The samples were loaded and separated with a flow rate of 0.15 ml/min using the following elution steps: 0-36 min, 100% solvent A (3% acetonitrile/0.1% TFA) and 0% solvent B (80% acetonitrile/0.1% TFA); 36-92 min, 0-80% B; 92-120 min, 80-100% B, followed by 100% B. Elution was recorded at 290 nm. A preparative Kromasil C_{18} column (50.8 × 250 mm; Akzo Nobel, Sweden) with a flow rate of 15 ml/min was used under the same conditions to prepare larger amounts of compounds. The purified compounds (purity >95%) were analyzed and verified by ESI-MS and ESI-MS-MS. All compounds were vacuum-dried several times after adding water and stored at a concentration of about 10 mM (aqueous stock solution) at –20 °C.

Cell culture

Glioma cell line LN229 (from brain) was a generous gift from Dr. K. Frei (Department of Neurosurgery, University Hospital Zurich). LN229 cells were maintained in DMEM supplemented with 1 g/L glucose, 10% FBS (Life Technologies), 20 μg/ml gentamycine (Fluka) in a humidified 5% CO_2 atmosphere at 37 °C. HMC-1 (a human mastocytoma cell line) cells were a generous gift from Dr J. Butterfield (Mayo Clinic, Rochester, Minn, USA) and maintained in Iscove's modified DMEM supplemented with 10% FBS in a humidified 5% CO_2 atmosphere at 37 °C. For measuring cell growth, cells were seeded (2.5 - 5 x 10^4 cells per well) and incubated in 0.5 ml medium containing 5% FBS or NBCS and 1% penicillin/streptomycin in 24-well plate. After one day, cells were incubated for the indicated times in the absence or presence of the compounds at the indicated concentrations. Cells were counted with a Coulter counter (ZM Coulter Electronics) as described (38).

Enzyme activities

ODC activity was measured by the released $^{14}CO_2$ from L-[1-^{14}C]ornithine as described (27). Polyamine oxidase activity was determined as described (31). LN229 cells were seeded in 6-well plates at a density of ~1.6 x 10^5 cells per well with 5%

FBS for one day and treated in the absence or presence of the indicated compound during 2 days. Cells were then lysed and polyamine oxidase activities measured. SSAT activity was determined essentially according to a published procedure (39). LN229 cells were seeded in 6-well plates at a density of ~1.6 x 10^5 cells per well with 5% FBS for one day and treated in the absence or presence of the indicated compound during 2 days. Cells were then lysed in 50 mM Tris-HCl (pH 7.8) by two cycles of freezing (liquid nitrogen) and thawing (37 °C, 2 min). After centrifugation, the supernatants (70 µL) were incubated with 0.4 µCi [^{14}C]acetyl-CoA and unlabeled spermidine (3 mM) for 15 min.

Molecular modeling

Modeling of phosphopyridoxyl conjugates into the active site of hODC was performed as described (27) for POB (Figure 1, **14**).

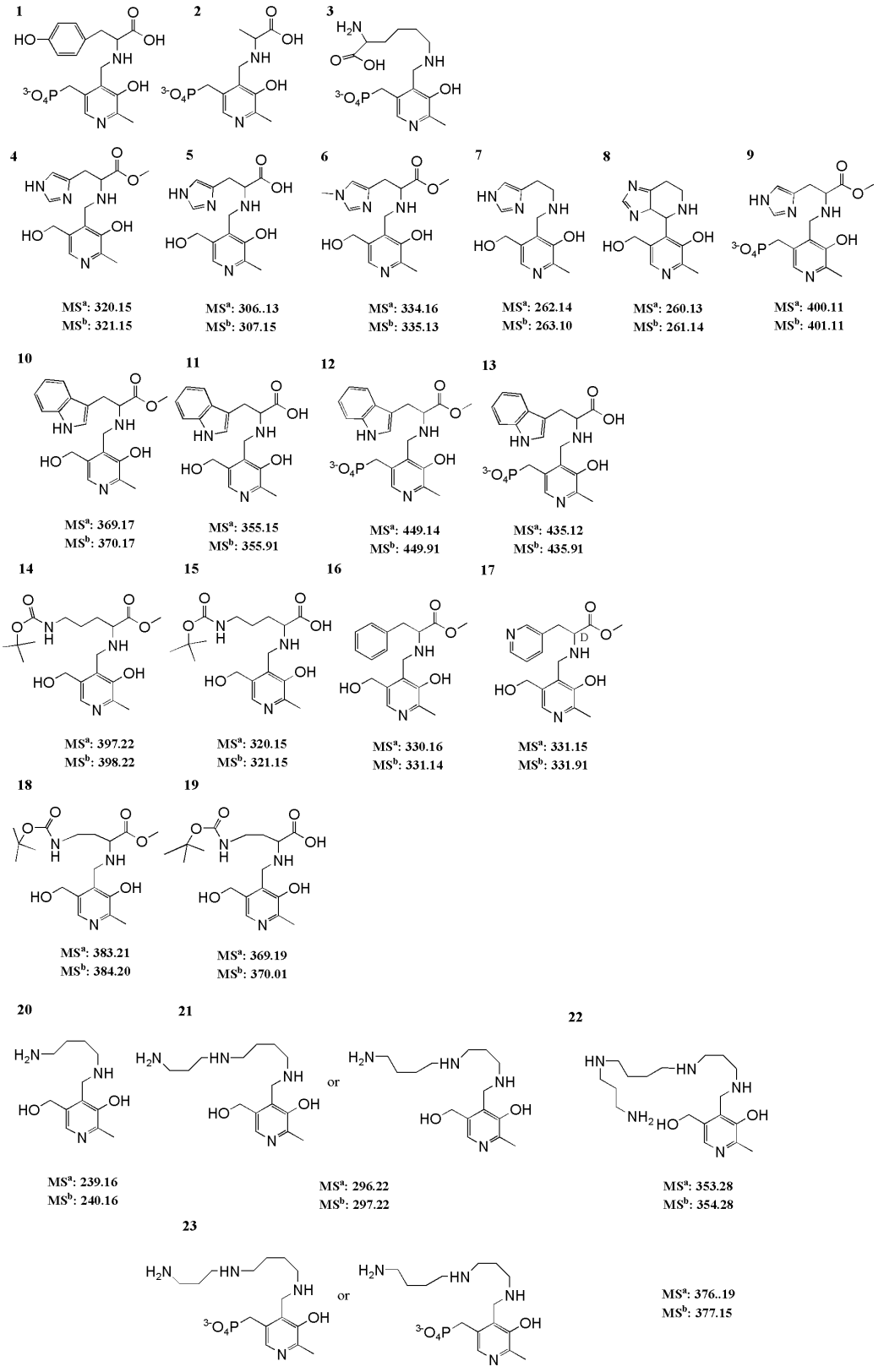

Fig. 1 Chemical structure of designed pyridoxyl-substrate derivatives.
The compounds were synthesized, purified and verified by ESI-MS methods as described in Materials and Methods. MS^a: theoretical mass. MS^b: measured mass $[M+H]^+$.

3.4 Results and Discussion

Inhibiting proliferation of tumor cells and cellular hODC

As demonstrated previously (27), a hydrophobic pocket is present at the active site of hODC, where the ε-amino group of ornithine is embedded between the two hODC subunits. The pocket is formed by the aromatic residues TyrA389, TyrA331, PheB397, and TyrB323. Only the dimer of ODC is catalytically active, as an active site consists of residues from both subunit A and B. This hydrophobic pocket is not occupied by the substrate ornithine (27) and can be utilized in designing hydrophobic derivatives of inhibitors with improved binding affinity. Indeed, this pocket favored the binding of the leading compound POB which carried a BOC group at the ε-amino group. Here we conjugated PL or PLP with different amino acid derivatives or PAs (**1** to **23**, Figure 1). As shown in Figure 2A, DFMO, the synthesized and purified (see Materials and Methods) vitamin B_6 conjugates **1** to **23** (Figure 1), the PAs (PUT, SPD, SPM) and the cellular active forms of vitamin B_6 (PL, PMP or PLP) as well as amino acid derivatives (BOM and BLM) were screened for their property to prevent proliferation of LN229 cells. Only the compounds **10**, **12**, **14**, **16** and **17** which contain a hydrophobic amino acid side chain such an aromatic ring or a BOC group together with a methyl ester at the α-carboxylate group inhibited proliferation of LN229 cell at 100 μM concentration more or equally efficiently than DFMO at 500 μM concentration. Cell inhibition was totally abolished, if the side chain of the conjugate was positively (**4-9** and **20-23**) or negatively charged (**3**) (Figure 2A). The de-esterified forms (**11**, **13**, and **15**) of compound **10**, **12** and **14** also lost the inhibitory effect. Thus, a bulky hydrophobic group in the side chain favors the binding to ODC and the methyl esterification seems to be crucial for uptake into cells (27).

In agreement with their inhibitory effect on cell proliferation inhibition, pyridoxyl- and phosphopyridoxyl-L-tryptophan methyl ester (PTME, **10** and pPTME**, 12**), the BOC-protected pyridoxyl-L-ornithine methyl ester (POB, **14**) and the pyridoxyl-L-phenylalanine methyl ester (**16**) also significantly affected serum-induced intracellular ODC activity, while conjugates with an imidazole motif (**4-6**), pyridine

D-alanine methyl ester (**17**) or BOC-protected α, γ-diaminobutyric acid methyl ester (**18**) did not (Figure 2B). Phosphorylated PTME (**12**) suppressed the induced intracellular ODC activity nearly completely if LN229 cells were treated at a concentration of 50 µM for 3 days, an inhibition comparable to that with PTME (**10**) and POB (**14**) at 100 µM (Figure 2B). The pPTME and phosphopyridoxyl-L-tryptophan (**13**, Figure 1), that is the cellular active form of pPTME and PTME, were found to inhibit the ODC activity in LN229 cell extracts with an IC_{50} ~ 50 µM, whereas unphosphorylated PTME, POB, **16** and **17** as well as compound **18** did not. The simple conjugates pyridoxyl-ornithine and pyridoxyl-lysine failed to inhibit cell proliferation and the activity of ODC *in vitro* (25) as we observed with pyridoxyl-putrescine (**20,** Figure 1 and Figure 2A).

The inhibition of cell proliferation and ODC activity by compounds bearing an ornithine-like side chain with a -NH-$(CH_x)_4$-NH- motif (**10**, **12** and **14)** was more pronounced than that of compounds lacking the distal N atom in the side chain (**16**) or having it in the wrong position (**18** and **19)**. Compound **18,** a mimic of POB, was synthesized as a control compound. It has a hydrophobic BOC group but one methylene group less and a -NH-$(CH_2)_3$-NH- motif instead of the -NH-$(CH_x)_4$-NH-PA motif. The missing inhibition of hODC and cell proliferation of the various compounds (Figure 2) strongly indicates that the inhibitory effect of POB, pPTME and PTME is due to quite specific interactions. Pyridoxyl-L-lysine, with a -NH-$(CH_2)_5$-NH- motif, is not an inhibitor of hODC *in vitro* either, as reported (25).

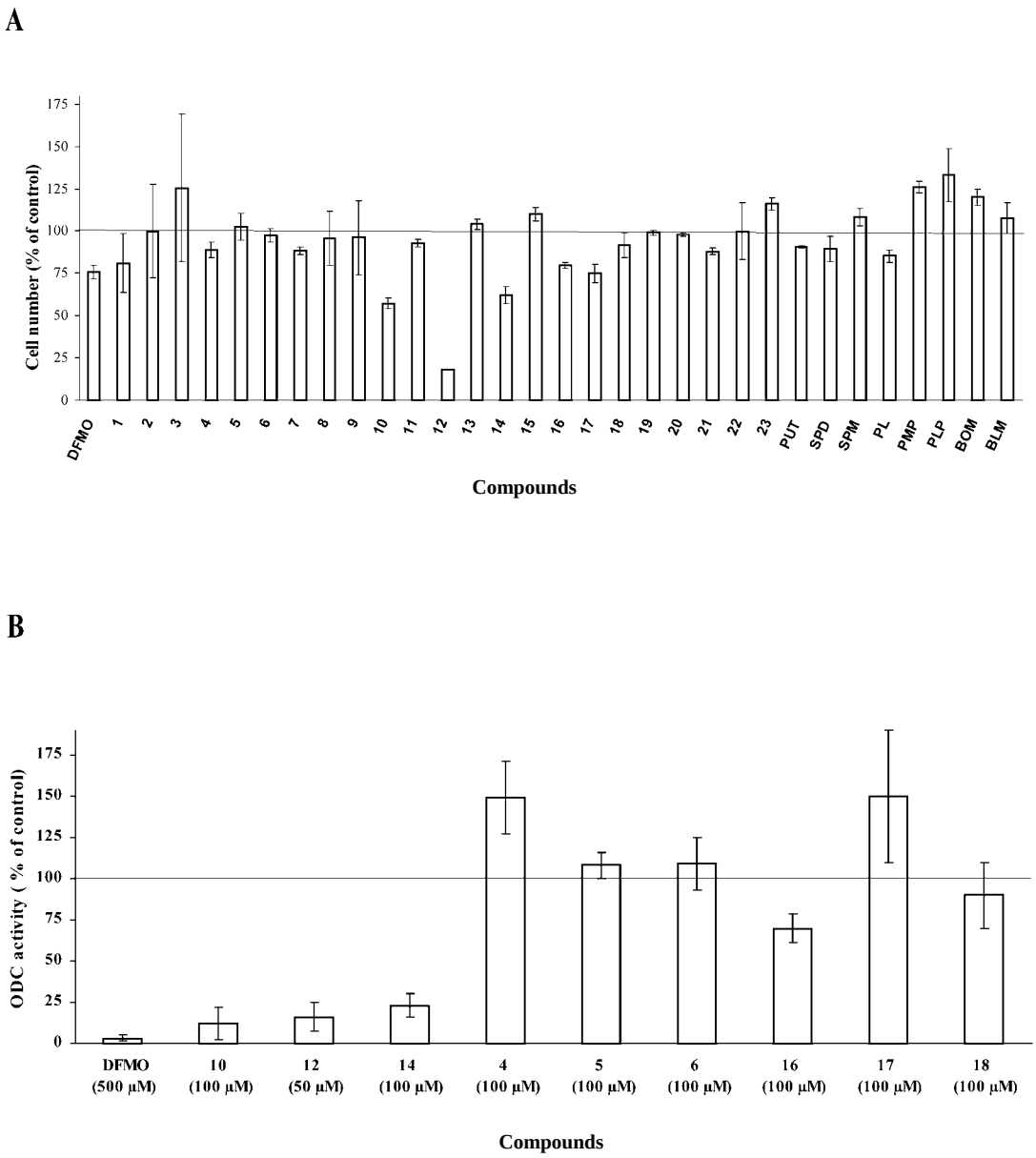

Fig. 2 Effect of pyridoxyl-substrate derivatives on cells.

A) Effect on cell proliferation. Glioma LN229 cells were treated for 3 days with the indicated compounds. DFMO, α-DL-difluoromethylornithine; compounds **1 to 23** (Fig. 1); PUT, putrescine; SPD, spermidine; SPM, spermine; PL, pyridoxal; PMP, pyridoxamine 5'-phosphate; PLP, pyridoxal 5'-phosphate; BOM, BOC-protected ornithine methyl ester and BLM, BOC- protected lysine methyl ester. The concentration used was 100 µM except for DFMO (500 µM), compound **12** (50 µM), PLP, BOM and BOL (200 µM each). Cells were counted as described in Materials and Methods. Error bars represent the standard deviation (n=3). To prevent exogenous oxidation of PUT, SPD and SPM, 2 mM aminoguanidine was added to inhibit serum oxidases.

B) Effect on serum-induced intracellular ODC activity. LN229 cells were treated with the indicated compounds for 3 days. Cells were collected, lysed and ODC activity was measured as described in Materials and Methods. Error bars represent the standard deviation (n=3).

The conjugate of pyridoxal with pyridyl-D-alanine methyl ester (**17**), which has a -NH-$(CH_x)_4$-NH- motif and a hydrophobic side chain but a D instead of a L chiral centre, showed no inhibition of hODC activity in cells and in cell extracts. These results demonstrate that maintaining the -NH-$(CH_x)_4$-NH- motif of the L-ornithine backbone is essential for binding to ODC and that additional hydrophobic modifications at the ε-amino group of ornithine or appropriate bulky hydrophobic side chains increase the binding affinity. PTME and pPTME (**10** and **12**) were the most potent inhibitors of cell proliferation of LN229 cells (Figure 1) with an IC_{50} value ~ 25 μM and ~ 50 μM, respectively (Figure 3). The phosphorylated PTME exceeded the potency of POB, the previously reported leading compound **14** (27), due to better binding properties and uptake kineticses, indicated by an earlier cell growth arrest of pPTME and PTME than with POB. After a one-day treatment, the inhibition was already comparable to that of POB after two-days (data not shown).

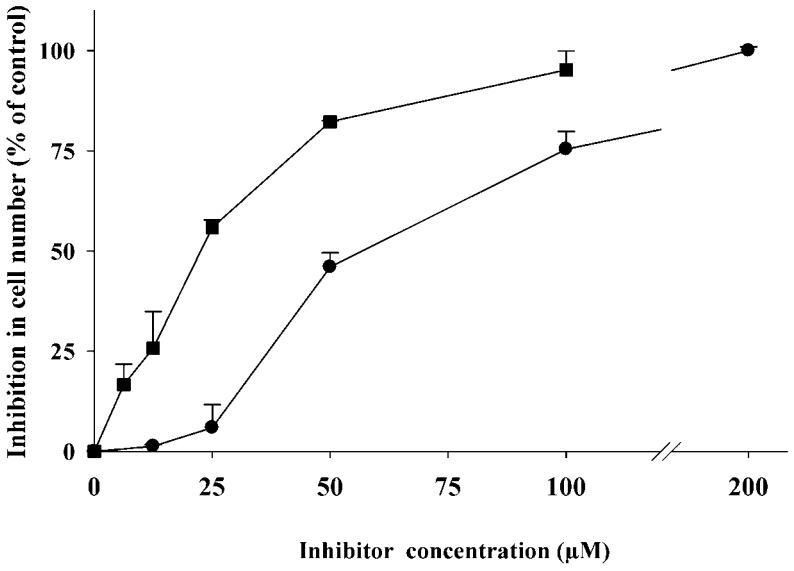

Fig. 3 Dose-dependent cell growth inhibition by PTME (10) and pPTME (12). Glioma LN229 cells were incubated with different concentrations of PTME (●) or with pPTME (■) for 3 days, counted and compared with the untreated controls (0%). Error bars represent the standard deviation (n=3).

Binding mode of designed compounds

The presumably active form of PTME (**10**) and pPTME (**12**) in the cell is phosphopyridoxyl-tryptophan (**13**, Figure 1). A binding model of compound **13** was constructed by molecular modeling (see Materials and Methods, Figure 4A). It showed a tight interaction with hODC. The side chain of tryptophan is embedded in a hydrophobic pocket composed of resides TyrA331, TyrA389, TyrB323 and PheB397, and binding is supported by stacking effects between the aromatic rings of the indole (white in Figure 4A) and tyrosine TyrA389. The N atom of the indole ring is able to form a hydrogen bond with the Asp332 (Figure 4A), which is situated at the entrance of the hydrophobic pocket and normally interacts with the ε-amino group of ornithine (40). The presumed intracellular forms of the inactive compounds **17** and **18** cannot properly occupy the cofactor or substrate binding site and lack the favorable interactions (Figure 4B, red and brown). The substantial loss of affinity of compound **4** with an imidazole ring (cyan, Figure 4B) or of **16** with a bulky hydrophobic benzene ring (blue), could be due to the loss of this hydrogen bond and less pronounced hydrophobic interactions and ring stacking effect.

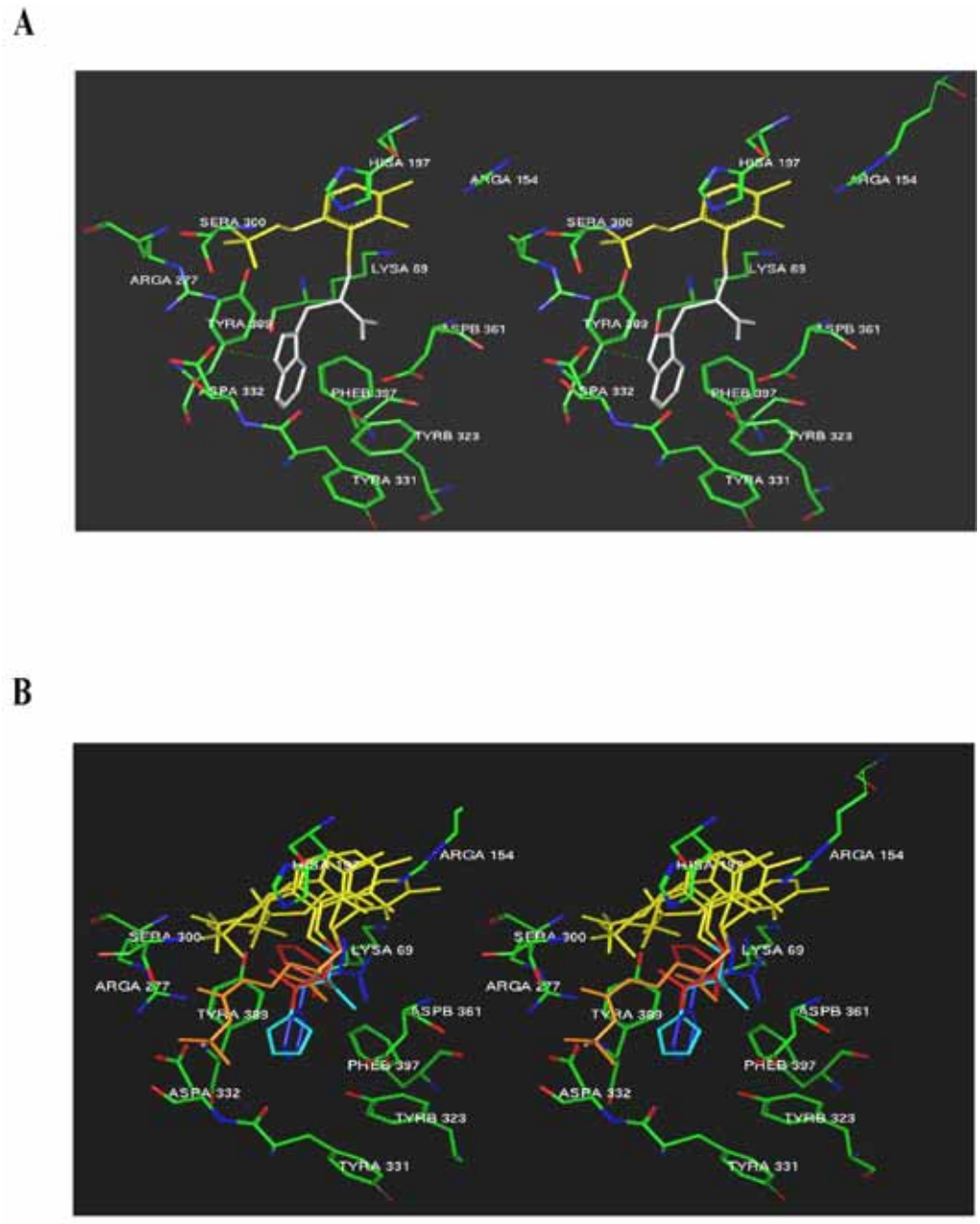

Fig. 4 Stereo view of the binding model of the phosphopyridoxyl conjugates in the active site of hODC

A) The putative strong binding mode of phosphopyridoxyl (yellow)-tryptophan (white). The active site residues within 3 Å of the phosphopyridoxyl-tryptophan conjugate and the hydrogen bond between phosphopyridoxyl-tryptophan and Asp332 are displayed in green. B) The putative binding mode of phosphopyridoxyl (yellow)-histidine (cyan), phosphopyridoxyl-phenylalanine (blue), phosphopyridoxyl -pyridine-D-Ala (red) and the BOC-protected phosphopyridoxyl -α,γ-diaminobutyric acid (brown).

Mode of action of the designed inhibitory compounds

DFMO, the suicide inhibitor of ODC, irreversibly binds to the active site of the holo enzyme by covalently attaching to Cys360. Cell inhibition caused by DFMO can be reversed by adding PAs to the cells (41). This effect was considered as one of the reason for the low efficiency of DFMO (3). PTME and pPTME (**10** and **12**) inhibited the proliferation of tumor cells more efficiently than DFMO but their inhibition of LN229 and HMC-1 cells could not be reversed by adding PAs (Figure 5) as was already observed and discussed with POB (27). This observation strongly indicates that pyridoxyl-amino acid derivatives inhibit cell growth not only by depletion of endogenous PAs but also by perturbing the complex PA metabolism in other ways.

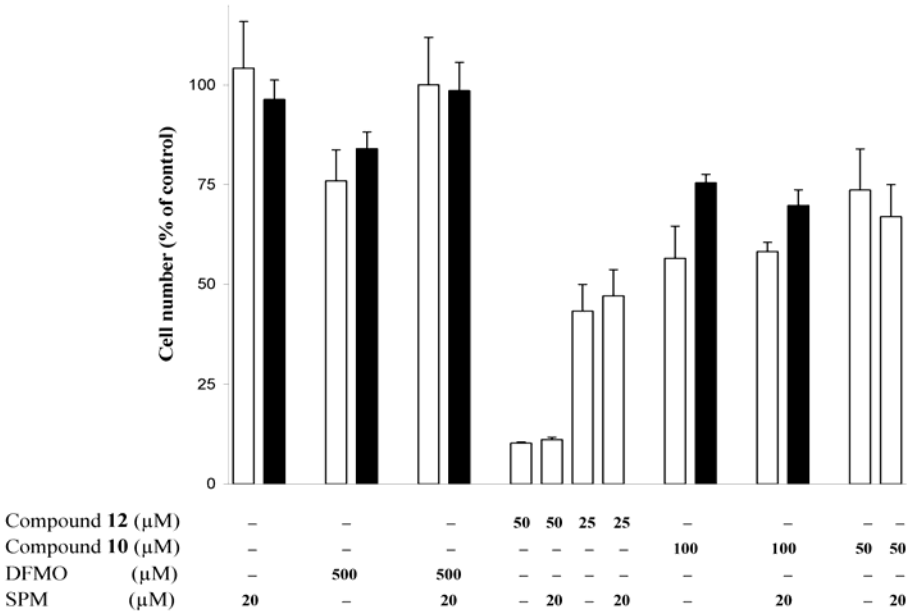

Fig. 5 Effect of exogenous polyamines on cell growth inhibition.
LN229 cells were treated or not (control, 100%) as indicated during 3 days in the presence of 2 mM aminoguanidine, which inhibits the oxidation of polyamines by serum oxidases. White column, LN229 cells; Black column, HMC-1 cells. Error bars represent the standard deviation (n=3).

PA analogs strongly induce the catabolic enzymes SSAT and PAO of PA metabolism by acting in a complex PA regulatory system (42, 43) and stop cell proliferation with or without depleting the PA pools (2, 18). POB suppressed the

proliferation of many types of tumor cells without depleting the intracellular PA pools more than in the control (27). PTME and pPTME inhibited cell growth more strongly than POB and did also not deplete intracellular PA. The putrescine, spermidine and spermine concentration in LN229 cells treated with 100 μM PTME for 3 days, were 0.4, 2.7 and 3.6 nmol per 10^6 cells, respectively. The corresponding values for untreated LN229 cells were 0.2, 2.4 and 3.0 nmol per 10^6 cells, respectively. Reasons for maintaining the intracellular PA concentration could be that, despite the inhibition of intracellular ODC, the intracellular conversion of PAs is accelerated by PTME, pPTME and POB through enzyme induction. Indeed, intracellular PAO activity was upregulated to 195%, 270% and 206%, when LN229 cells were incubated for 2 days at the indicated concentrations of PTME, pPTME and POB, respectively (Figure 6A). DFMO (500 μM) and other conjugates had no effect. SSAT activity of LN229 cells, under the same conditions, was also induced to 620%, 790% and 194%, respectively, whereas DFMO had no such effect (Figure 6B). Probably, the PA motif (-NH-$(CH_x)_4$–NH-) present in PTME, pPTME and POB seems to be recognized by the PA regulatory system and thus induces the PA catabolic enzymes. The upregulation of PA catabolism might explain why this kind of inhibitors exert a more pronounced inhibition of cell growth than DFMO, which did not influence PAO and SSAT activity. Instead of only inhibiting intracellular hODC, these particular pyridoxyl-amino acid derivatives seem to act as PA analogs and induce SSAT and PAO. In the PAO-catalyzed reaction, H_2O_2 is produced, which is regarded as the main reason of cell death caused by PA analogs (1). The induced catabolism of PA regenerates PUT and SPD from SPD and SPM, respectively (44), and might explain why the PAs were not completely depleted even if ODC was inhibited.

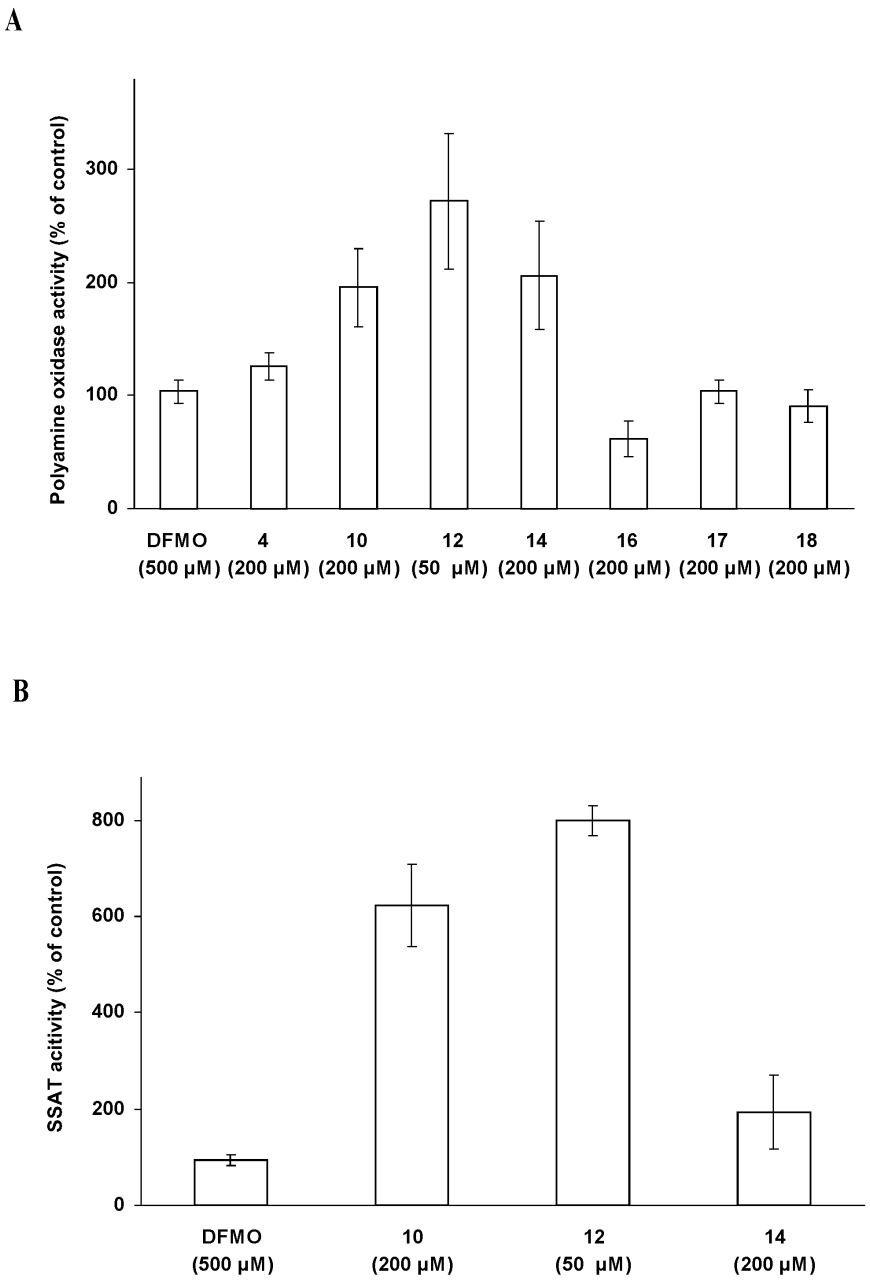

Fig. 6 Effect of pyridoxyl-substrate derivatives on polyamine catabolic enzymes. LN229 cells were treated with the indicated compounds or not (control, 100%) for two days. Cells were collected, lysed and the activity of polyamine oxidase (A) or of spermine/spermidine *N*1-acetyltransferase (B) measured as described in the Materials and Methods. Error bars represent the standard deviation (for A, n=3; for B, n=2).

Remarkably in this context is that the phosphorylated derivative of PTME **12** was able to inhibit intracellular ODC and cell proliferation, indicating that it is taken up by cells. Apparently, its hydrophobicity is such that it can pass the cell membrane. Its overall clogP of 1.1, which is in the range of cell-permeable compounds (45), and the

strong retardation of pPTME on a C_{18} column (eluted only with 100% solvent B, see Materials and Methods) support this conclusion. Because it is already phosphorylated, it will be more prone to bind to freshly synthesized apoODC than unphosphorylated conjugates, which have to be phosphorylated in cells by pyridoxal kinase.

In conclusion, the application of structurally diverse compounds to map the binding requirement of ODC proved an efficient tool to develop new inhibitors. ODC inhibitors of the kind presented in this study seem to be efficient agents for preventing proliferation of tumors cells. Besides ODC inhibition, the compounds PTME, pPTME and POB, which share the same PA motif (-NH-$(CH_x)_4$-NH-) (Figure 7), exert an additional effect, which seems to derive from mimicking PA by their ability to induce the PA catabolic enzymes SSAT and PAO. The overall action of these compounds on cells combines both, the effect of ODC inhibitors and that of PA analogs. In the search for alternative new therapeutic agents to treat malignant tumors such as gliomas the inhibitory pyridoxyl-derivatives as summarized and defined in Figure 7 could be used as lead compounds for developing even better inhibitors.

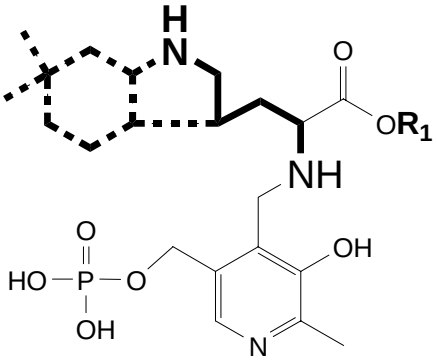

Fig. 7 Schematic representation of active inhibitors.

Bold solid line, the required -N-$(CH_x)_4$-N- motif; bold dashed line, overlap of the skeleton of the hydrophobic fragments supporting binding. R_1, moiety required for cell permeability.

3.5 Acknowledgment

We acknowledge the financial support by COST Switzerland (Action 922, Grant number C02.0017). We thank Dr. S. Bienz and collaborators (Institute of Organic Chemistry, University Zurich) for the assistance in the synthesis of the designed analogs. Dr. K. Frei for kindly providing glioma cell lines, Dr. P. Christen (Department of Biochemistry, University Zurich) for providing us with some of the compounds and for critical reading of the manuscript, Dr. J. Butterfield and co-workers for providing HMC-1 cells, Dr. R. D. Walter and Dr. I. B. Müller for helpful discussions.

3.6 Reference

1. Casero RA, Jr., Marton LJ. Targeting polyamine metabolism and function in cancer and other hyperproliferative diseases. Nat Rev Drug Discov 2007;6:373-90.
2. Wallace HM, Fraser AV, Hughes A. A perspective of polyamine metabolism. Biochem J 2003;376:1-14.
3. Seiler N. Thirty years of polyamine-related approaches to cancer therapy. Retrospect and prospect. Part 1. Selective enzyme inhibitors. Curr Drug Targets 2003;4:537-64.
4. Jackson LK, Brooks HB, Myers DP, Phillips MA. Ornithine decarboxylase promotes catalysis by binding the carboxylate in a buried pocket containing phenylalanine 397. Biochemistry 2003;42:2933-40.
5. Igarashi K, Kashiwagi K. Polyamine transport in bacteria and yeast. Biochem J 1999;344 Pt 3:633-42.
6. Pegg AE. Regulation of ornithine decarboxylase. J Biol Chem 2006;281:14529-32.
7. Nickel KP, Belury MA. Inositol hexaphosphate reduces 12-O-tetradecanoylphorbol-13-acetate-induced ornithine decarboxylase independent of protein kinase C isoform expression in keratinocytes. Cancer Lett 1999;140:105-11.
8. Glikman P, Manni A, Demers L, Bartholomew M. Polyamine involvement in the growth of hormone-responsive and -resistant human breast cancer cells in culture. Cancer Res 1989;49:1371-6.
9. Gerner EW, Meyskens FL, Jr. Polyamines and cancer: old molecules, new understanding. Nat Rev Cancer 2004;4:781-92.
10. Auvinen M, Paasinen A, Andersson LC, Holtta E. Ornithine decarboxylase activity is critical for cell transformation. Nature 1992;360:355-8.
11. Nilsson JA, Keller UB, Baudino TA, et al. Targeting ornithine decarboxylase in Myc-induced lymphomagenesis prevents tumor formation. Cancer Cell 2005;7:433-44.
12. Wheeler DL, Ness KJ, Oberley TD, Verma AK. Inhibition of the development of metastatic squamous cell carcinoma in protein kinase C epsilon transgenic mice by alpha-difluoromethylornithine accompanied by marked hair follicle degeneration and hair loss. Cancer Res 2003;63:3037-42.
13. Qu N, Ignatenko NA, Yamauchi P, et al. Inhibition of human ornithine decarboxylase activity by enantiomers of difluoromethylornithine. Biochem J 2003;375:465-70.
14. Messing E, Kim KM, Sharkey F, et al. Randomized prospective phase III trial of difluoromethylornithine vs placebo in preventing recurrence of completely resected low risk superficial bladder cancer. J Urol 2006;176:500-4.
15. Vlastos AT, West LA, Atkinson EN, et al. Results of a phase II double-blinded randomized clinical trial of difluoromethylornithine for cervical intraepithelial neoplasia grades 2 to 3. Clin Cancer Res 2005;11:390-6.

16. Wallace HM, Fraser AV. Inhibitors of polyamine metabolism: review article. Amino Acids 2004;26:353-65.
17. Levin VA, Hess KR, Choucair A, et al. Phase III randomized study of postradiotherapy chemotherapy with combination alpha-difluoromethylornithine-PCV versus PCV for anaplastic gliomas. Clin Cancer Res 2003;9:981-90.
18. Fraser AV, Woster PM, Wallace HM. Induction of apoptosis in human leukaemic cells by IPENSpm, a novel polyamine analogue and anti-metabolite. Biochem J 2002;367:307-12.
19. Li CM, Tyler PC, Furneaux RH, et al. Transition-state analogs as inhibitors of human and malarial hypoxanthine-guanine phosphoribosyltransferases. Nat Struct Biol 1999;6:582-7.
20. Singh V, Evans GB, Lenz DH, et al. Femtomolar transition state analogue inhibitors of 5'-methylthioadenosine/S-adenosylhomocysteine nucleosidase from Escherichia coli. J Biol Chem 2005;280:18265-73.
21. Eliot AC, Kirsch JF. Pyridoxal phosphate enzymes: mechanistic, structural, and evolutionary considerations. Annu Rev Biochem 2004;73:383-415.
22. Christen P, Mehta PK. From cofactor to enzymes. The molecular evolution of pyridoxal-5'-phosphate-dependent enzymes. Chem Rec 2001;1:436-47.
23. Flamigni F, Guarnieri C, Caldarera CM. Characterization of highly purified ornithine decarboxylase from rat heart. Biochim Biophys Acta 1984;802:245-52.
24. Raso V, Stollar BD. The antibody-enzyme analogy. Characterization of antibodies to phosphopyridoxyltyrosine derivatives. Biochemistry 1975;14:584-91.
25. Heller JS CE, Bussolotti DL, Coward JK. Potent inhibition of ornithine decarboxylase by N-(5'-phosphopyridoxyl)-ornithine. Biochim Biophys Acta 1975;403:197-207.
26. Khomutov RM, Dixon HB, Vdovina LV, et al. N-(5'-phosphopyridoxyl)glutamic acid and N-(5'-phosphopyridoxyl)-2-oxopyrrolidine-5-carboxylic acid and their action on the apoenzyme of aspartate aminotransferase. Biochem J 1971;124:99-106.
27. Wu F, Grossenbacher D, Gehring H. New transition state-based inhibitor for human ornithine decarboxylase inhibits growth of tumor cells. Mol Cancer Ther 2007;6:1831-9.
28. Wu F, Yu J, Gehring H. Inhibitory and structural studies of novel coenzyme-substrate analogs of human histidine decarboxylase. Submitted 2007.
29. Zhang ZM, McCormick DB. Uptake of N-(4'-pyridoxyl)amines and release of amines by renal cells: a model for transporter-enhanced delivery of bioactive compounds. Proc Natl Acad Sci U S A 1991;88:10407-10.
30. Tang L, Li MH, Cao P, et al. Crystal structure of pyridoxal kinase in complex with roscovitine and derivatives. J Biol Chem 2005;280:31220-9.
31. Dai H, Kramer DL, Yang C, et al. The polyamine oxidase inhibitor

MDL-72,527 selectively induces apoptosis of transformed hematopoietic cells through lysosomotropic effects. Cancer Res 1999;59:4944-54.

32. Vujcic S, Halmekyto M, Diegelman P, et al. Effects of conditional overexpression of spermidine/spermine N1-acetyltransferase on polyamine pool dynamics, cell growth, and sensitivity to polyamine analogs. J Biol Chem 2000;275:38319-28.
33. Duranton B, Holl V, Schneider Y, et al. Cytotoxic effects of the polyamine oxidase inactivator MDL 72527 to two human colon carcinoma cell lines SW480 and SW620. Cell Biol Toxicol 2002;18:381-96.
34. Gramatikova SI, Christen P. Pyridoxal 5'-phosphate-dependent catalytic antibody. J Biol Chem 1996;271:30583-6.
35. Gramatikova S, Mouratou B, Stetefeld J, Mehta PK, Christen P. Pyridoxal-5'-phosphate-dependent catalytic antibodies. J Immunol Methods 2002;269:99-110.
36. Hidehiko KumagaI, Hideaki Yamada and Hiroshi Fukami. A Modified Method for Synthesis of Pyridoxylhistamine. Agr. Biol. Chem. 1969;33:1210-12.
37. Kametani T, Koizumi M, Okui K, Nishii Y, Ono M. Biochemical studies on drugs and the central nervous system. 1. Synthesis and activity of pyridoxal derivatives. (Studies on the syntheses of heterocyclic compounds. 438). J Med Chem 1972;15:203-4.
38. Geistlich A, Gehring H. CDGF (chicken embryo fibroblast-derived growth factor) is mitogenically related to TGF-beta and modulates PDGF, bFGF, and IGF-I action on sparse NIH/3T3 cells. Exp Cell Res 1993;204:329-35.
39. Ulrich S, Loitsch SM, Rau O, et al. Peroxisome proliferator-activated receptor gamma as a molecular target of resveratrol-induced modulation of polyamine metabolism. Cancer Res 2006;66:7348-54.
40. Jackson LK, Brooks HB, Osterman AL, Goldsmith EJ, Phillips MA. Altering the reaction specificity of eukaryotic ornithine decarboxylase. Biochemistry 2000;39:11247-57.
41. Wallick CJ, Gamper I, Thorne M, et al. Key role for p27Kip1, retinoblastoma protein Rb, and MYCN in polyamine inhibitor-induced G1 cell cycle arrest in MYCN-amplified human neuroblastoma cells. Oncogene 2005;24:5606-18.
42. Pavlov V, Lin PK, Rodilla V. Biochemical effects and growth inhibition in MCF-7 cells caused by novel sulphonamido oxa-polyamine derivatives. Cell Mol Life Sci 2002;59:715-23.
43. Vujcic S, Liang P, Diegelman P, Kramer DL, Porter CW. Genomic identification and biochemical characterization of the mammalian polyamine oxidase involved in polyamine back-conversion. Biochem J 2003;370:19-28.
44. Casero RA, Jr., Pegg AE. Spermidine/spermine N1-acetyltransferase--the turning point in polyamine metabolism. Faseb J 1993;7:653-61.
45. Lipinski CA, Lombardo F, Dominy BW, Feeney PJ. Experimental and computational approaches to estimate solubility and permeability in drug discovery and development settings. Adv Drug Deliv Rev 2001;46:3-26.

4. Inhibitory and structural studies of novel coenzyme-substrate analogs of human histidine decarboxylase

Fang Wu, Jing Yu, Heinz Gehring

4.1 ABSTRACT

Histamine, a biogenic amine with important biological functions, is produced from histidine by histidine decarboxylase (HDC), a pyridoxal 5'-phosphate (PLP)-dependent enzyme. HDC is thus a potential target to attenuate histamine production in certain pathological states. Targeting mammalian HDC with novel inhibitors and elucidating the structural basis of their specificity for HDC are challenging tasks, because the 3D structure of mammalian HDC is still unknown. In the present study, we designed, synthesized and tested potentially membrane-permeable pyridoxyl-substrate conjugates as inhibitors for human HDC and modeled an active site of hHDC, which is compatible with the experimental data. The most potent inhibitory compound among 9 tested structural variants was the pyridoxyl-histidine methyl ester conjugate (PHME), indicating that the binding site of hHDC does not tolerate other groups than the imidazole side chain of histidine. PHME inhibited 60% of TPA-induced newly synthesized HDC in human HMC-1 cells at 200 μM and was also inhibitory in cell extracts. The proposed model of hHDC, containing phosphopyridoxyl-histidine in the active site, revealed the binding specificity of HDC towards its substrate and the structure-activity relationship of the designed and investigated compounds.

4.2 INTRODUCTION

The biogenic amine histamine plays an important role in a number of physiological processes, including inflammatory as well as allergic reactions, control of gastric acid secretion and neurotransmission (1-5). Histidine decarboxylase (HDC), a pyridoxal 5'-phosphate (PLP) dependent homodimeric enzyme catalyzes the decarboxylation of histidine to histamine (**Fig. 1)** and is regarded as a potential target to attenuate histamine production in certain pathological states (3).

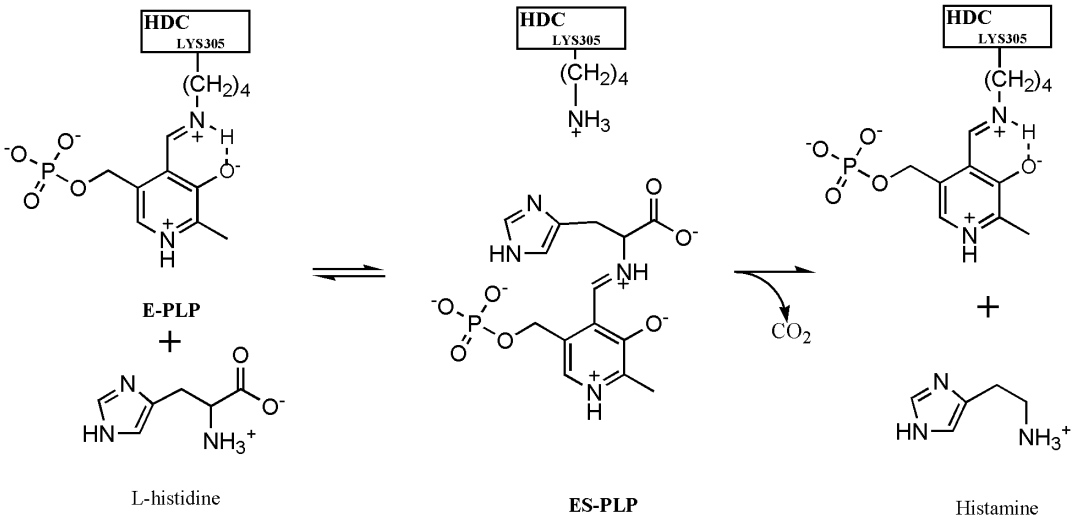

Figure 1. Reaction mechanism of ODC with L-histidine. E-PLP, HDC-pyridoxal 5'-phosphate (internal aldimine); ES-PLP, enzyme-coenzyme-substrate intermediate (external aldimine).

Human HDC is initially translated as a 74 kD form and then post-translationally processed to the 53–55 kD form through a complex reaction, which is catalyzed by caspase-9 and cleaves off a C-terminal part (1). HDC shares high homology (51% identity) in primary sequence with dopa or aromatic acid decarboxylase (6). The 74 kD form of HDC has a very low enzymic activity and is mainly recovered in the

insoluble fraction, whereas the 53-55 kD form is soluble and has a high activity if expressed in baculovirus-insect or mammalian cells (1). Endogenous hHDC is expressed only in histamine releasing cells such as mast cells, basophils, enterochromaffin-like cells in the stomach, neurons in the brain or macrophages (7).

To date, the crystal structure of mammalian HDC is unknown due to its difficulties in preparation, heterogeneity and instability (3, 6). A structure of dimeric rat HDC with the cofactor PLP has been constructed by homology modeling using pig dopa decarboxylase (DDC) with the inhibitor carbiDOPA (**Fig. 2*A*)** as template (3, 6, 8). The proposed model contains no ligand, the interactions of binding-site residues of HDC with its ligands still being undefined.

Numerous inhibitors of mammalian HDC have been developed (9, 10). Alpha-fluoromethylhistidine (FMH), an enzyme-activated irreversible inhibitor of mammalian as well as pyruvoyl-dependent bacterial HDC, covalently attaches to active site residues after being activated by HDC itself, an inhibitory mechanism similar to α-DL-difluoromethylornithine, a suicide inhibitor of ornithine decarboxylase (11, 12). Most other inhibitors are substrate analogs and inhibit the enzyme competitively. They have been developed in the seventies, by adding substituents to histidine in the hope to gaining additional affinity (13). However, the binding affinity did not improved much, with the methyl ester of histidine (HME, **Fig. 2*A***) being an exception (IC_{50} of ~ 1.8 μM, *in vitro*). Unfortunately, HME proved to be inactive in cells, because it is hydrolysed to histidine, the substrate of HDC, after being taken up by cells (10). Bacterial pyruvoyl-dependent HDC was also reported to be inhibited by HME *in vitro* (10). Recently, (–)-epigallocatechin-3-gallate extracted from green tea was reported to inhibit rat HDC *in vitro* and in rat RBL-2H3 cells (14), but it also inhibited other PLP-dependent enzymes, such as ornithine decarboxylase (15).

Pyridoxal 5'-phosphate (PLP) is the cofactor for numerous enzymes, which catalyze a wide variety of amino acid transformations (16, 17). The external aldimine, a Schiff base of PLP with the α-amino group of the amino acid substrate (**ES-PLP**, **Fig. 1**), is the common intermediate of all transformation of amino acid catalyzed by

PLP-dependent enzymes (16). A stable analog of PLP-substrate adducts can be obtained by reduction of the Schiff base producing phosphopyridoxyl-amino acids. Such analogs of coenzyme-substrate adducts are, for obvious reasons, high-affinity inhibitors for PLP-dependent apoenzymes (18, 19). Based on the knowledge that such analogs strongly interact with the corresponding apoenzymes, we recently developed a strategy for delivering a novel Schiff base analog as inhibitor for intracellular PLP-dependent human ornithine decarboxylase. The inhibitor, a phosphopyridoxyl-ornithine based precursor (POB), efficiently suppressed ornithine decarboxylase activity in cells and also cell proliferation (20).

To develop novel bioavailable inhibitors for mammalian HDC and explore their interaction with the active site of mammalian HDC, we designed and synthesized several pyridoxyl-amino acid-based precursor inhibitors for hHDC and deduced a structural model composed of PLP as well as histidine analogs in the active site of hHDC. One of the designed compounds efficiently inhibited 12-O-tetradecanoylphorbol-13-acetate (TPA)-induced hHDC activity in cells and in cell extracts without affecting human ornithine decarboxylase activity. The generated interaction model describes the structure-activity relationship of the tested compounds and of previously reported inhibitors. Moreover, it explains the binding specificity of mammalian HDC for histidine.

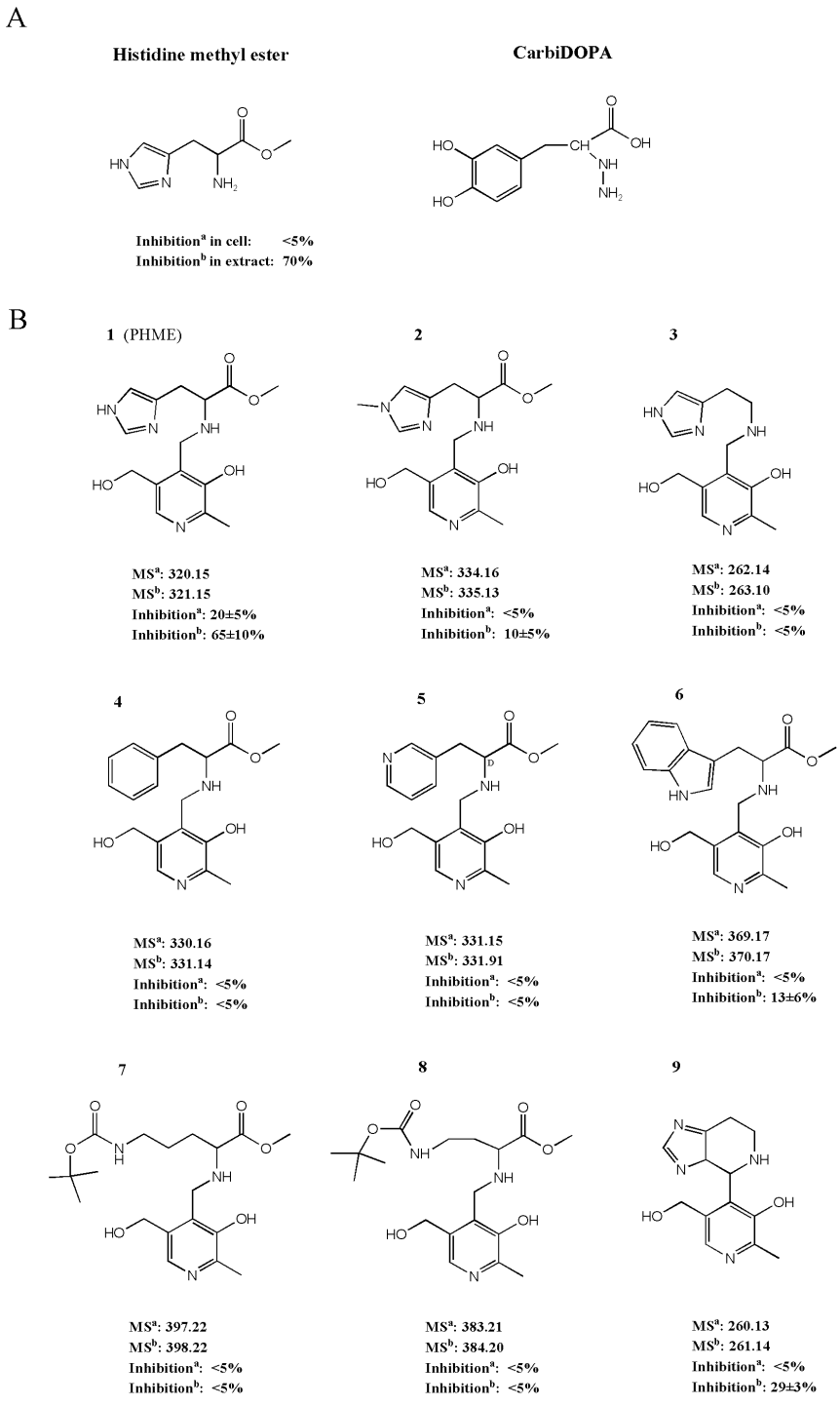

Figure 2. Chemical structure and inhibitory activity of various compounds. *A)* Substrate analogs of HDC and DDC. *B)* Designed and synthesized pyridoxyl-substrate analogs. The compounds **1** to **9** were synthesized, purified and verified as described in Materials and Methods. MS^a: theoretical mass. MS^b: measured mass $[M+H]^+$. $Inhibition^a$: HMC-1 cells were pre-treated with the indicated compounds (150 μM) for 3 h, then incubated with 100 nM TPA for additional 3 h

before cells were collected and lyzed. HDC activity was measured by trapping the released $^{14}CO_2$ from L-[1-^{14}C]histidine in assay buffer (see Materials and Methods). The inhibition values are expressed as the percentage of control (0%). Inhibition[b]: HMC-1 cells were pre-treated with 100 nM TPA for 3 h, then lyzed, incubated with the indicated compounds (150 µM). HDC activity was measured as described (inhibition of control, 0%). The results are listed as the average ± stdev (n=3).

4.3 MATERIALS AND METHODS

Materials

His·HCl and histamine·2HCl were bought from Sigma (Saint Louis, Missouri, USA). His-OMe·2HCl, His(1-Me)-OMe, Phe-OMe·HCl, ß-(3-pyridyl)-D-Ala-OMe·2 HCl, Trp-OMe·HCl, and α,γ-diaminobutyric acid(Boc)-OMe·HCl were from Bachem (Bubendorf, Switzerland). Protease inhibitors were obtained from Roche (Basel, Switzerland). L-[1-14C]histidine (55 mCi/mmol) was from American Radiolabeled Chemicals Inc (Saint Louis, Missouri, USA). Pyridoxal·HCl and 12-O-tetradecanoylphorbol-13-acetate (TPA) was from Fluka (Buchs, Switzerland).

General procedure for synthesis of the compounds

Compounds **1** to **6** (**Fig. 2*B***) were synthesized as described for the synthesis of pyridoxylhistamine (21). Briefly, pyridoxal (1mmol) and $NaHCO_3$ (2 mmol) were dissolved in 5 ml ethanol and the substrate analogs (1.05 mmol) together with $NaHCO_3$ (3 mmol) in 10 ml ethanol. Both solutions were mixed at 0 ºC and stirred at room temperature for 2 h. Then, $NaBH_4$ (125 mg) was added in small portions to the solution on ice. Acetic acid (100%) was added 30 min later to stop the reaction until pH 5 was reached. The solvents were removed with a vacuum dryer and the residues

were dissolved in water and subjected to FPLC or HPLC for purification and analysis. Compound **8** (**Fig. 2*B***) was synthesized as reported previously for compound **7** (20). Compound **9** (cyclized form of compound **3**) was obtained according to a reported procedure (22). Briefly, histamine (1.02 mmol) and KOH (4.2 mmol) were dissolved in water (2.5 ml) and stirred at 0 °C for 10 min. Then, solid pyridoxal (1 mmol) was added to the solution followed by ethanol (20 ml). The reaction mixture was stirred at 30 °C for 7 h and the solvent evaporated, yielding a white powder.

Compounds **1, 2, 3** and **9** were analyzed and purified with FPLC equipped with a mono S HR5/5 column (Amersham pharmacia biotech, Sweden) and a multiwavelengh detector. The samples were loaded and separated with a flow rate of 0.5 ml/min using the following gradient: 0-5 min, 100% solvent A (50 mM acetic acid pH 4.6) and 0% solvent B (50 mM acetic acid, pH 4.6, 1M NaCl); 5-30 min, 0-100% B; 30-40 min, 100% B. Detection was at 290 nm.

Compounds **4, 5, 6** and **8** were analyzed and purified with a HPLC equipped with a Kromasil C_{18} column (4.6 × 250 mm; Akzo Nobel, Sweden). The samples were loaded and separated with a flow rate of 0.15 ml/min using the following gradient: 0-36 min, 100% solvent A (3% acetonitrile/0.1% TFA) and 0% solvent B (80% acetonitrile/0.1% TFA); 36-92 min, 0-80% B; 92-120 min, 80-100% B, followed by 100% B. Elution was recorded at 290 nm. A preparative Kromasil C_{18} column (50.8 × 250 mm; Akzo Nobel, Sweden) with a flow rate of 15 ml/min was used under the same conditions to prepare larger amounts of compounds. All compounds were vacuum-dried several times after adding water and stored at a concentration of about 10 mM (water stock solution) at –20 °C. The obtained purified compounds (purity >95%) were analysed and verified by ESI-MS.

Cell culture

HMC-1 (a human mastocytoma cell line) cells were a generous gift from Dr J. Butterfield (Mayo Clinic, Rochester, Minn, USA) and maintained in Iscove's modified DMEM supplemented with 10% FBS in a humidified 5% CO_2 atmosphere at 37 °C.

HDC activity

HDC activity was measured by the released of $^{14}CO_2$ from labeled histidine as described (2, 23, 24). For measuring TPA-induced HDC activity, cells were cultured in 6-well plate at a density of ~6 x 10^5 cells per well (2 ml) with 5% FBS for one day and then treated in the absence or in the presence of the indicated compound for 3 h. The cells were induced with 100 nM TPA for 3 h, collected and washed twice with ice-cold phosphate-buffered saline (PBS, pH 6.8). The collected cells were lyzed by freezing (liquid nitrogen) and thawing twice (37 °C, 2 min) in 310 µl lysis buffer (10 µM EDTA, 10 µM PLP, 20 µM DTT and protease inhibitor cocktail in 100 mM PBS, pH 6.8). The reaction was started by adding 30 µl L-[1-^{14}C]histidine (final concentration, 130 µM; 0.09 µCi) to 270 µl supernatant of lyzed cells. After an 3-h incubation, the reaction was stopped by injecting 200 µL 4 N H_2SO_4 and the mixture was kept for one h at room temperature to ensure complete absorption of released CO_2 by the capture reagent (tissue solubilizer NCSII, Amersham). The captured $^{14}CO_2$ was measured by scintillation counting in a Wallac 1450 MicroBeta liquid scintillation counter. The protein concentration in the supernatant of lyzed cells was determined by the BioRad protein assay kit.

In order to measure inhibition in cell extracts of TPA-induced untreated HMC-1 cells, supernatants of lyzed cells were incubated with the respective compound and HDC activity determined as describe above.

Molecular modeling

The protein sequence of hHDC (Swiss-Prot access number: P19113) was aligned with the sequence of pDDC obtained from the PDB structure (PDB code: 1JS3; (8)), and rHDC (Swiss-Prot access number: P16453) with ClustalIW (25). Based on the sequence alignment of pDDC and hHDC, the structure of the dimeric hHDC was

constructed by superposing two monomeric HDCs, obtained from Swiss-Model database (http://swissmodel.expasy.org/), into the crystal structure of dimeric (subunit A and B) pDDC by using InsightII (version 2000, Accelrys Corporate, San Diego, USA). The structure of phosphopyridoxyl-histidine was constructed into hHDC based on the known 3D coordinates of the phosphopyridoxyl-carbiDOPA (PDB code: 1JS3), followed by energy minimization performed with the InsightII/Built module (steepest descents until a maximum derivative of 20 kcal/mol, CVFF force field). The assembled structures consisting of hHDC and phosphopyridoxyl-histidine analog were further optimized by energy minimization using InsightII/Discover module (conjugation gradient until a maximum derivative of 0.01 kcal/mol, CVFF force field).

4.4 RESULTS

Coenzyme-substrate analogs as inhibitors of hHDC

To target HDC in mammalian cells, we designed and synthesized potential coenzyme-histidine-based precursor inhibitors for hHDC (compounds **1, 2, 3** and **9**; **Fig. 2*B***), which we assumed to be membrane permeable and phosphorylated by intracellular pyridoxal kinase (26, 27). Recently we showed that intracellular ODC could be targeted with this kind of transition-state-based inhibitor (20). ODC (half life, 20 ~ 60 min) and HDC (half life, 1 ~ 2 h) are inducible and short-lived enzymes (12, 28) and the freshly synthesized apoenzymes will be excellent targets for these inhibitors. As the knowledge of the structural prerequisite in the active site environment was marginal, we synthesized and tested compounds with variations in the substrate moiety (Compound **4** to **8**, **Fig. 2*B***).

To identify effective inhibitors for newly synthesized apo HDC, HMC-1 cells were induced with TPA and HDC activities measured after cells have been pre-treated with the various compounds (**Fig. 2*B***). Among the 9 tested structural diverse compounds, pyridoxyl-histidine methyl ester (PHME, compound **1**, **Fig. 2*B***) was found to be the most potent inhibitor for HDC in HMC-1 cells and in cell extracts if subjected to 150 μM pyridoxyl-substrate conjugate. The phosphorylated PHME was also found to be a potent inhibitor (IC_{50} ~ 50 μM) for hHDC when tested in cell extracts of HMC-1, but was inactive in cells. All the other analogs did not significantly inhibit HDC in HMC-1 cells, although some (compounds **2**, **6** and **9**) slightly inhibited HDC activity in cell extracts (**Fig. 2*B***).

Non-induced (TPA) HMC-1 cells exhibited already a basal activity, which was slightly (15%) affected by 200 μM PHME (**Fig. 3**). Under these conditions, the inhibitor has to compete bound PLP (intracellular concentration, ~ 20 to 50 μM (29)) out of the active site of HDC, which probably is a slow process. After induction (black columns,

Fig. 3), freshly synthesized apoenzyme, indicated by a 2.5-fold increase in enzyme activity, is the main target of the inhibitor in the cells. This fraction is inhibited to ~ 60%, comparable to the inhibition caused by HME (**Fig. 2*A***) *in vitro*. Furthermore, PHME specifically inhibited hHDC in cells without affecting the activity of human ornithine decarboxylase and cell viability (unpublished observation).

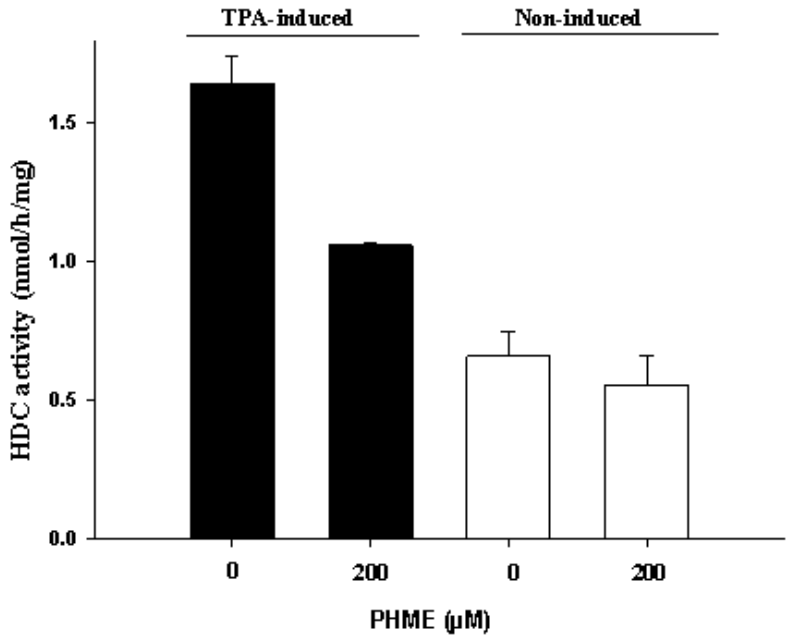

Figure 3. PHME inhibition of TPA-induced HDC activity in HMC-1 cells. HMC-1 cells were treated with or without PHME for 3 h followed by an 3-h incubation with or without TPA (100 nM). Cells were collected, lyzed and HDC activities measured as described in the legend of **Fig**. **2**. The results are listed as the average ± stdev (n=3).

Modeling the active site of hHDC

In order to understand the structure-activity relationship of the synthesized compounds (**Fig. 2*B***) and the active site of HDC, we built up by molecular modeling the active site of HDC together with the presumed intracellularly active form of PHME (phosphorylated and deesterified compound **1**, **Fig. 2*B***). The crystal structure of pig DDC (51% sequence identity with mammalian HDC, **Fig. 4**) served as template for constructing dimeric hHDC. Residues of hHDC and pDDC as well as rat HDC

surrounding the coenzyme-substrate analog within a distance of 4-5 Å were listed in **Table 1**, aligned as previously reported (6), and shown in **Fig. 4**. Most residues in the active site of pDDC and hHDC are identical (71%), except the seven conservative, semi-conservative or non-conservative substitutions (Ile101 (pDDC) → Leu102 (hHDC), Gly354 (pDDC) → Ser354 (hHDC), Phe80 (pDDC) → Tyr81 (hHDC), Thr82 (pDDC) → Ala83 (hHDC), Ser147 (pDDC) → Thr149 (hHDC), Ala148 (pDDC) → Val150 (hHDC) and His302 (pDDC) → Ser304 (hHDC)) shown in **Fig. 5*C*** and **Table 1**. Among them, Ala83 and Ser304 have been shown to be important residues for maintaining the activity of mouse HDC (6).

In the active site of hHDC, the imidazole ring was located in a pocket composed by residues Tyr81B, Asn302B, Ser304B, Lys305B, Leu102A, Phe104A and Ser354A (**Fig. 5*A***), whereas in pig DDC, the aromatic ring is surrounded by residues PheB80, AsnB300, HisB302, LysB303, IleA101, PheA103 and GlyA354 (**Fig. 5*B***).

```
Human_HDC          1   MMEPEEYRE---RGREMVDYICQYLSTVRERRVTPDVQPGYLRAQLPESAPEDPDSWDSIFGDIERIIMPGVVHWQSPHM 77
Rat_HDC            1   MMEPSEYHEYQARGKEMVDYICQYLSTVRERQVTPNVKPGYLRAQIPSSAPEEPDSWDSIFGDIEQIIMPGVVHWQSPHM 80
Pig_DDC            1   -MNASDFRR---RGKEMVDYMADYLEGIEGRQVYPDVQPGYLRPLIPATAPQEPDTFEDILQDVEKIIMPGVTHWHSPYF 76
Clustal Consensus  1   :*:..:::.   **:*****:.:**. :. *:* *:*:*****. :* :**::**:::.*: *:*:******.**:**:: 62

Human_HDC          78  HAYYPALTSWPSLLGDMLADAINCLGFTWASSPACTELEMNVMDWLAKMLGLPEHFLHHHPSSQGGGVLQSTVSESTLIA 157
Rat_HDC            81  HAYYPALTSWPSLLGDMLADAINCLGFTWASSPACTELEMNIMDWLAKMLGLPDFFLHHHPSSQGGGVLQRTVSESTLIA 160
Pig_DDC            77  FAYFPTASSYPAMLADMLCGAIGCIGFSWAASPACTELETVMMDWLGKMLQLPEAFLAGEAG-EGGGVIQGSASEATLVA 155
Clustal Consensus  62  .**:*: :*:*::*.***.**.*:**:**:******** :****.*** **: ** ... :****:* :.**:**:* 123

Human_HDC          158 LLAARKNKILEMKTSEPDADESCLNARLVAYASDQAHSSVEKAGLISLVKMKFLPVDDNFSLRGEALQKAIEEDKQRGLV 237
Rat_HDC            161 LLAARKNKILEMKAHEPNADESSLNARLVAYASDQAHSSVEKAGLISLVKIKFLPVDDNFSLRGEALQKAIEEDKQQGLV 240
Pig_DDC            156 LLAARTKVVRRLQAASPGLTQGAVLEKLVAYASDQAHSSVERAGLIGGVKLKAIPSDGKFAMRASALQEALERDKAAGLI 235
Clustal Consensus  124 *****.: : .::: .*.  :..:  :*************:****. **:* :* *.:*::*..***:*:*.**  **: 180

Human_HDC          238 PVFVCATLGTTGVCAFDCLSELGPICAREGLWLHIDAAYAGTAFLCPEFRGFLKGIEYADSFTFNPSKWMMVHFDCTGFW 317
Rat_HDC            241 PVFVCATLGTTGVCAFDKLSELGPICAREGLWLHVDAAYAGTAFLRPELRGFLKGIEYADSFTFNPSKWMMVHFDCTGFW 320
Pig_DDC            236 PFFVVATLGTTSCCSFDNLLEVGPICHEEDIWLHVDAAYAGSAFICPEFRHLLNGVEFADSFNFNPHKWLLVNFDCSAMW 315
Clustal Consensus  181 *.** ******. *:** * *:**** .*.:***:******:**: **:* :*:*:*:****.*** **::*:***:.:* 246

Human_HDC          318 VKDKYKLQQTFSVNPIYLRHAN--SGVATDFMHWQIPLSRRFRSVKLWFVIRSFGVKNLQAHVRHGTEMAKYFESLVRND 395
Rat_HDC            321 VKDKYKLQQTFSVNPIYLRHAN--SGVATDFMHWQIPLSRRFRSIKLWFVIRSFGVKNLQAHVRHGTDMAKYFESLVRSD 398
Pig_DDC            316 VKRRTDLTGAFKLDPVYLKHSHQGSGLITDYRHWQLPLGRRFRSLKMWFVFRMYGVKGLQAYIRKHVQLSHEFEAFVLQD 395
Clustal Consensus  247 ** : .*  :*.::*:**:*::  **: **: ***:**.*****:*:***:* :***.***::*: .:::: **::* .* 308

Human_HDC          396 PSFEIPAKRHLGLVVFRLKGPNCLTENVLKEIAKAGRLFLIPATIQDKLIIRFTVTSQFTTRDDILRDWNLIRDAATLIL 475
Rat_HDC            399 PVFEIPAERHLGLVVFRLKGPNCLTESVLKEIAKTGQVFLIPATIQDKLIIRFTVTSQFTTKDDILRDWNLIREAANLVL 478
Pig_DDC            396 PRFEVCAEVTLGLVCFRLKGSDGLNEALLERINSARKIHLVPCRLRGQFVLRFAICSRKVESGHVRLAWEHIRGLAAELL 475
Clustal Consensus  309 * **: *:  **** *****.: *.* :*:.* .: ::.*:*. ::.:::::**:: *: .  ..:   *: **  *  :* 356

Human_HDC          476 SQHCTSQPSPRVGNLIS--QIRGARAWACGTSLQSVSGAGDDPVQARKIIKQPQRVGAGPMKRENGLHLETLLDPVDDCF 553
Rat_HDC            479 SQHCTSQPSPRAKNLIPPPVTRDSKDLTNGLSLESVNEGGDDPVQVRKIFRLP-----------GDSLETTMDPFDDCF 546
Pig_DDC            475 ---------------------------------------------------------------------------- 475
Clustal Consensus                  ::               :  :       :    ::     :    :       :   :  .   :

Human_HDC          554 SEEAPDATKHKLSSFLFSYLSVQTKKKTVRSLSCNSVPVSAQKPLPTEASVKNGGSSRVRIFSRFPEDMMMLKKSAFKKL 633
Rat_HDC            547 SEEASDTTKHKLSSFLFSYLSVQNKKKTMRSLSCNSMPMSAQKSPPPDASVKHGGFFRARIFSGFPEEMMMMKKGGFKKL 626
Pig_DDC            475 ---AAEEGKAEIKS---------------------------------------------------------------- 486
Clustal Consensus        *.:  * ::.*:::  : :      :  :    : :          :         ::  :   ::::    :  :

Human_HDC          634 IKFYSVPSFPECSSQCG-LQLPCCPLQAMV 662
Rat_HDC            627 IKFYSVPSFPECSSQCGTLQLPCCPLQAMV 656
Pig_DDC            486 ---------------------------- 486
Clustal Consensus  394 : :  :  :         : :    :  :: 402
```

Figure 4. Sequence alignment of human HDC, rat HDC and pig DDC. The protein sequence of hHDC (Swiss-Prot access number: P19113) was aligned with the sequence of pDDC obtained from the PDB structure (PDB code: 1JS3 (8)), and rHDC (Swiss-Prot access number: P16453) with ClustalIW (25). * = identical residues in all sequences in the alignment; : = conserved substitutions; . = semi-conserved substitutions. Arrows indicate the non-identical residues of active sites (see **Table 1** and **Fig. 5*C***).

Table 1. Comparison of residues in the active site of pDDC, hHDC and rHDC. Residues indicated by italic fonts are the non-identical substitutions. Bold residues are the non-conservative substitutions. * = identical residues; : = conserved substitutions; . = semi-conserved substitutions.

pDDC	hHDC	rHDC	Clustal Consensus
ILE A101	*LEU 102A*	*LEU 102A*	:
PHE A103	PHE 104A	PHE 104A	*
GLY A354	***SER 354A***	***SER 354A***	.
TRP B71	TRP 72B	TRP 72B	*
TYR B79	TYR 80B	TYR 80B	*
PHE B80	*TYR 81B*	*TYR 81B*	:
PRO B81	PRO 82B	PRO 82B	*
THR B82	*ALA 83B*	*ALA 83B*	:
SER B147	*THR 149B*	*THR 149B*	:
ALA B148	***VAL 150B***	***VAL 150B***	.
SER B149	SER 151B	SER 151B	*
HIS B192	HIS 194B	HIS 194B	*
SER B194	SER 196B	SER 196B	*
THR B242	THR 244B	THR 244B	*
GLY B244	GLY 246B	GLY 246B	*
THR B245	THR 247B	THR 247B	*
THR B246	THR 248B	THR 248B	*
ASP B271	ASP 273B	ASP 273B	*
ALA B273	ALA 275B	ALA 275B	*
ASN B300	ASN 302B	ASN 302B	*
HIS B302	***SER 304B***	***SER 304B***	
LYS B303	LYS 305B	LYS 305B	*
PHE B309	PHE 311B	PHE 311B	*
ARG B447	ARG 447B	ARG 447B	*

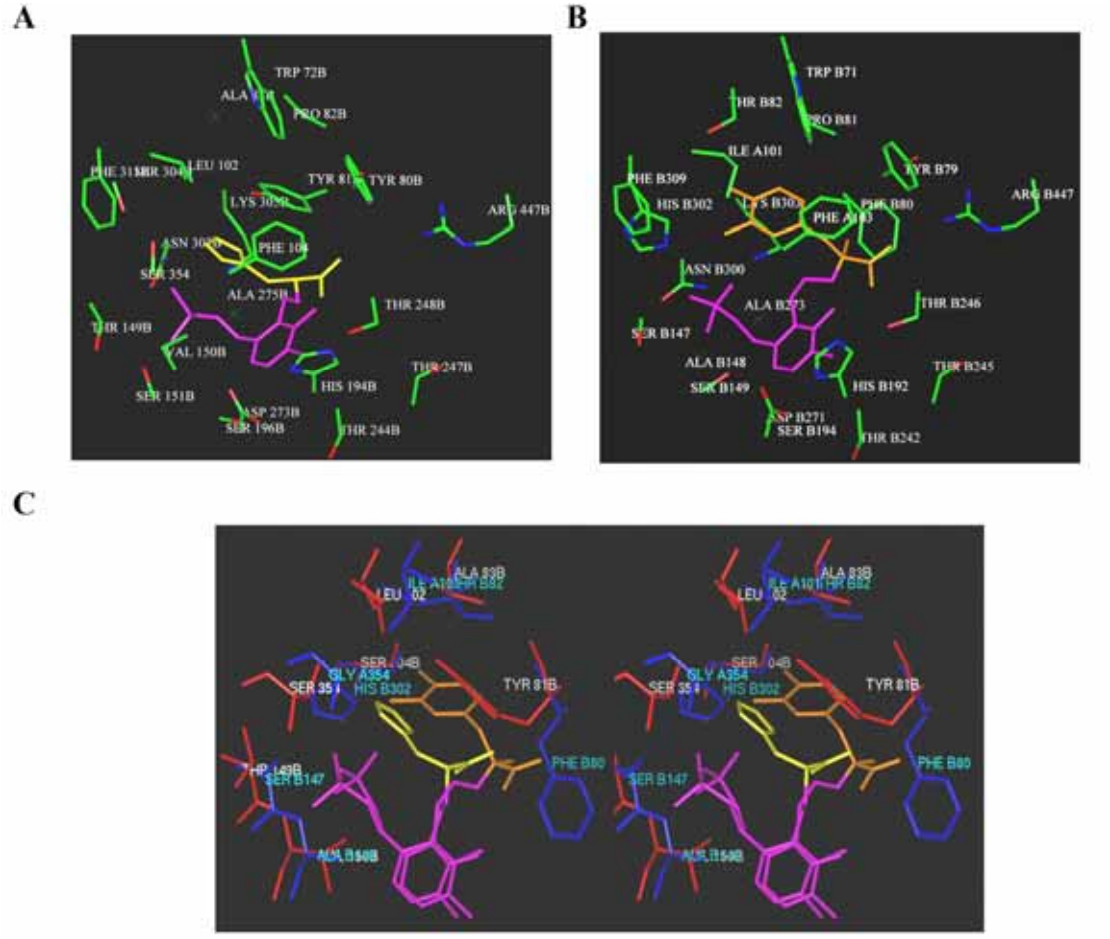

Figure 5. Active site model of hHDC and pDDC, containing a coenzyme-substrate analog. *A)* The modeled active site of hHDC (green) and the phosphopyridoxyl-histidine conjugate (pink-yellow). *B)* The active site of pDDC together with the phosphopyridoxyl-carbiDOPA (pink-brown) (PDB code: 1JS3). *C*) Superposed stereo view of the of non-identical residues of the active site of hHDC (red, the side chains are labeled with white fonts) and pDDC (blue, labels in cyan) together with phosphopyridoxyl (pink)-histidine (yellow) and phosphopyridoxyl (pink)-carbiDOPA (brown) conjugates. Residues surrounding the coenzyme-substrate analog within a distance of 4-5 Å are indicated.

4.5 DISCUSSION

Exploring the steric constraints in the binding-site by attaching additional groups on the mimic of a reaction intermediate is a robust methodology in understanding the structural requirements of the active site and in developing inhibitors (20, 30). The present study describes the successful action of PHME, a newly developed inhibitor of this kind of intracellular hHDC. The development strategy was based on the external aldimine, an obligatory intermediate in the mechanism of action of hHDC. In the tested 9 pyridoxyl derivatives, the 5'-phosphate group is eliminated and the carboxyl group is esterified with methanol. The rationale behind the design was that these compound have no negative net charge and very likely cross the cell membrane as it was reported for several pyridoxyl-amines (27, 31), a pyridoxyl-methionine analog (32) and compound **7** (20). The methyl ester group in the compounds will be hydrolysed by endogenous esterase (10), and the resulting inhibitors, after being phosphorylated by intracellular pyridoxal kinase (26, 31), will bind the cellular newly synthesized apo HDC with a high affinity.

Here, we tested several structural diverse mimics of a reaction intermediate of HDC (ES-PLP, **Fig. 1**) with variations in the substrate motif (**Fig. 2**). Only PHME showed remarkable inhibition both in cell extract and in cells, which already indicated that the binding site of hHDC is rather specific and seems not to accept variations in the substrate moiety.

To understand the structural basis of the binding specificity of hHDC, a model consisting of dimeric hHDC and phosphopyridoxyl-histidine, the cellular active from of PHME, was constructed by homologous modeling methods. With this model, the substrate specificity of these two proteins can be explained by the substitutions Gly354 (pDDC) → Ser354 (hHDC), Phe80 (pDDC) → Tyr81 (hHDC) and His302 (pDDC) → Ser304 (hHDC) (**Fig. 5A-C** and **Table 1**). The imidazole side chain of the substrate is in a favorite position to form hydrogen bonds with the hydroxyl groups of Tyr81, Ser304 or Ser354 of hHDC, whereas the hydroxyl groups of carbiDOPA are

favorably interacting with the imidazole ring of His302 of pDDC as reported (6, 33). Mutation of Ser304 of hHDC to Gly decreased the enzymic activity but not completely (6) indicating Ser304 participates in substrate binding rather than in the catalytic conversion as also suggested by the present model. This binding mode of the coenzyme-substrate conjugate in the active site of hHDC demonstrates that the imidazole binding moiety of substrate consists of a tightly packed and specific pocket in contrast to that of pDDC (**Fig. 5A-C**, (34)). Tyr81B in hHDC adopted a 'closed conformation' in contrast to the 'open conformation' of the corresponding residue Phe80B in pDDC and can form a stacking interaction with the imidazole ring and an additional hydrogen bond with the N1 atom of the imidazole ring (**Fig. 5C**). This different conformation forms a small but specific binding pocket for the imidazole ring of the substrate histidine, which cannot accept bigger ligands like pDDC (**Fig. 5C**). The model displays also a more tightly packing in hHDC than in pDDC of active site residues surrounding the phosphate group (**Fig**. **5A-C**).

The small but specific binding site of hHDC as analyzed above explains why the conjugates with a larger amino acid moiety (His(1-Me), **2**; Phe, **4**; ß-(3-Pyridyl)-D-Ala, **5**; Trp, **6**; tert-butoxycarbonyl (BOC) protected ornithine, **7** and BOC protected α,γ-diaminobutyric acid, **8**; **Fig. 2B**) do not significantly inhibit hHDC in cells. Compound 2, which has an additional methyl group at the imidazole ring, showed already much less inhibition than compound **1** (**Fig. 2**). The model indicates that the methyl group at N1 of the imidazole ring disturbs the formation of a hydrogen bond to Tyr81B, Ser304B or Ser354A in the active site of hHDC and exerts steric constraints (**Fig. 2B**, **5A** and **5C**). The failure of inhibition by compound **3** and **9** (cyclized form of **3**) is mostly likely due to the missing carboxylate group, which could interact with the conservative positively charged Arg 447B during catalysis **(Fig. 2** and **5A**).

Besides the structure-activity relationship gained from the designed compounds, the proposed model reasonably explains previous experimental data. The hHDC model points out that hHDC contains a narrow side chain-binding pocket and a relatively large binding site for the carboxylate group. Additional modifications on

histidine, such as α- and ß- substitutions (9) as well as substitutions at the imidazole ring (10), will decrease the binding affinity due to steric hindrance in this region. The small binding site does not accept a bulky fragment such as α-methyl dopa either (Fig. 5C), which is a potent inhibitor for DDC but not for rHDC (35). The relatively large free binding region around the carboxylate group in hHDC (**Fig. 5A**) could accept additional moieties, whereas in DDC this is not the case (**Fig. 5B**). Indeed, PHME, phosphopyridoxyl-histidine methyl ester (see above), HME (10), the dipeptide His-Phe (13, 36) as well as others (37) inhibited mammalian HDC in vitro. This fact could be utilized to develop more potent inhibitors for hHDC by modifications at the carboxylate group.

In conclusion, the present investigation with pyridoxyl-histidine analogs as possible precursor ligands for hHDC revealed a novel intracellular inhibitor of hHDC and a structural model of its active site containing not only the coenzyme but also substrate analogs. These findings can serve as structural basis for functional studies of HDC and to develop more potent inhibitors for this enzyme of pharmaceutical interest.

4.6 ACKNOWLEDGMENT

We acknowledge the financial support by COST Switzerland (Action 922, Grant number C02.0017). We thank Dr. S. Bienz and collaborators (Institute of Organic Chemistry, University Zurich) for providing excellent facilities for organic synthesis, Dr. J. Butterfield and co-workers for providing HMC-1 cells and Dr. P. Christen (Department of Biochemistry, University Zurich) for his valuable advice and critical reading of the manuscript.

4.7 REFERENCES

1. Furuta, K., Nakayama, K., Sugimoto, Y., Ichikawa, A., and Tanaka, S. (2007) Activation of histidine decarboxylase through post-translational cleavage by caspase-9 in a mouse mastocytoma P-815. *J. Biol. Chem.* **282**, 13438-13446
2. Maeda, K., Taniguchi, H., Ohno, I., Ohtsu, H., Yamauchi, K., Sakurai, E., Tanno, Y., Butterfield, J. H., Watanabe, T., and Shirato, K. (1998) Induction of L-histidine decarboxylase in a human mast cell line, HMC-1. *Exp. Hematol.* **26**, 325-331
3. Moya-Garcia, A. A., Medina, M. A., and Sanchez-Jimenez, F. (2005) Mammalian histidine decarboxylase: from structure to function. *Bioessays* **27**, 57-63
4. Fleming, J. V., and Wang, T. C. (2000) Amino- and carboxy-terminal PEST domains mediate gastrin stabilization of rat L-histidine decarboxylase isoforms. *Mol. Cell. Biol.* **20**, 4932-4947
5. Medina, M. A., Urdiales, J. L., Rodriguez-Caso, C., Ramirez, F. J., and Sanchez-Jimenez, F. (2003) Biogenic amines and polyamines: similar biochemistry for different physiological missions and biomedical applications. *Crit. Rev. Biochem. Mol. Biol.* **38**, 23-59
6. Fleming, J. V., Sanchez-Jimenez, F., Moya-Garcia, A. A., Langlois, M. R., and Wang, T. C. (2004) Mapping of catalytically important residues in the rat L-histidine decarboxylase enzyme using bioinformatic and site-directed mutagenesis approaches. *Biochem. J.* **379**, 253-261
7. Watanabe, T., and Ohtsu, H. (2002) L-histidine decarboxylase as a probe in studies on histamine. *Chemical record* **2**, 369-376
8. Burkhard, P., Dominici, P., Borri-Voltattorni, C., Jansonius, J. N., and Malashkevich, V. N. (2001) Structural insight into Parkinson's disease treatment from drug-inhibited DOPA decarboxylase. *Nat. Struct. Biol.* **8**, 963-967
9. DeGraw, J. I., Engstrom, J., Ellis, M., and Johnson, H. L. (1977) Potential histidine decarboxylase inhibitors. 1. alpha- and beta-substituted histidine analogues. *J. Med. Chem.* **20**, 1671-1674
10. Kelley, J. L., Miller, C. A., and White, H. L. (1977) Inhibition of histidine decarboxylase. Derivatives of histidine. *J. Med. Chem.* **20**, 506-509
11. Watanabe, T., Yamatodani, A., Maeyama, K., and Wada, H. (1990) Pharmacology of alpha-fluoromethylhistidine, a specific inhibitor of histidine decarboxylase. *Trends in pharmacological sciences* **11**, 363-367
12. Seiler, N. (2003) Thirty years of polyamine-related approaches to cancer therapy. Retrospect and prospect. Part 1. Selective enzyme inhibitors. *Curr. Drug Targets* **4**, 537-564
13. Hammar, L., and Ragnarsson, U. (1979) Peptide inhibition of mammalian histidine decarboxylase. *Agents Actions* **9**, 314-318

14. Rodriguez-Caso, C., Rodriguez-Agudo, D., Sanchez-Jimenez, F., and Medina, M. A. (2003) Green tea epigallocatechin-3-gallate is an inhibitor of mammalian histidine decarboxylase. *Cell Mol. Life. Sci.* **60**, 1760-1763
15. Facchini, A., Zanella, B., Stefanelli, C., Guarnieri, C., and Flamigni, F. (2003) Effect of green tea extract on the induction of ornithine decarboxylase and the activation of extracellular signal-regulated kinase in bladder carcinoma ECV304 cells. *Nutr. Cancer* **47**, 104-110
16. Eliot, A. C., and Kirsch, J. F. (2004) Pyridoxal phosphate enzymes: mechanistic, structural, and evolutionary considerations. *Annu. Rev. Biochem.* 73, 383-415
17. Mehta, P. K., and Christen, P. (2000) The molecular evolution of pyridoxal-5'-phosphate-dependent enzymes. *Advances in enzymology and related areas of molecular biology* **74**, 129-184
18. Heller JS, C. E., Bussolotti DL, Coward JK (1975) Potent inhibition of ornithine decarboxylase by N-(5'-phosphopyridoxyl)-ornithine. *Biochim Biophys Acta* **403**, 197-207
19. Khomutov, R. M., Dixon, H. B., Vdovina, L. V., Kirpichnikov, M. P., Morozov, Y. V., Severin, E. S., and Khurs, E. N. (1971) N-(5'-phosphopyridoxyl)glutamic acid and N-(5'-phosphopyridoxyl)-2-oxopyrrolidine-5-carboxylic acid and their action on the apoenzyme of aspartate aminotransferase. *Biochem. J.* **124**, 99-106
20. Wu, F., Grossenbacher, D., and Gehring, H. (2007) New transition state-based inhibitor for human ornithine decarboxylase inhibits growth of tumor cells. *Molecular cancer therapeutics* **6**, 1831-1839
21. Hidehiko KumagaI, H. Y. a. H. F. (1969) A Modified Method for Synthesis of Pyridoxylhistamine. *Agr. Biol. Chem.* **33**, 1210-1212
22. Kametani, T., Koizumi, M., Okui, K., Nishii, Y., and Ono, M. (1972) Biochemical studies on drugs and the central nervous system. 1. Synthesis and activity of pyridoxal derivatives. (Studies on the syntheses of heterocyclic compounds. 438). *J. Med. Chem.* **15**, 203-204
23. Dartsch, C., Chen, D., and Persson, L. (1998) Multiple forms of rat stomach histidine decarboxylase may reflect posttranslational activation of the enzyme. *Regulatory peptides* **77**, 33-41
24. Levine, R. J., and Watts, D. E. (1966) A sensitive and specific assay for histidine decarboxylase activity. *Biochem. Pharmacol.* **15**, 841-849
25. Thompson, J. D., Higgins, D. G., and Gibson, T. J. (1994) CLUSTAL W: improving the sensitivity of progressive multiple sequence alignment through sequence weighting, position-specific gap penalties and weight matrix choice. *Nucleic Acids Res.* **22**, 4673-4680
26. Tang, L., Li, M. H., Cao, P., Wang, F., Chang, W. R., Bach, S., Reinhardt, J., Ferandin, Y., Galons, H., Wan, Y., Gray, N., Meijer, L., Jiang, T., and Liang, D. C. (2005) Crystal structure of pyridoxal kinase in complex with roscovitine and derivatives. *J. Biol. Chem.* **280**, 31220-31229
27. Zhang, Z. M., and McCormick, D. B. (1991) Uptake of

N-(4'-pyridoxyl)amines and release of amines by renal cells: a model for transporter-enhanced delivery of bioactive compounds. *Proc. Natl. Acad. Sci. U. S. A.* **88**, 10407-10410

28. Zhao, C. M., Chen, D., Yamada, H., Dornonville de la Cour, C., Lindstrom, E., Persson, L., and Hakanson, R. (2003) Rat stomach ECL cells: mode of activation of histidine decarboxylase. *Regulatory peptides* **114**, 21-27
29. Robson, L. C., and Schwarz, MR (1980) In Vitamin B6 Metabolism and Role in Growth (Tryfiates G.P., ed) pp.205, Food and Nutrition Press, Westport Conn.
30. Knight, Z. A., Gonzalez, B., Feldman, M. E., Zunder, E. R., Goldenberg, D. D., Williams, O., Loewith, R., Stokoe, D., Balla, A., Toth, B., Balla, T., Weiss, W. A., Williams, R. L., and Shokat, K. M. (2006) A pharmacological map of the PI3-K family defines a role for p110alpha in insulin signaling. *Cell* **125**, 733-747
31. Zhang, Z., and McCormick, D. B. (1992) Uptake and metabolism of N-(4'-pyridoxyl)amines by isolated rat liver cells. *Arch. Biochem. Biophys.* **294**, 394-397
32. Ogier, G., Chantepie, J., Deshayes, C., Chantegrel, B., Charlot, C., Doutheau, A., and Quash, G. (1993) Contribution of 4-methylthio-2-oxobutanoate and its transaminase to the growth of methionine-dependent cells in culture. Effect of transaminase inhibitors. *Biochem. Pharmacol.* **45**, 1631-1644
33. Bertoldi, M., Castellani, S., and Bori Voltattorni, C. (2001) Mutation of residues in the coenzyme binding pocket of Dopa decarboxylase. Effects on catalytic properties. *Eur. J. Biochem.* **268**, 2975-2981
34. Sakamoto, Y., Watanabe, T., Hayashi, H., Taguchi, Y., and Wada, H. (1985) Effects of various compounds on histidine decarboxylase activity: active site mapping. *Agents Actions* **17**, 32-37
35. Smissman, E. E., and Warner, V. D. (1972) Specificity in enzyme inhibition. 2. -Aminohydroxamic acids as inhibitors of histidine decarboxylase and 3,4-dihydroxyphenylalanine decarboxylase. *J. Med. Chem.* **15**, 681-682
36. Mattsson, M., Henningsson, A. C., Henningsson, S., and Hammar, L. (1982) Effect of His-Phe, a competitive inhibitor of histidine decarboxylase, on gastric acid secretion in chronic gastric fistula rats: delay in acid secretion response to pentagastrin. *Agents Actions* **12**, 176-178
37. Taylor, R. J., Jr., Leinweber, F. J., and Braun, G. A. (1973) 4-imidazolyl-3-amino-2-butanone (McN-A-1293), a new specific inhibitor of histidine decarboxylase. *Biochem. Pharmacol.* **22**, 2299-2310

5. Appendix

The nanoelectrospray mass spectra of phosphopyridoxyl-tryptophan methyl ester (pPTME).

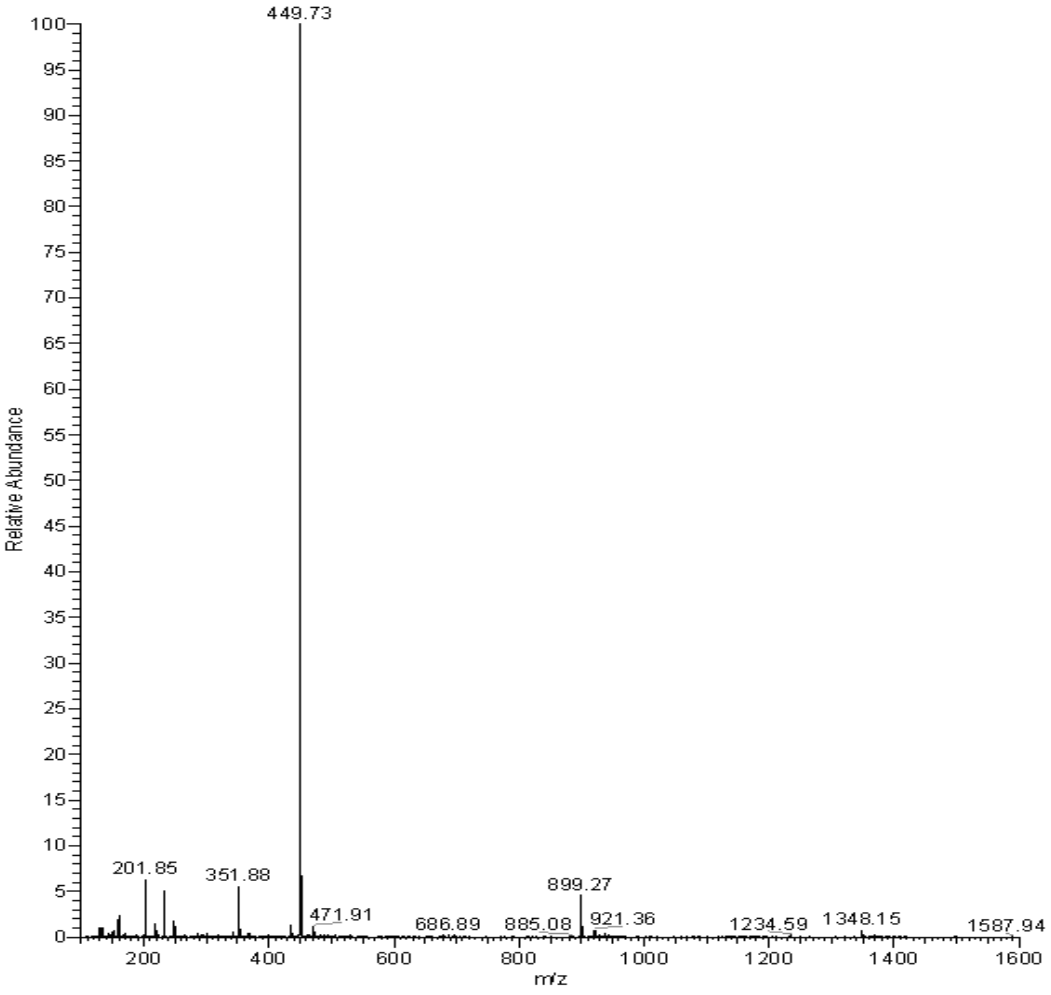

The nanoelectrospray mass spectra of pyridoxyl-tryptophan methyl ester (PTME).

The nanoelectrospray mass spectra of pyridoxyl-ornithine (BOC) methyl ester (POB).

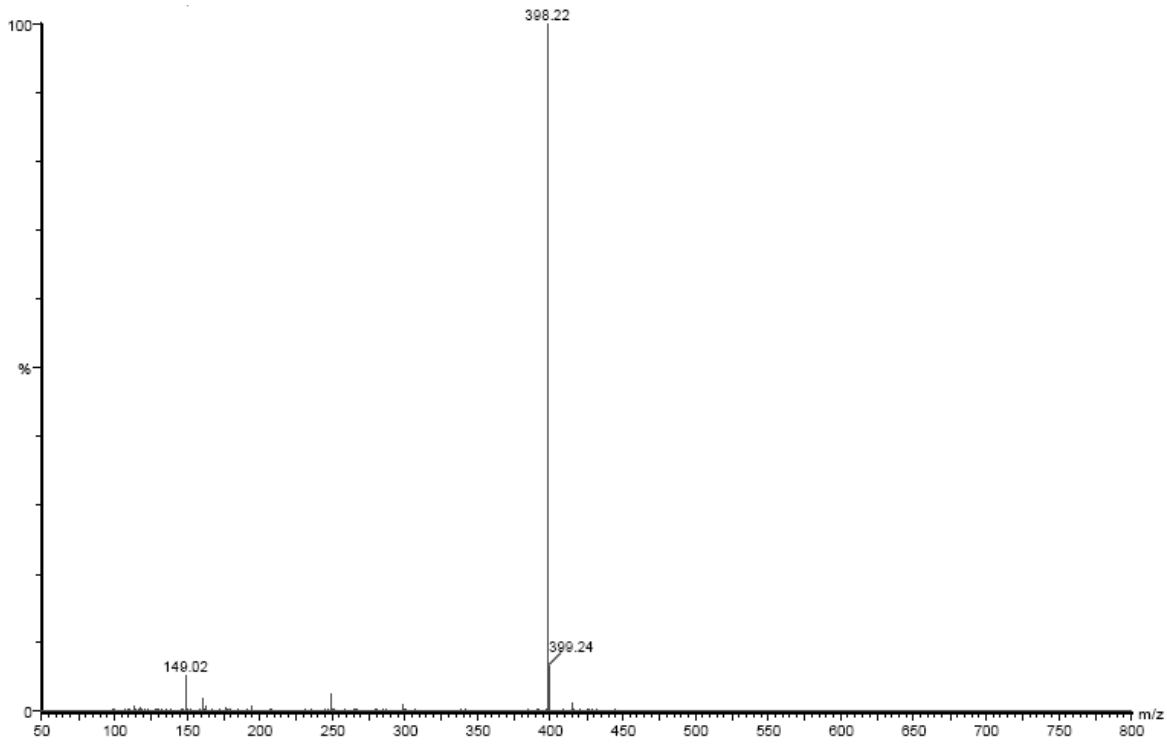

The nanoelectrospray mass spectra of pyridoxyl-histidine methyl ester (PHME).

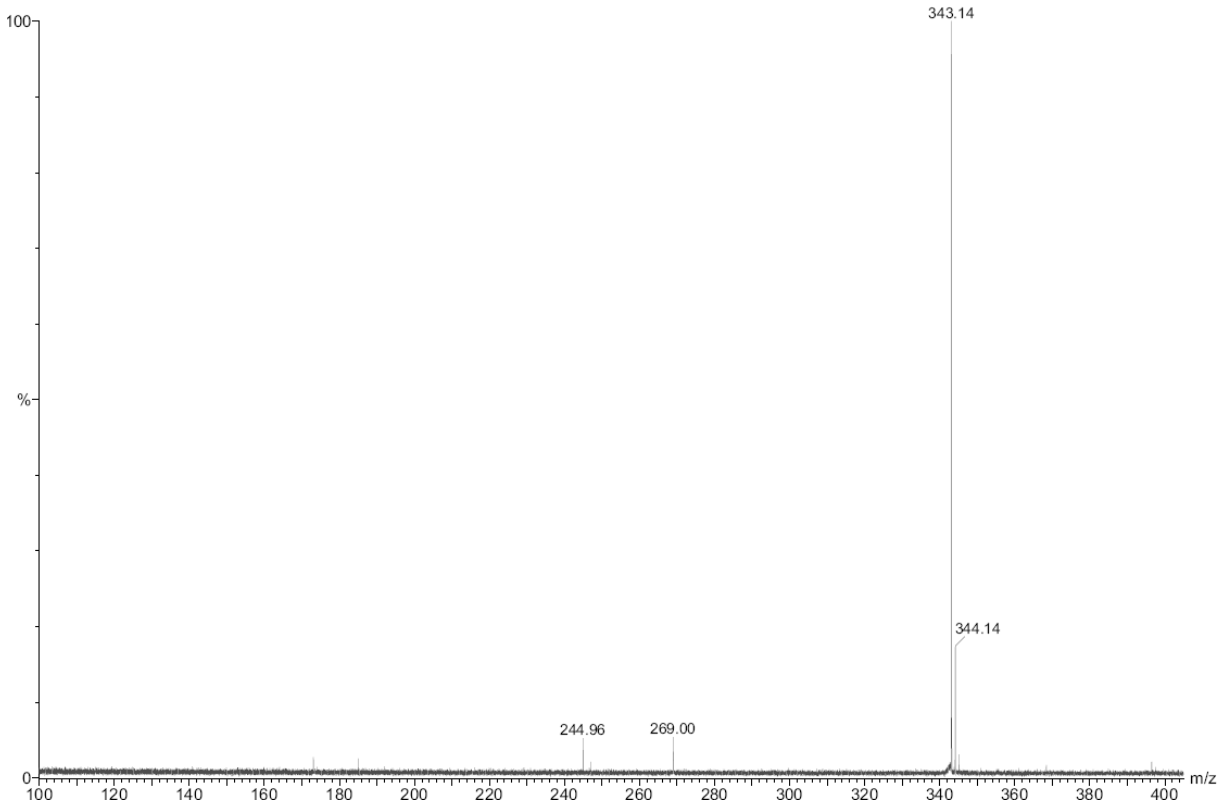

Acknowledgements

Here, I would like to thank many people who help me during my PhD study.

Prof. Heinz Gehring, my supervisor, who gives me the opportunity to work in his group, provides such dynamic and interdisciplinary projects and initiates fruitful collaborations.

Prof. Philipp Christen, who generously shares his ideas, knowledge and experience, and reviewed my dissertation.

Prof. Peter Sonderegger, who supervises my PhD dissertation as the responsible faculty member.

Prof. Stefan Bienz, who gives me the opportunity to work in his laboratory and provides the excellent organic chemistry facilities.

Margrit, Mathys Würfl who helps me a lot in preparing the dissertation and administrative issues.

Doris Grossenbacher, Christine Lüthi, Rahel Siegenthaler, Wanjiang Han, Rouzanna Zakaryan, Lilian Quero, Steffen Pahlich and Karim Bschir for their collaborations and technical assistance.

Maurizio Campagna, Pascal Bisegger, Michael Méret and Xinjun Luan for their substantive help in organic synthesis and analytical methods.

My wife, Jing, who gives me great support not only in daily life but also in bioscience.

My friends Hu Guoquan, Zhou Yueyang, Reto Kreuzer, Huang Zhixin, Lu Jianjun, Chen Shangjun, Liu Huanfa, Xue Gongda, Yang Zhou, Liu Junguo, Huang Danzhi, Tao Minli, Liu Peng, Zhou Ting and Wei Ren for their kind help and having fun together.

All my colleagues in University Zurich, for their valuable and generous help.

WU Fang
born on June 2nd, 1976 in Xi'an, China
Nationality: China

1992- 1995	Qing An High School, Xi'an, Shannxi, China
1995- 1999	Department of biochemistry Shanghai Jiao Tong University, Shanghai, China. B.Sc, Major in Biochemistry. Bachelor thesis: Study on the production of PUFAs in the *P. tricornutum*
1999- 2002	Shanghai Research Centre of Biotechnology Shanghai Institutes for Biological Sciences Chinese Academy of Science. M.Sc in biochemistry and molecular biology Master thesis: Design and study the biomimic ligands for the human tissue plasminogen activator
2002- 2003	Pre-clinical Safety, Novartis Pharma, Basel, Switzerland.
2003- 2007	Department of Biochemistry University Zürich, Switzerland. PhD student, supported by COST Switzerland, Action 922 Supervised by Prof. Dr. Heinz Gehring Dissertation: Design, synthesis and characterization of coenzyme-substrate inhibitors targeting intracellular pyridoxal 5'-phosphate-dependent enzymes

.